Universität für Bodenkultur Wien
Department für Agrarbiotechnologie IFA Tulln
Institut für Umweltbiotechnologie

Felice QUARTINELLO M.Sc.

DISSERTATION

Enzymes for textile applications: advances in surface functionalization and recycling

Zur Erlangung des Doktorgrades an der Universität für Bodenkultur Wien

Univ. Prof. Dr. Georg Guebitz

Universität für Bodenkultur Wien
Department für Agrarbiotechnologie IFA Tulln
Institut für Umweltbiotechnologie

2020

Table of contents

Preamble

The research described in this doctoral thesis was supervised by Univ.Prof. Dipl.-Ing. Dr.techn. Georg M. Gübitz at the University of Natural Resources and Life Sciences, Department for Agrobiotechnology, Institute of Environmental Biotechnology, Tulln an der Donau, between September 2016 and May 2020. The work of this thesis was carried out as part of several projects and received financial support from the European Union´s H2020 research and innovation program under the grant agreement 641942 (Resyntex Project) and under grant agreement FOLSMART [grant number 683356].

This PhD thesis is divided in four main sections.

The first section (Chapter 2) introduces the reader towards Textile and Clothing Industry and its actual fabric apparel technology. Afterwards, it also introduce the potential applications of biotechnology into this sector in order to reduce the environmental impact of such sector.

Chapter 3 and 4 include publications published during this thesis period where surface functionalization of textile has been demonstrated. Specifically, Poly(ethylene terephthalate), Nylon-6 and cotton/PET blend were “activated” *via* a limited surface treatment using enzymes. Thus, those obtained new functional groups were used to covalently immobilize finishing agents and then give new functional properties to the apparel. In the third section (chapter 5 and 6), it is described a selective enzymatic recycling technology to reduce the environmental impact of landfilled textile waste. Moreover, both chapters introduce the chemical characterization and the potential re-utilization of the obtained building blocks produced during the biochemical processes. This technology allows the production of aminoacids and glucose, which can be used as platform for the production of bio-based valuable molecules, while PET degradation products can be used to re-synthetize pure recycled PET, instead of using fossil-based monomers.

The latter section (chapter 7 and 8) includes a general conclusion, appendix and listing of the scientific publications, oral and poster presentation.

Abstract

The main objective of the thesis has been to assess enzymatic surface hydrolysis for smart textiles formulation and finally complete degradation for reduction of environmental impact of textile waste.

Regarding enzymatic functionalization, *Humicola insulens* cutinalse (HiC) has been demonstrated capable to introduce new reactive functional groups on PET and nylon-6 surfaces, without reduction of their mechanical properties. The limited depolymerization was confirmed by HPLC, FT-IR and *via* colorimetric reactions. In the next steps, the obtained reactive groups (-COOH and -OH from PET; $-NH_2$ and -COOH for nylon) were subsequently exploited for coupling of finishing textile agents. DNA was immobilized on pure polyester and polyamide for potential flame retardant application. Different coupling reaction were studied, where finally tyrosine coating system resulted the most effective as results of the lowest burning rate and totally burning time (35 sec, 150 mm and 4.3 mm sec^{-1} for untreated nylon and 3.5 sec, 17.5 mm and 5 $mm*sec^{-1}$ for enzymatically treated nylon coated with tyrosine/DNA) as also confirmed by FT-IR, ESEM/EDS measurements. Moreover, TGA analysis proved a lower thermal degradation between 450 and 625 °C when compared to the untreated sample.

The second study of surface functionalization involved the enzymatic treatment of hospital bed sheet (50 % cotton/PET) with HiC and then the immobilization of antimicrobial protein-based nanoparticles, in order to reduce the possible nosocomial infections. Briefly, pH responsive human serum albumin/silk fibroin nanoparticles were prepared and loaded with a natural antimicrobial compound, eugenol. Among different in vitro release studies of eugenol, the nanoparticles with the lowest amount of silk fibroin and lower degradation degree shown higher release, almost 41 % at pH 6.00. After the immobilization *via* EDC/NHS coupling system, functionalized cotton/PET blends were tested against Gram positive and negative bacteria. It resulted in antimicrobial activity against *Staphylococcus aureus* (81 %) and against *Escherichia coli* (31 %).

Beside textile waste composition, wool, cotton and polyester and their related blends are the most representative: therefore, it has been developed an enzyme-based strategy for recovery of valuable compounds from those materials. Either model and real textile waste blends were subjected to a step-wise enzymatic process. Accordingly, to pH and enzymatic activities, fabrics were first incubated with a protease from *Bacillus subtilis* for protein-based material removal (95 % efficiency) and related amino acids extraction. Subsequently, glucose was obtained after incubation with cellulase from cellulose part degradation (85 % efficiency). The purity of the remaining polyester was, finally, tested with FT-IR spectroscopy. The amino acids recovered were characterized via elementary analysis (ToN and ToC) and molecular sized determination (SDS-PAGE), in the same the obtained glucose has been used for bio-ethanol production *via Saccharomyces cerevisiae* fermentation.

Finally, PET was depolymerized via a chemo-enzymatic combination. In a first stage, the polyester was subjected to a chemical treatment under neutral conditions (with water at T=250 °C and P=40 bar), which allowed the 85 % depolymerization of PET into monomer (TPA) and oligomers. The latters were further hydrolyzed using HiC and yielding 97 % of pure TPA. In this work, it was also developed a method to monitor the degree of PET depolymerization *via* FT-Raman spectroscopy. The peak of free carboxylic group of TPA (1632 cm^{-1}) is able to shift after the deprotonation into two peaks (1604 and 1398 cm^{-1}) in presence of tryethylamine (ratio 1:5). Thus, this ability of shift was exploited in order to determine the purity of TPA after the different hydrolysis steps.

Kurzfassung

Das Hauptaugenmerk dieser Arbeit lag darin Enzyme für die Hydrolyse von Textiloberflächen einzusetzen um so genannte „smarte Textilien“ damit herzustellen. Andererseits wurden Enzymen zum vollständigen Abbau von Textilabfällen erforscht, um den negativen Umwelteinfluss dieser Abfälle zu reduzieren.

Für die enzymatische Funktionalisierung wurde das Enzym *Humicola insulens* cutinase (HiC) verwendet um neue, reaktive und funktionelle Gruppen auf den Oberflächen von PET und Nylon-6 Textilien zu generieren, ohne dabei die mechanischen Eigenschaften der Stoffe zu verändern. Diese Funktionalisierung wurde mittels HPLC, FT-IR und der Hilfe kolorimetrischer Methoden nachgewiesen. In einem nächsten Schritt wurden die enzymatisch-erzeugten, reaktiven Gruppen (-COOH und -OH bei PET; $-NH_2$ und -COOH bei Nylon) verwendet, um daran unterschiedliche Stoffe zu koppeln. Unter anderem wurde DNA auf der Polyester- und Polyamid-Oberfläche immobilisiert, um den Textilien flammhemmende Eigenschaften zu verleihen. Von den verschiedenen Reaktionen zur Kopplung der DNA, welche getestet wurden, stelle sich Tyrosin als Kopplungs-Reagenz als besonders effektiv heraus. Die über das Tyrosin gebundene DNA führte zur geringsten Abbrand Rate und einer reduzierten Abbrand Zeit (35 Sek., 150 mm und 4.3 mm $Sek.^{-1}$ bei unbehandeltem Nylon; 3.5 Sek., 17.5 mm und 5 mm $Sek.^{-1}$ bei Nylon mit Tyrosin/DNA Kopplung). Diese Ergebnisse wurden des Weiteren mittels FT-IR und ESEM/EDS Messungen bestätigt. Analysen mit Hilfe von TGA Messungen zeigten außerdem eine niedrigere thermische Zersetzung zwischen 450 und 625 °C verglichen mit den unbehandelten Proben.

In einer weiteren Studie wurde HiC zur enzymatischen Funktionalisierung von Krankenhaus-Bettwäsche (50 % Baumwolle/PET) verwendet um danach antimikrobielle, auf Proteinen basierende Nanopartikel darauf zu immobilisieren. Dies sollte dazu dienen, Infektionen nach Operationen zu verhindern. Dazu wurden pH-reaktive, human Serum Albumin - Seiden Fibroin Nanopartikel hergestellt und mit dem natürlich-vorkommenden, antimikrobiellen Stoff Eugenol beladen. Bei den unterschiedlichen in vitro Studien zur Freisetzung von Eugenol stellte sich heraus, dass jene Nanopartikel mit dem geringsten Gehalt an Seiden-Fibroin und dem geringsten Abbaugrad die effektivste Freisetzung

gewährleisten (41 % bei pH 6.00). Nach Immobilisierung der Nanopartikel mittels EDC/NHS Kopplungssystem wurde der antimikrobielle Effekt der funktionalisierten Baumwolle/PET Stoffe gegen *Staphylococcus aureus* (81 %) *Escherichia coli* (31 %) nachgewiesen.

Im Kontext von Textilabfällen machen Wolle, Baumwolle und Polyester den größten Anteil aus. Daher wurde weiters ein auf Enzymen basierendes Konzept zur Gewinnung von wertvollen Bestandteilen aus diesen Abfällen entwickelt. Dabei wurde der schrittweise, enzymatische Abbau von vordefinierten Mischungen der unterschiedlichen Materialien, aber auch von echten Textilabfällen getestet. Im ersten Schritt wurden die Stoffe mit einer *Bacillus subtilis* Protease inkubiert um Proteine (95 % Effektivität) und Aminosäuren zu extrahieren. Gefolgt von einer enzymatischen Behandlung mittels Cellulose konnten bis zu 85 % Glukose rückgewonnen werden. Die Reinheit des resultierenden Polyesters am Ende wurde mittels FT-IR analysiert. Gewonnene Aminosäuren wurden mittels Elementaranalyse (ToN und ToC) und Ermittlung der Molekülgröße (SDS-PAGE) charakterisiert. Die produzierte Glukose kam bei der Bio-Ethanol Produktion durch Fermentation mit *Saccharomyces cerevisiae* zum Einsatz.

Abschließend wurde ein Prozess zum chemisch-enzymatischen Abbau von PET getestet. Im ersten Schritt wurde das Polyester einer chemischen Behandlung unter neutralen Bedingungen (mit Wasser bei T=250 °C und P=40 bar) unterzogen, was zu einer de-Polymerisierung (85%) von PET in Monomer- (TPA) und Oligomer-Bestandteile führte. Diese Bestandteile wurden einer enzymatischen Hydrolyse mit HiC unterzogen, welche zu 97 % reinem TPA führte. Inhalt dieser Studie war des Weiteren die Entwicklung einer Methode zum Monitoring der PET de-Polymerisierung mittels FT-Raman Spektroskopie. Der Peak der freien Carboxy-Gruppe von TPA (1632 cm^{-1}) verlagert sich nach der de-Protonierung und resultiert in zwei Peaks bei 1604 und 1398 cm^{-1} in der Gegenwart von Triethylamin (Verhältnis 1:5). Diese Verschiebung wurde verwendet, um die Reinheit von TPA nach den unterschiedlichen Hydrolyse-Prozessen zu analysieren

1

Aim of the thesis

It is common to refer to Clothing industry as “traditional industry” since it is one of the oldest sectors of industrial development. This is the main reason which drive textile research to find more innovative productions and improvement of the product quality.

Textile and clothing industry represent a very heterogenous field, with its products mostly used either in domestic or in industrial applications. Primarily, clothes were produced from natural protein-based (wool and silk), natural cellulosic (cotton and linen). In the last century, thanks to the implement and introduction of chemical industry, a switch in apparel composition has been observed, especially after the discovery of polyesters and polyamide synthesis.

In Europe, textile and clothing sector has a turnover of around € 170 billion and employing about 2 million people, and still is undergoing in a profound transformation. European clothing industry is mostly dominated by small-medium size companies, where their process is still possible to be identified as conventional textile productions. This represent the driving main reason of research interest to produce new technologies for yarn and composite production. Finally, in the last decade the “smart textiles” concept was introduced in such system. This new approach involves the formulation of new fabrics able to respond, react, monitor and as well protect humans to a certain environment.

A big interest is observed for production of technical textile using natural and promptly available compounds, which provides “smart “properties to these materials and finally applied for medical implants, personal protection, or healthcare application for example.

Textile and Clothing industry, as well other manufacturing sectors, involves transformation of the raw material into the final valuable product, which also include a tremendous amount of chemicals and energy. For example, during fabric production, different steps a require a large amount dyeing, water and energy. On the other hand, the fast end-life of textile products increase the environmental concern of textile industry. More intensified restrictions in terms on energy efficiency, reduction of CO_2 emission and wastewater, bring this sector to the constant research of novel methodologies to combine cost efficiency with lower environmental impact.

Therefore, Circular economy concept shows the highest potential in terms of innovation and market potential. If it is also combined with Biotechnology, it can be provided new guidelines for industries for a cleaner production, more sustainable products which focus also on a better recycling.

Hereby, various strategies were investigated to achieve the following aims:

1- Development and improvement of enzymatic surface functionalization and further characterization of the reactive groups generated
2- Studies of coupling systems for immobilization of finishing agents (flame retardant and antimicrobial compounds) and determination of their properties with different analytics
3- Investigation of enzymatic degradation of man-made polymers (optimal enzyme/substrate and mass transfer ratios)
4- Evaluation of release products and potential conversion into value-added products
5- Combination of chemical/enzymatic approach for synthetic polyester degradation and evaluation of monomer purity

Introduction
(Bioprocess of polyesters)

2

2.1 Textile functionalization

The great potential of fibre processing is the ability to produce highly purposed-targeted materials. This process can start at the fibre level where different additive and/or finishes are added during fibre or filament production leading different properties to the same type of fibre[1], [2]. Then, textile finishing chemicals are used to convert a basic fabric into a technical textile with a novel functional property. Traditionally, many of the functional properties given to textiles are achieved at the final finishing stage, where the chemical treatment of the fibres changes their appearance and improves their functional and comfort properties. Such high-performance fabrics require an activated surface prior the functionalization with the textile chemical finishing[3] [4].

Unlikely natural fibres, most of synthetic polymers (i.e. polyesters and polyamides) used in textile application show high hydrophobicity, which is also responsible of the reduced possibility of finishing agent applications (such antistatic or antimicrobial agents and dyes), due to minimal presence of reactive groups on polymer surface[5], [6]. Different methodologies have been investigated for increasing the hydrophilicity of such polymers. Chemical treatments, in combination with high temperatures are the most well-known processes. In particularly alkaline treatment performed with 4-20 % alkaline solution (NaOH or KOH)[7], phase catalyst is performed in presence of titanium[8], while acid hydrolysis involves high concentration of mineral acid[9]. Such treatments are very costly, and on the other hand, toxic while different neutralization and purification steps are needed. Furthermore, chemical processes are affected from a mechanism “all or nothing”,

where the adsorption of high concentrations (as NaOH) does not only affect the polyester surface but also the bulk structure of the polymeric chain, resulting into pitting corrosion and reduced tensile strength. An alternative developed for surface modification are plasma treatments. These methods are rather expensive and difficult to control on non-planar surfaces. Moreover, the non-specific behaviour of this process can cause ageing of the polyester, as possible results for the rearrangement and different orientation of the polar groups. is also responsible of the reduced possibility of finishing agent applications (such antistatic or antimicrobial agents and dyes, due to minimal presence of reactive groups on polyester surface. The strong interest of new sustainable chemistry technologies increased since the beginning of the twenty-first century. In this sense, biotechnologies proved to be a useful resource of tool and methodologies for polymer chemistry applications. In textile industry, “green processes“ are already applied for laundry and design of biodegradable and reusable fibres. The reason of such strong influence is mainly correlated to the widespread diversity of microorganisms (bacteria and fungi) and their relative enzymes, which can find a broad range of application for both natural and synthetic fibres [4]. Enzymatic polymer functionalization and hydrolysis take advantages from the milder reaction conditions, high specificity/selectivity and moreover less damages over the chemical methods, as mentioned before.

2.1.1 Poly(ethylene terephthalate) (PET)

Among these different polymer[10] PET (also commonly termed polyester) is considered as one of the most important manmade polymers. The chemical structure of polyesters is characterized by the presence of an ester group. Synthesis of polyesters is achieved by a polycondensation of molecules containing both a carboxylic acid and an alcohol group or from a polycondensation between a dicarboxylic acid and a diol. Linear polyesters were first synthetized by Wallace Carothers in 1928, which discovered that these polymers can be used for fibres production. Advancing the research Carothers in 1941, used terephthalic acid (TPA) (as aromatic dicarboxylic acid) and ethylene glycol (as diol) into a polycondensation reaction to synthetize Poly(ethylene terephthalate) (PET). In the first step, TPA reacts with ethylene glycol at a temperature between 240 °C and 260 °C and

pressure between 300 and 500 KPa. The second reaction is trans-esterification reaction where dimethyl terephthalate (DMT) is reacted with EG at 150 °C. The output of this reaction is bis(hydroxylethyl) terephthalate (BHET), which is further polymerized to a degree of carboxylation of up to 30. Further, the polycondensation continues at 290 °C and 50-100 KPa until a degree of polymerization of 100 is reached (**Figure 1**).

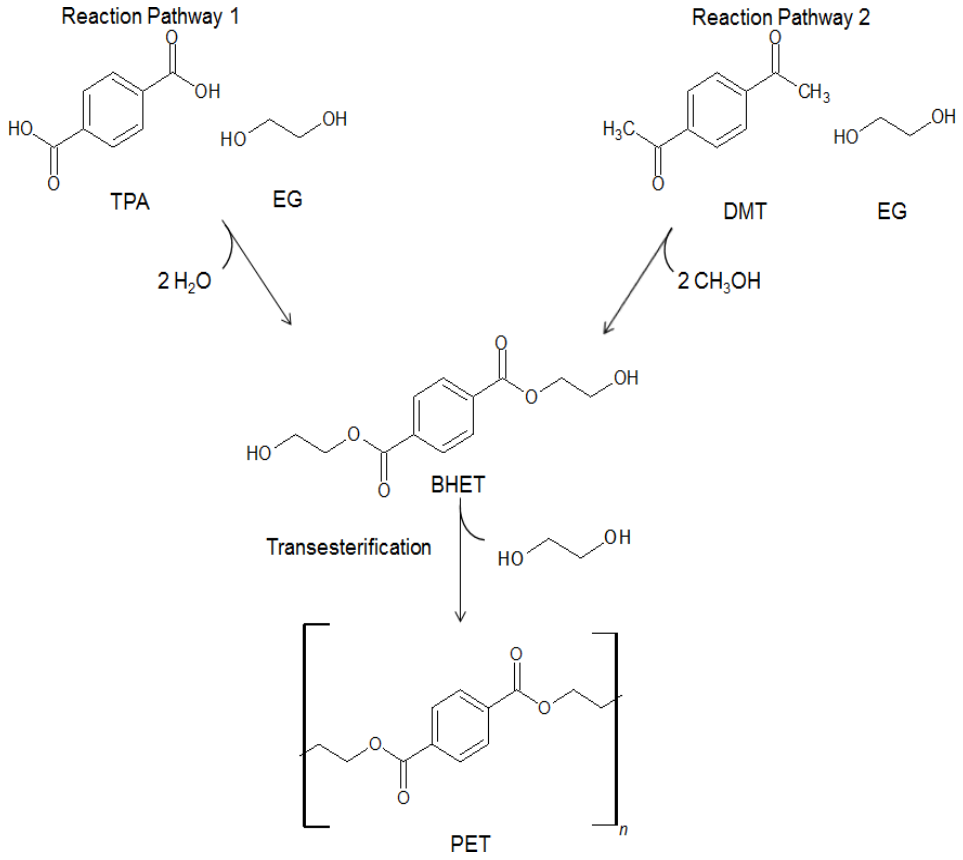

Figure 1 Chemical synthesis of Poly(ethylene terephthalate)

Enzymatic functionalization of PET

In nature, most reactions are catalysed by enzymes to run at mild conditions like temperature and pH [10]. Polymers, like polyesters present in fruit shells (i.e. cutin) are first hydrolysed by extracellular enzymes from bacteria and fungi before the building block are transported into the microbial cells. Esterases belong to *α/β* fold hydrolases representing the largest protein family, including epoxy-hydrolase, dehalogenase, amidase, cutinase and lipase. The common domain consists of *β*-strands connected by

α-helixes. Furthermore, the catalytic triad involves a nucleophile (serine, cysteine or aspartic acid) positioned after *β*5, an acid residue (aspartate) after *β*7 and a highly conserved histidine located after the last *β*-strand [11]. The nucleophilic amino acid is in a sharp turn named as “nucleophilic elbow” and identifies by the conservative sequence G-X-S-X-G. The arrangement of the nucleophilic elbow gives a contribution to the formation of oxyanion-binding site, which is required to stabilize the transition during the hydrolysis reaction (**Figure 2**).

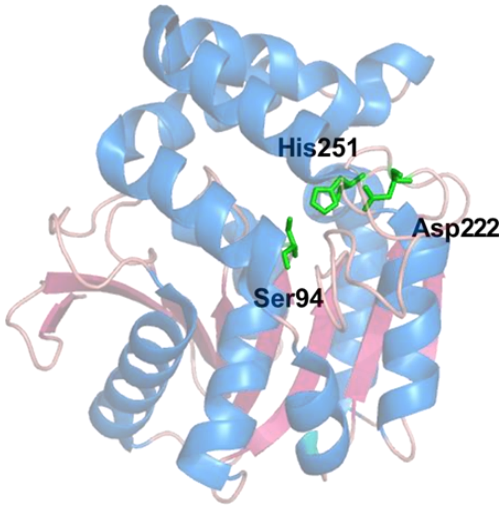

Figure 2 Structure of α/β hydrolase from *Pseudomonas fluorescens*, PDB ID: 1VA4. Red: beta sheet, blue: alpha helix, green: amino acids from catalytic triade (Ser94, Asp222, His251)

Lipase (EC number 3.1.1 and EC number 3.1.4) is an enzyme capable of performing fat hydrolysis, transforming triglycerides into glycerol and fatty acids, in the lipolysis process. Different lipases were characterized and studied for polyester functionalization[12]. Moreover, this subgroup of esterases contains a typical domain defined as “lid”. This lid is made of α-helices that cover the catalytic domain and lead to a peculiar phenomenon known as “interfacial activation”. This results in lower accessibility towards polymeric structures. In contrast, improving of lipase activity can be observed in presence of water-oil, like in presence of surfactants[13], [14] (**Figure 3A**)**.** Cutinases (or cutin-hydrolases) are extracellular degradative enzymes produced by plant pathogenic fungi. Their main role is to decompose cutin (a polyester composed of hydroxy and hydroepoxy fatty acids) facilitating fungus penetration through the cuticle[15], [16] (**Figure 3B**).

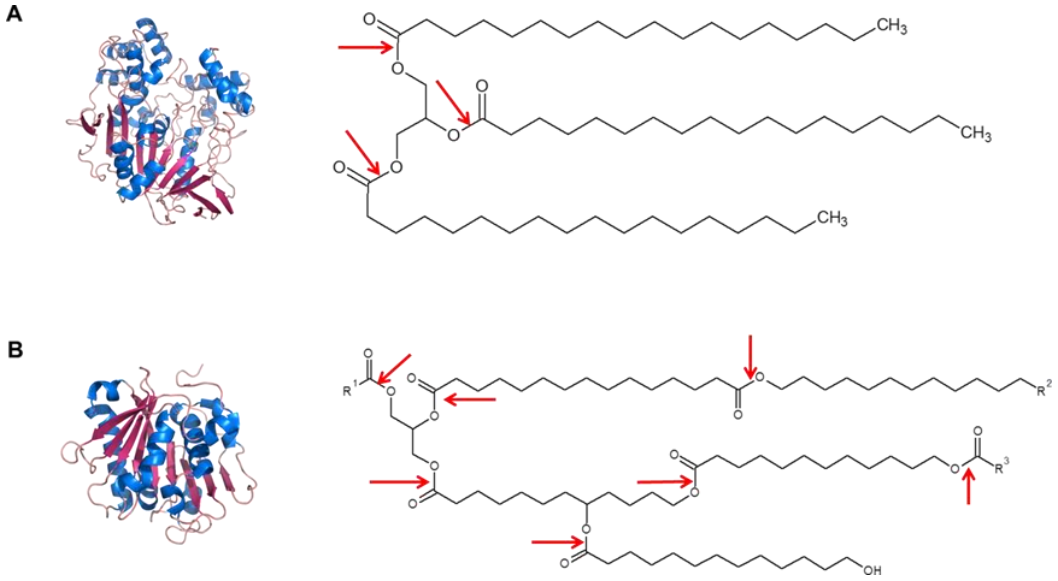

Figure 3 A) *Candida rugosa* Lipase (open lid structure) PDB ID: 1CRL and chemical structure of stearin (substrate of lipase). B) *Thermobifida cellulosilytica* Cutinase1 PDB ID: 5LUI and chemical structure of cutin (substrate of cutin)

As described above, PET shows different crystallinity degrees while higher enzymatic hydrolysis is detected at temperature close to the glass transition (Tg) of PET (65 °C)[17]. At this temperature, the PET amorphous region is more flexible and susceptible to enzymatic cleavage. On the other hand, at this operative temperature higher enzyme stability is required. However, a thermostable LC-cutinase was hydrolyzed around 25% of low crystalline PET for 24 hours at 70°C. a complete degradation of lower crystalline polyester occurs, also, with *Humicola insulens* cutinase incubation, after 96 hours at 70 ° C[18]. Both results demonstrate that crystalline regions of PET can be hydrolyzed. The ultimate goal of biotechnologist is to understand how enzymes work mechanistically and determine their properties, such as stability. Bivalent metal ions, such as calcium and magnesium (Ca^{2+}- Mg^{2+}) enhanced the thermostability of different esterases from actinomycetes resulting in an increasing of PET depolymerization[19]–[21]. Furthermore, the substitution of the metal-binding site with a salt brigde of disulphur bond in TfCut2 from *Thermobifida fusca* KW3 was allowed degradation of PET at 70 °C even in absence of bivalent ions. The activity of cutinase is also promoted by phosphate anions with concentration up to 1 M[22]. In order to reduce the product inhibition effect, PET hydrolysis

was performed in an enzyme reactor coupled with ultrafiltration membrane, where released products ad MHET and BHET were removed. This resulted as 1.7 –fold higher amount of hydrolysis within 24 hours of reaction. In a similar way, synthetic polymer was incubated with a dual enzyme reaction system composed of a polyester hydrolase and the immobilized TfCa from *Thermobifida fusca* KW3, giving two times higher amount of products obtained without TfCa. In this enzyme coupled system the immobilized enzyme has the role to reduce the product inhibition, hydrolyzing MHET and BHET into the monomer[23]. The same process was performed with other two different esterases: HiC and *Candida Antarctica* Lipase B (CalB) with an increasing of reaction of 7.7 fold in the yield of TPA[24]. Since cutinases operate only on the polymer surface, the adsorption of such catalyst represents a crucial factor[25]. Hydrophobins are small proteins secreted by the rodlet of layer of fungi in order to prevent microorganisms attack[26]–[28]. Hydrophobins contain 8 cystein residues responsible for their adsorption onto hydrophobic surfaces. The class I hydrophobin are from *Tricoderma reesei* (RolA) while the class II was defined from Aspergillus oryzae (HBF II), both were reported to improve the hydrolytic activity of enzymes on synthetic polymers. As reported from Espino-Rammer[29], in the presence of the class II of hydrophobins (HFB4 and HFB7) the enzymatic activity towards PET has been 2.5 higher than without. In nature, many polymer active enzymes carry so-called substrate binding domains connected with the catalytic domains. Cellulases show carbohydrate-binding modules (CBMs)[30], increasing the concentration of the enzyme in a small subarea of polymer and enhancing the cellulose degradation. Another example is given by the Polymer-binding domain (PBM) present in the polyhydroxyalcanoate depolymerase from *Alcaligenes feacalis* for it adsorption onto the polymer[31]. Taking inspiration from such natural process, cutinase 1 from *Thermobifida cellulosilytica* (Thc_Cut1) was fused with PBM, where 11-fold higher activity on PET was demonstrated. In the same way, the same Thc_Cut1 was fused with hydrophobins from *Tricoderma spp*[32]. Such variants of enzymes released 16 times higher amounts of products in comparison with wild type enzyme. Some regions present on the enzyme surface are also responsible for the interaction of the catalyst with the polymer. Therefore, exchanges of amino acids present on the surface of the esterase from

T.alba from Est119 to more hydrophobic residues lead to enhanced thermal stability and activity towards polyester[33]. In the work of Herrero-Acero[34], the role of specific amino acids located on the enzyme surface from the two homologous cutinases from *Thermobifida cellulosylitica* (Thc_Cut1 and Thc_Cut2) was demonstrated. A double substitution (R29N_A30V) from Thc_Cut1 to Thc_Cut2 led to an improvement of the second esterase, which was even higher than the native Cut1[35].In addition enzyme engineering, physical strategies were able to increase the efficiency of esterase towards poly(ethylene terephthalate) modification. In this sense, the use of ultrasound energy represents a process which greatly increases the enzymatic activity which was demonstrated for different classes of enzymes. In the work from Pellis, it was shown that after 30 min of sonication, Thc_Cut1 released 3.3 fold higher amounts of terephthalic acid[36].

2.1.2 Nylon 6

Nylon 6 is produced by a polymerization reaction which is initiated with the ring opening of caprolactam (CL) by the addition of water. In this reaction aminocaproic acid is produced to a certain extend. When a certain concentration of aminocaproic acid has been produced, further CL units are linked to the already growing chain to produce a polymer with 2 or more repeats. The last step is a condensation reaction, where two chains which have both, amine and carboxylic groups, react to form an amide linkage. The whole reaction is performed at a temperature between 240 and 270 °C (**Figure 4**).

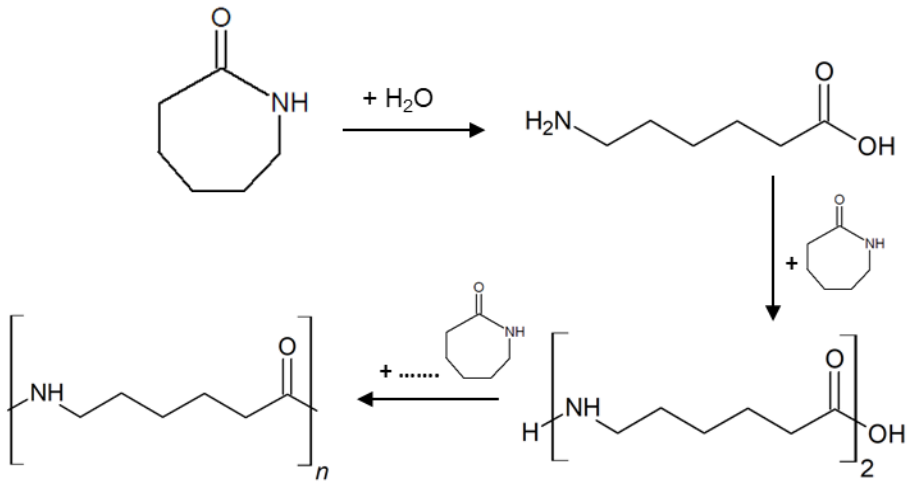

Figure 4 Synthesis of Nylon 6 via caprolactam

Enzymatic treatment of PA

The applications of nylon 6 are quite similar to the ones of PET but nylon fibres play a more important role in the textile industry. Due to its properties like high strength, elasticity, abrasion resistance, dyability and shape holding, Nylon is used in clothing and home furnishing. It is most often produced as fibre and finds applications in socks, sporting goods, carpets and in upholstering of furniture. As well PET, textile materials made of polyamide are uncomfortable to wear due to low water permeability. In the last two decades, enzymatic functionalization of polyamide surface has been applied for improving their adhesion properties. The enzymatic hydrolysis of nylon fabric leads the breakage of the amide bond into resulting amino and carboxylic moieties. Therefore, the most used enzymes able to cleave amide bonds are proteases, amidases and cutinases. An alkali stable polyamidase was isolated from *Nocardia farcinica*[37] and directly applied to water insoluble polyamide oligomers. In the same way, a polyamidase from *Beavueria brongniartii*[37] was used to hydrolyze polyamide fibers. Cutinase have demonstrated the ability to functionalize nylon-substrate and fibers. In the work of Araujo *et al*, site-directed mutagenesis of *Fusarium solani* cutinase was performed in order to enlarge the active site and better accommodate the synthetic oligomers and polymers. Several of its variants

shown higher activity towards nylon substrate then the wild-type[38]. Through enzyme rational desing, *Humicola insol*ens cutinase and *Thermobifida cellulosylitica* cutinase 1 were engineered in order to improve the amidase activity and then cleaving synthetic amide containing polymers. Briefly, site directed mutagenesis was performed in order reallocate the water network adapted for the hydrogen bonds formations with substrate containing amide bonds. On the other hand, it resulted also in a reduced activity on PET[39]. In addition to hydrolases, different studies have been shown that oxidative enzymes can act on polyamide depolymerization. Manganese peroxide was able to modify PA 6 and PA 6,6 surfaces without reducing the fibre diameter. Moreover, Fujisawa *at al* investigated the laccase mediator system for nylon degradation, using 1-hydroxybenzotriazole (HBT) as mediator. They have shown that PA was hydrolysed after 2 days of treatment[40].

2.1.3 Flame retardant applications

In Europe, every year 2.0 – 2.5 million fires are reported resulting in about 25.000 fire deaths and about 500.000 fire injuries every year. Most of the incidents, about 80 %, occur in private homes were easy ignitable materials, like synthetic polymers, contribute to a fast fire spreading[41]. The application of flame retardants has the possibility to reduce the annual costs resulting from the fires. Flame-retardant compound (FRC) can be a potential material for fire extinguishing by acting as a flame-retardant compound and removing one of the three elements within the fire triangle (**Figure 5**).

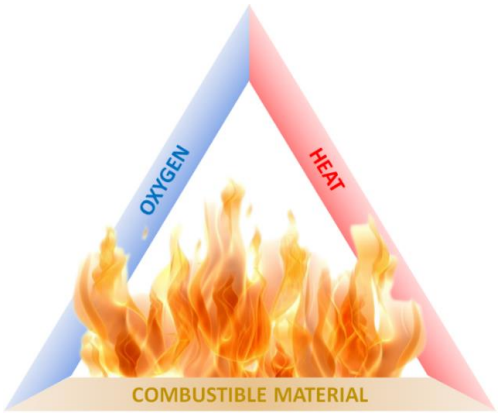

Figure 5 Fire triangle, showing the three elements necessary to start a fire

Flame retardants are compounds which are added to surfaces as pre-treatment or post-treatment of organic materials like textiles and plastics. Their purpose is the inhibition of combustion by blocking the ignition, interfering with the heating of surfaces as well as preventing the degradation of the material. Even when a fire already started, flame retardants can help to prevent the spreading of the flames and provide extra time to extinguish the fire in the early stage of development[42].

The most often used inorganic flame retardants are metal hydroxides with aluminium and magnesium compounds like aluminium trihydrate (AlH_6O_3), bauxite (AlOOH) and magnesium hydroxide ($Mg(OH)_2$) , which are able to release water during endothermically degradation leading a cooling effect and dilution in the gas phase (**Figure 6A**) .The second class of FRC are chlorine and bromine compounds where their main reaction occurs in the gas phase. Briefly they remove H and OH radicals and therefore prevent further heat formation and thermal combustion (**Figure 6B**).

Fluorinated flame retardant compounds are the most often used for natural and synthetic fibres and fabrics. Their main mode of action is during the solid phase of combustible material in which the phosphorus, when heated, reacts to form phosphoric acid. The phosphoric acid leads to char formation and inhibits the pyrolysis necessary for the growth of the flame. They can be applied to the materials during the polymerization of plastics or by coating of the surface, where they can be chemically bound. In combination with phosphorus containing flame retardants, often nitrogen compounds are applied. These compounds can release ammonia during combustion, which can lead to a dilution in the gas phase, resulting in the extinguishing of the flame (**Figure 6C**).

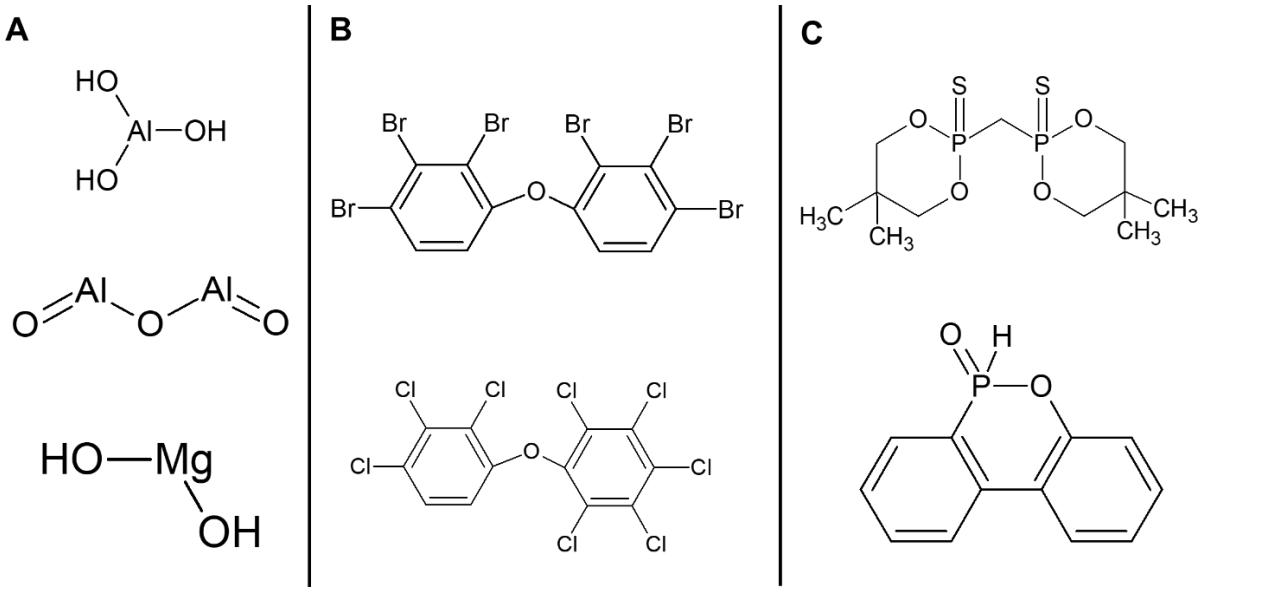

Figure 6 Chemical structure of FRCs. **A**) inorganic **B**) chlorinated and brominated **C**) fluorinated compounds

Due to the high toxicity and environmental impact the use of these kinds of flame retardants has drastically decreased. Furthermore, since 2003 the EU declared them as dangerous for the environment and very toxic to aquatic organism. As results of the negative impact of the mentioned FRC, the research of eco-friendly alternatives is needed.

DNA as flame retardant

The DNA double helix consists of two single strands of nucleotides. Each nucleotide contains one of the four nitrogen-containing bases adenine, guanine, cytosine or thymine. Together with a deoxyribose unit and a phosphate group, they built up the sugar phosphate backbone of the DNA[43]. The two antiparallel single strands are connected *via* hydrogen bonds to form the well-known α-helical structure with minor and major

groove in between. The availability of DNA has already become competitive to those of other chemicals as described by Grote and co-workers, which developed a large-scale method for the extraction of DNA out of salmon milt and roe sacks in waste products of Japanese fishing industry[44]. Furthermore, alternative sources of waste like spend brewer's yeast and vegetable waste have been proven to be potential sources for DNA and can present a cheap alternative to chemical flame retardants. Several studies already proved the potential of DNA as flame retardant for example on cotton and wool fabrics[45]. By comparing DNA with the commercially available flame retardants, DNA provides all requirements to be used as a flame-retardant compound in only one molecule (**Figure 7**). The nitrogen present in adenine, guanine, cytosine and thymine as well as deoxyribose units acting as carbon source, have the potential to release ammonia and carbon dioxide upon heating, which are non-combustible gases and can lead to self-extinguishing by displacing the oxygen. Furthermore, the sugar-phosphate backbone can release phosphoric acid during combustion, which leads to degradation and char formation and in further consequence to the barrier of the combustible material. Another advantage of using DNA is that a high purity is not necessary because also impurities like proteins can have positive effects due to their nitrogen content.

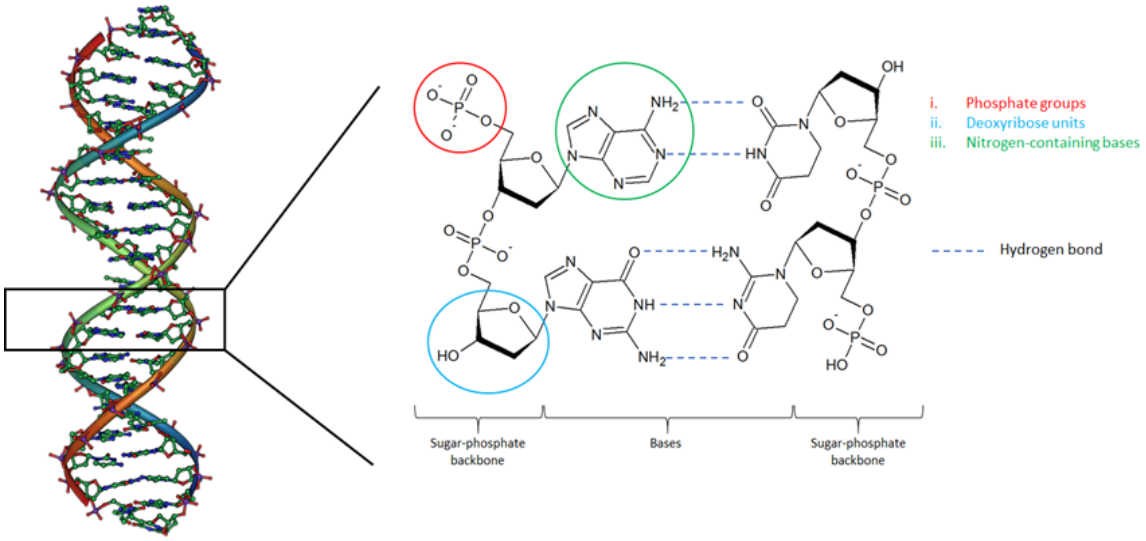

Figure 7 DNA chemical structure

2.1.4 Antimicrobial textiles

Due to their large surface area and ability to retain moisture, textiles are known as being conducive to microorganisms' growth, such as bacteria and fungi. The microorganism's growth on textiles causes a range of undesirable effects, including generation of unpleasant odours, reduction in mechanical strength, stains and discoloration and an increased likelihood of user contamination. On the other hand, the presence of microorganism on textile can also affect the customer; due to the growing public health awareness of the pathogenic effects, over the last few years, intensive research and development have been promoted in order to minimize or even eliminate microbial presence on textiles[46]. This microbial contamination is a great concern, mainly for textiles used in hospitals as medical devices or for health and hygienic care, but also in sports clothing, water purification systems, animal feed and the food industry. The infections acquired in hospitals may be caused by several species, such as *Escherichia coli*, *Klebsiella pneumonia*, *Pseudomonas aeruginosa* and *Acinetobacter baumannii.* Moreover, microorganisms in the presence of some antimicrobial agents may become resistant and the appearance of multi-drug-resistant bacteria is increasing at a worrying rate, being for the medical world one of the biggest challenges to face. Thus, the development of new and efficient antimicrobial treatments is still an important current topic of research, mostly regarding an alternative therapeutic strategy based on plant-derived antimicrobials[47]. Antimicrobial agents used in commercial textiles are biocides acting in different ways according to their chemical and structural nature and affinity level to certain target sites within microbial cells. Those different modes of action may be:

- Damage or inhibition of cell wall synthesis,
- Inhibition of cell membrane function,
- Inhibition of protein synthesis,
- Inhibition of nucleic acid synthesis (DNA and RNA)
- Inhibition of other metabolic processes

Nowadays, in pharmaceutical and medical fields nanotechnology is gaining a key role. Nanoparticles (NP) are materials in which the basic unit in three-dimensional space falls within the nanometre scale range (1-100nm), which present different many advantages[48]:

- High drug-loading
- Incorporation of drug with or without chemical cross-linking
- The possibility to bind specific ligand to surface

Protein-based nanoparticles

Nanoparticles have emerged as a novel alternative to overcome bacterial multidrug resistance encountered globally due to misuse of antibiotics. Using protein for particles preparation has the advantage to have low toxicity, either regarding metabolites or degradation products[49].

Use of nanoparticles as antimicrobial agents could overcome mechanisms of bacterial resistance as the microbicidal nature of nanoparticles result from direct contact with the bacterial cell wall, without the need to penetrate into the cell. It is suggested that multiple mechanisms may contribute to the antimicrobial mechanisms. The physical structure of the nanoparticle itself may have inherent antibacterial properties due to its membrane damaging abrasiveness[50].

Human serum albumin

Human serum albumin (HSA) is the most abundant blood plasma protein (60-65 % of total plasma protein) in the human body. It is synthesized in the liver by hepatocytes and then secreted into the blood stream where it has a half-life of around 19 days[51]. It has a molecular weight of approximately 66.5 kDa and in its sequence are present a large amount of acidic (Glu & Asp) and basic residues (Lys & Arg). This results in high water solubility and high binding property for small ligands, fatty acids, hormones caused, which is its natural role as depot and reporter protein. Based on these properties, HSA is an ideal candidate for the application in targeted drug delivery in form of nanoparticles[52].

Silk fibroin

Silk as a natural biomaterial produces from silk spiders (e.g. *Nephila clavipes*) or from insects such as silkworms such as *Bombyx mori* (mulberry silkworm). Generally, raw silk is composed of two strains of silk fibroin (SF) fibres covered with a layer of sericin. SF is a protein complex with molecular weight of around 2.3 MDa [52]. This protein complex consists of both heavy (H, 391.6 kDa) and light (L, 27.7 kDa). The heavy chain consists of crystalline, hydrophobic structure domains and amorphous, hydrophilic domains, resulting in an overall anionic molecule at neutral pH. The hydrophobic core contains a repetitive hexapeptide sequence, where a repetitive domain GAGAGS able to self-assemble into anti-parallel β-sheet structure. This secondary structure is highly crystalline and shows the capability to form intra- and intermolecular hydrogen bonds together with van der Waals interactions, giving a strong mechanical property. The content of β-sheet can be regulated by physical and chemical treatments, defining the high versatility of such polymer. As results of such properties, SF is already been investigate for drug delivery into nanofiber, films and implants.

Eugenol

Different studies define the antibacterial activity against gram-positive and gram-negative using either plant extracts of clove (*Caryophyllus aromaticus*) , basil (*Ocimun basilucum*), cinnamon bark (*Cinnamomum zeylanicum*) where the major bioactive component is eugenol (4-Allyl-2-methoxyphenol), which is an amphipathic hydroxyphenyl propene (**Figure 8**).

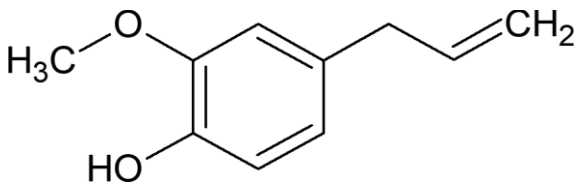

Figure 8 Chemical structure of eugenol

The antimicrobial activity of eugenol can be ascribed to the presence of a free hydroxyl group in the molecule, which cause the destabilization of the bacterial cell membrane. This hyper permeability is followed by leakage of ions and extensive loss of other cellular contents, and ultimately results in cell death. Eugenol also modified the fatty acid profile of the cell membrane of different bacteria[53].

2.2 Textile waste recycling

World fibre production has been rising continuously over last decades and a tremendous increase is expected in the near future. Referring to Fast Food, in the last decade is widely taking place the phenomenon so called “Fast Fashion”, which is trying to capture fashion trends and quickly delivering them to customers at cheap prices the textile industry created an environmental challenge. The average number of fashion collections each year has increased drastically. Companies, like H&M and Zara now offer between 12 and 24 collections per year, while in 2011 there were just five. Consumers more often loose a sense of value for clothing and exchange their wardrobe more frequently, either because it is “out of fashion” or damaged, as similar to Fast Food the materials used for these products most often are of cheaper and lower quality[1].

In 2007 the total consumption of textiles, including clothing and household textiles like bed sheets and carpets, in the EU was 9.55 million tonnes. A more recent estimation of the Waste and Resources Action Programme (WRAP UK) mentions 6.4 million tonnes of clothing in the EU in 2015[2]. At the end of their use more than 50 % of European textiles were disposed of through the mixed household waste eventually being landfilled or incinerated. While the data used in this article is from 2004 more recent studies indicate, though there is a large variance between countries, that the overall situation in the EU did not change much till today. On average only 36 % of textiles are collected separately. Germany has an exceptionally high share with 75 %, while in Italy only 11 % of clothes are collected separately.

A total of 738 billion tonnes of waste were treated within the EU in 2016, whereof 57 % were recycled, 24 % were landfilled and 18 % were incinerated or used for energy

recovery. Landfilling and incineration are least preferred of these waste treatment methods as many valuable resources and energy are thrown away. During incineration and energy recovery waste is combusted. The difference, as the name suggests, is that during combustion in Waste to Energy (WTE) plants energy is recovered in the form of heat and electrical energy, while during incineration no energy recovery takes place. Therefore, WTE plants are preferred over incineration. However, WTE plants are no complete alternative to landfills, as toxic substances are collected in bottom ashes and air filters which again are stored in landfills[54]. The circular material rate, a measure indicating how much material is recovered and reused in economy, steadily increased from 11 % in 2010 to 11.7 % in 2016. In textile industry specifically the rate of textile waste being reused in the production of new textiles lies beneath 1 %[55].

Many of today's textiles are no longer composed of one material but are blends of different fibres like cotton and polyester. In combining multiple materials, the properties of the fabric can be fine-tuned. Cotton is soft and brings a high-water absorbency to the fabric, strong PET fibres make fabrics more wrinkle resistant, contribute to textiles durability and lower the cost, due to their cheaper production. The combination of those properties makes polycotton the most common combination of synthetic and natural fibres. It is widely used in service textiles like bed sheet and towels where the lower moisture absorbency of polyester saves cost and energy in drying of garments.

But while textile blends have advantageous properties compared to pure materials, their end-of-life poses a new challenge. The mixed composition of most fabrics does not allow simple reprocessing as it would be able with pure fibres, therefore separation techniques are needed in order to recover the individual materials[56].

2.2.1 Protein based fibres

The worldwide wool retail sale per annum is around $ 80 billion with more than 2.1 million tonnes of greasy wool produces every year.

Wool fibres are made out of three different types of spindle-shaped cortical cells surrounded by a rectangular cell (cuticle), which is thick around 500 nm and represent the main component of the external layer of the fibre (**Figure 9**). About 90% of the cortical cells are composed by intermediate filaments (IFs) (40-65 KDa), where are located the membranes and remnants from cytoplasm and nucleus. The main building block are fibrous and low-sulfur α-keratins, which belong to the IFs proteins which. The last show helical structure, consisting of four α-helical segments (which are heptad) linked via a non-helical domain. On the other hand, matrix proteins are present high-sulfur proteins (HSPs)(11-26 KDa) or ultra-high sulfur proteins (UHSPs) (depending on their cysteine content) and in high glycine-tyrosine proteins (HGTPs) (6-9 KDa). These proteins are designed to surround the IFs at the last step of the developments of the follicle and interact to them via molecular disulphide bonds[57].

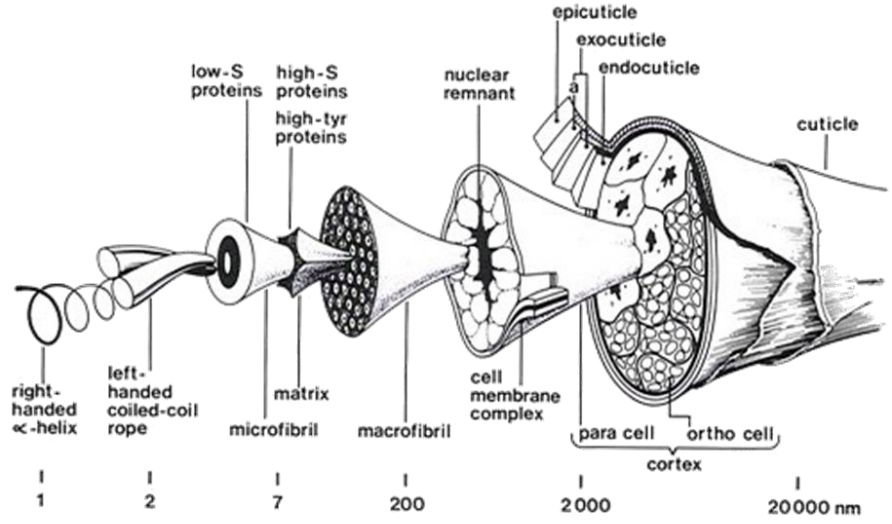

Figure 9 micro and macroscopic structure of wool

Enzymatic applications on wool fibres.

The applications of enzymes on protein-based materials is a process well established in the last twenty years in terms of surface activation, especially regarding enzymatic scouring and finishing. In particular, Hydrolases enzymes (like lipases and cutinases) have been used in wool production and leather industry to remove the lipidic surface from the materials and improving the wettability[58]. Moreover, different approaches with proteases were performed to achieve shrink resistance on wool. In terms of surface functionalization, the hydrolytic cleavage performed by protease is not only limited on fibre surface, therefore causing strength loss. From this point, different studies were involved into protease modification via chemical and enzymatic approaches[59], [60].

Proteases are grossly subdivided into two major groups, i.e., exopeptidases and endopeptidases, depending on their site of action. Exopeptidases cleave the peptide bond proximal to the amino or carboxy termini of the substrate, whereas endopeptidases cleave peptide bonds distant from the termini of the substrate. Based on the functional group present at the active site, proteases are further classified into four prominent groups, i.e., serine proteases, aspartic proteases, cysteine proteases, and metalloproteases. In terms of fibres applications, serine alkaline proteases are the most often used[61]. This class of enzyme can hydrolyze a peptide bond which has tyrosine, phenylalanine, or leucine at the carboxyl side of the splitting bond. The optimal pH of alkaline proteases is around pH 10, and their isoelectric point is around pH 9. Their molecular masses are in the range of 15 to 30 kDa. One of the weill known serine alkaline protease is Savinase™ (EC3.4.21.14) is secreted by the alkalophilic bacterium *Bacillus lentus* and is a representative of that subgroup of subtilisin enzymes with maximum stability in the pH range 7 to 10 and high activity in the range 8 to 12. It is therefore of major industrial importance for use in detergents[62].

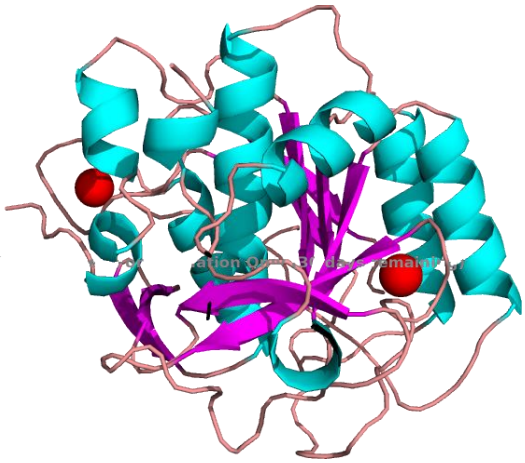

Figure 10 Savinase :3D structure PDB ID: 1SVN

2.2.2 Cotton

Cotton by far is the most produced natural fibre, and only second to polyester when considering all fibre types. Worldwide, 25.6 million tonnes of cotton were produced in 2018[2]. Cotton consists of 90 % cellulose and therefore is the purest natural form of cellulose. The non-cellulosic fraction of cotton contains proteins, pectins, waxes and other substances. The specific composition of cotton varies depending on the species and environmental conditions and has an influence on the fibre length. Higher quality cotton has fibre lengths between 25 and 65 mm, while lower quality fibres have lengths between 10 and 25 mm. The structure of cotton fibres is built up by multiple layers. Outermost is the wax-coated primary cell wall. Beneath several layers of secondary cell wall spiral around a channel called lumen, which transports a nutritious sap during fibre growth. As stated earlier, the main component of cotton is cellulose. Cellulose is a polysaccharide built up from repeating units of cellobiose. Cellobiose itself is a dimer consisting of two β1,4glycosically bound β-D-glucopyranose units[63] (**Figure 11**). The degree of polymerisation (DP) represents the number of glucose units aligned in a cellulose chain. Cellulose in the primary cell wall has a degree of polymerisation between 2000 and 6000. The secondary cell wall is made of cellulose of higher molecular weight with a degree of polymerisation of up to 14,000. Cellulose strains are directional as they exhibit one

reducing end, due to the reactive hemiacetal group, and one non-reducing end. Since each glucose unit contains three hydroxyl groups which can interact with neighbouring oxygen atoms, a tight network of inter- and intra-molecular hydrogen bonds holds the cellulose chains together, forming a strong and rigid crystalline structure. Depending on the orientation of cellulose chains different forms can be distinguished. In cellulose I, the chains are aligned parallel with all reducing ends pointing in the same direction. This form is found in naturally occurring cellulose. Cellulose II, on the other hand, is obtained by dissolving and regenerating cellulose I and occurs in fibres like viscose or Lyocell. In cellulose II chains are oriented with reducing and non-reducing ends alternating, which is called anti-parallel. Crystalline regions or varying length are intercepted by more loosely arranged, or amorphous, regions which are more susceptible to reactions than the tight crystalline structures. Cellulose is easily degraded by oxidising agents like hypochlorides, peroxides and acids like sulfuric acid while being recalcitrant towards alkaline treatment.

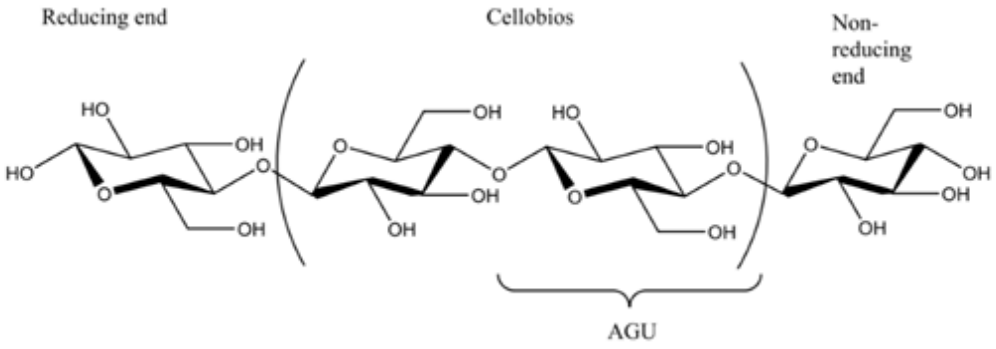

Figure 11 Cellulose structure

Enzymatic degradation of cellulose

Cellulases are enzymes capable of hydrolysing β-1,4-glycosidic bonds. Three major types of cellulases are necessary for the fully hydrolysis of cellulose to glucose:

- Endoglucanases (EC 3.2.1.4),
- Exoglucanases like exo-1,4-beta-glucosidases (EC 3.2.1.74) and cellobiohydrolases (EC 3.2.1.91)

- β-glucosidases or cellobiases (EC 3.2.1.21)

In general microorganisms produce multiple types of enzymes from each of the cellulase classes. *Tricoderma reesei*, for instance, is a filamentous fungus, known for more than 50 years for its capability to degrade cellulose, that produces two exoglucanases, five endoglucanases and two cellobiases[64]. Endoglucanases are responsible for rapidly decreasing cellulose's degree of polymerisation by randomly cutting cellulose in amorphous regions, creating new chain ends. The generation of new chain ends results in a synergism with exoglucanases. Exo-1,4-beta-glucosidases and cellobiohydrolases start the degradation of cellulose specifically at reducing or non-reducing chain ends, releasing glucose and cellobiose respectively. In Exoglucanases the active site in shape of a tunnel is formed by four loops in the case of cellobiohydrolases 1 (CBH1) and two loops in CBH2. Once CBH1 and CBH2 attached to cellulose chain ends they consecutively cleave multiple bonds before the enzyme dissociates. Most endo- and exoglucanases have cellulose binging modules (CBM) which help adhere to the polysaccharide. Commonly CBMs are attached to the catalytic domain through a flexible linker, while CBH1 has just one and EG3 lacks a CBM other enzymes contain multiple binding modules. The adherence of CBMs to cellulose is thought to be driven by van der Waals forces and interaction of polarised aromatic amino acids with the pyranose rings of glucose. The degradation of cellulose is finalised in another enzymatic cooperation as cellobiose, released through cellobiohydrolases, is hydrolysed to glucose by β-glucosidase[65](**Figure 12**). Moreover, some oxidative enzymes like polysaccharide monooxygenases (PMOs) and cellobiose dehydrogenases (CDHs) have been found that synergistically help to cleave the crystalline part of cellulose matrix.

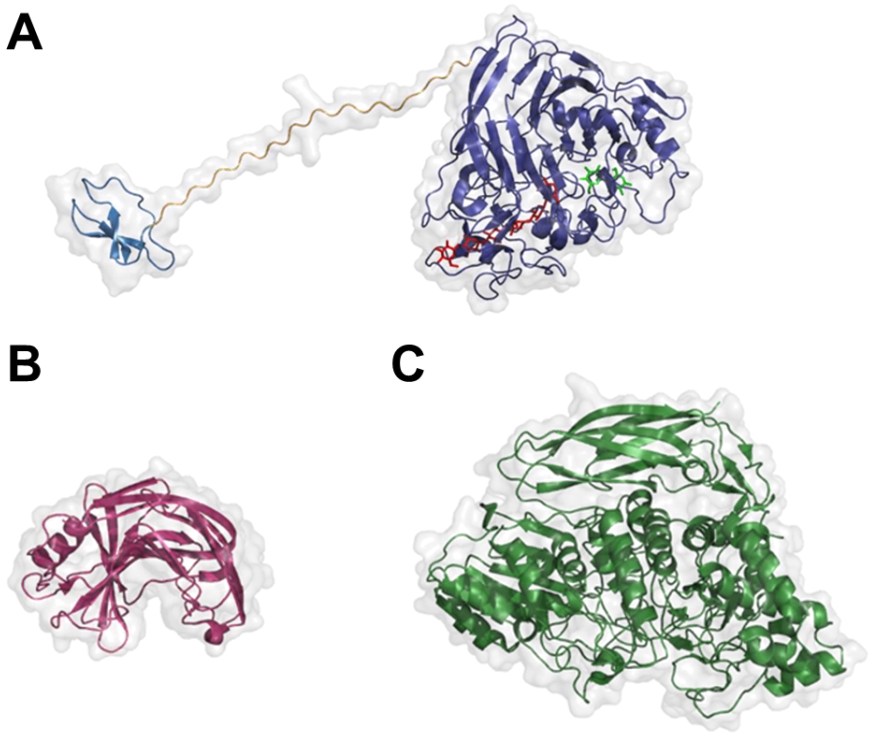

Figure 12 A)Exoglucanase 1 from T. reesei. Catalytic domain (dark blue) and cellulose binding module (light blue) are connected through a flexible linker (yellow). PyMOL with structures for the catalytic domain (7CEL) and CBM (1CBH) obtained from protein data base. **B**) structure of endoglucanase 3 (pink) and **C**) β-glucosidase 1 (green) from *T. reesei*; Structures were obtained from protein data base EG3: 1H8V; β-glucosidase: 3ZYZ. Rendered in PyMOL

2.3 Value-added products

The main goal of circular economy is to re-design waste materials into new valuable and usable products. Moreover, this process involves and promotes innovation through the value chain instead of relying only on the “end-life products” solution. Products obtained from enzymatic processes can potentially be applied as substitute to the conventional industrial processes or as starting point to produce new bio-based compounds, *via* fermentation processes for example.

Amino acids

The worldwide market of amino acids has greatly grown in the last decades due to the many applications of these products in different fields. Amino acids are used in feeds, food, parenteral and enteral nutrition, medicine, cosmetics and raw materials for the chemical industry[66], [67]. In last years, new bio-materials have been prepared from the protein waste stream and then recently proposed for packaging, active filtration of air and water and biomedical applications[68], [69].Peculiar attentions were invested into nanofibrous materials for medical applications, due to their high surface to volume ratio and high porosity, make them promising candidates for several applications such as filter membranes, wound dressing, cell-growth scaffolds, vascular grafts and drug deliver.

Glucose

Glucose, which is the monomer unit of cellulose in biomass, has gained increasing attention due to its abundance, environmental friendliness and wide distribution in nature. The efficient production of glucose from waste has great potential due to the rapid development of biorefinery. It is well established the process of production of biofuel from biomass-derived glucose *via Saccharomyces cerevisiae* fermentation. Besides as an alternative to fossil fuels, ethanol is an important platform chemical for the production of ethylene and ethylene glycol through chemical catalysis that are used for the production of polyethylene and poly(ethylene terephthalate).

Fermentation processes for production of bio-based chemicals and/or building blocks are strictly dependent of development of wild-type or genetically engineered microbial strains which are able to produce the final compounds with high efficiency and effective downstream separation. As reported from Pellis *et al*[15] ,different fermentation methodologies are already available for production of monomers for polyester synthesis.

PET monomers

The most common end products are PET’s monomers, purified terephthalic acid (TPA) and ethylene glycol (EG), the necessary building blocks to make new, virgin quality PET

resin. Thus, in order to obtain 100% bio-PET both precursors should be obtained from renewable sources[70]. As defined previously EG is already available on a large scale from biomass, that means the remaining monomer (TPA) is still produced from fossil sources. Para-xylene (PX), the main precursor of TPA, is traditionally obtained in large quantities cheaply from the catalytic reforming of crude oil (BTX – benzene, toluene and xylenes), then it represents a cheap method for TPA production. Due to strict request regarding the greenhouse emissions, different studies have been involved the production recycled PET (rPET) from recycled monomer[16], [71].

2.4 References

[1] N. M. Van Der Velden, M. K. Patel, and J. G. Vogtländer, “LCA benchmarking study on textiles made of cotton, polyester, nylon, acryl, or elastane,” *Int. J. Life Cycle Assess.*, vol. 19, no. 2, pp. 331–356, 2014.

[2] European technology Platform, “Towards a 4 th Industrial Revolution of Textiles and Clothing,” no. October, 2016.

[3] J. Allwood, S. Laursen, C. de Rodriguez, and N. Bocken, “Well dressed?: The present and future sustainability of clothing and textiles in the United Kingdom,” *J. Home Econ. Inst. Aust.*, 2015.

[4] G. M. Guebitz and A. Cavaco-Paulo, “Enzymes go big: surface hydrolysis and functionalisation of synthetic polymers,” *Trends Biotechnol.*, vol. 26, no. 1, pp. 32–38, 2008.

[5] A. Pellis *et al.*, “Biocatalyzed approach for the surface functionalization of poly(L-lactic acid) films using hydrolytic enzymes,” *Biotechnol. J.*, vol. 10, no. 11, pp. 1739–1749, 2015.

[6] A. Ortner *et al.*, “activated poly (lactic acid) surfaces †,” pp. 816–822, 2017.

[7] M. Y. Abdelaal, T. R. Sobahi, and M. S. I. Makki, “Chemical Degradation of Poly(Ethylene Terephthalate),” *Int. J. Polym. Mater.*, vol. 57, no. 1, pp. 73–80, 2008.

[8] M. Rahman and G. C. East, “Titanium Dioxide Particle-induced Alkaline Degradation of Poly(ethylene Terephthalate): Application to Medical Textiles,” *Text. Res. J.*, vol. 79, no. 8, pp. 728–736, 2009.

[9] T. Yoshioka, T. Sato, and A. Okuwaki, “Hydrolysis of waste PET by sulfuric acid at 150°C for a chemical recycling,” *J. Appl. Polym. Sci.*, vol. 52, no. 9, pp. 1353–1355, 1994.

[10] R. Wei and W. Zimmermann, “Microbial enzymes for the recycling of recalcitrant

petroleum-based plastics: how far are we?," *Microb. Biotechnol.*, vol. 10, no. 6, pp. 1308–1322, 2017.

[11] M. Holmquist, "Alpha Beta-Hydrolase Fold Enzymes Structures, Functions and Mechanisms," *Curr. Protein Pept. Sci.*, vol. 1, no. 2, pp. 209–235, 2000.

[12] G. Fischer-Colbrie, S. Heumann, S. Liebminger, E. Almansa, A. Cavaco-Paulo, and G. M. Guebitz, "New enzymes with potential for PET surface modification," *Biocatal. Biotransformation*, vol. 22, no. 5–6, pp. 341–346, 2004.

[13] T. Xu *et al.*, "Crystal structure of a mono- and diacylglycerol lipase from Malassezia globosa reveals a novel lid conformation and insights into the substrate specificity," *J. Struct. Biol.*, vol. 178, no. 3, pp. 363–369, 2012.

[14] A. Biundo *et al.*, "Characterization of a poly(butylene adipate-co-terephthalate)-hydrolyzing lipase from Pelosinus fermentans," *Appl. Microbiol. Biotechnol.*, vol. 100, no. 4, pp. 1753–1764, 2016.

[15] A. Pellis, E. Herrero Acero, V. Ferrario, D. Ribitsch, G. M. Guebitz, and L. Gardossi, "The Closure of the Cycle: Enzymatic Synthesis and Functionalization of Bio-Based Polyesters," *Trends Biotechnol.*, vol. 34, no. 4, pp. 316–328, 2016.

[16] C. Gamerith, M. Gajda, A. Ortner, E. H. Acero, G. M. Guebitz, and M. Ulbricht, "Enzymatic hydrolysis of poly(ethyleneterephthalate) used for and analysed by pore modification of track-etched membranes," *N. Biotechnol.*, vol. 39, pp. 42–50, 2017.

[17] I. Donelli, P. Taddei, P. F. Smet, D. Poelman, V. A. Nierstrasz, and G. Freddi, "Enzymatic surface modification and functionalization of PET: A water contact angle, FTIR, and fluorescence spectroscopy study," *Biotechnol. Bioeng.*, vol. 103, no. 5, pp. 845–856, 2009.

[18] Å. M. Ronkvist, W. Xie, W. Lu, and R. A. Gross, "Cutinase-Catalyzed hydrolysis of poly(ethylene terephthalate)," *Macromolecules*, vol. 42, no. 14, pp. 5128–5138, 2009.

[19] J. Then *et al.*, "Ca^{2+} and Mg^{2+} binding site engineering increases the degradation of polyethylene terephthalate films by polyester hydrolases from Thermobifida fusca," *Biotechnol. J.*, vol. 10, no. 4, pp. 592–598, 2015.

[20] P. Schmidt, M. R. Fernandez, J. M. Pastor, and J. Roda, "Study of the conformations of poly(ε-caprolactam) and poly(ε-caprolactam)-polybutadiene block copolymers by FT i.r. spectroscopy with photoacoustic detection and by micro-Raman confocal spectroscopy," *Polymer (Guildf).*, vol. 38, no. 9, pp. 2067–2075, 1997.

[21] T. Miyakawa, H. Mizushima, J. Ohtsuka, M. Oda, F. Kawai, and M. Tanokura, "Structural basis for the Ca2+-enhanced thermostability and activity of PET-degrading cutinase-like enzyme from Saccharomonospora viridis AHK190," *Appl. Microbiol. Biotechnol.*, vol. 99, no. 10, pp. 4297–4307, 2015.

[22] J. Schmidt *et al.*, "Effect of Tris, MOPS, and phosphate buffers on the hydrolysis of

polyethylene terephthalate films by polyester hydrolases," *FEBS Open Bio*, vol. 6, no. 9, pp. 919–927, 2016.

[23] M. Barth *et al.*, "A dual enzyme system composed of a polyester hydrolase and a carboxylesterase enhances the biocatalytic degradation of polyethylene terephthalate films," *Biotechnol. J.*, vol. 11, no. 8, pp. 1082–1087, 2016.

[24] A. Carniel, É. Valoni, J. Nicomedes, A. da C. Gomes, and A. M. de Castro, "Lipase from Candida antarctica (CALB) and cutinase from Humicola insolens act synergistically for PET hydrolysis to terephthalic acid," *Process Biochem.*, vol. 59, pp. 84–90, 2017.

[25] W. R. Gombotz, G. H. Wang, T. A. Horbett, and A. S. Hoffman, "Protein adsorption to poly(ethylene oxide) surfaces.," *J. Biomed. Mater. Res.*, vol. 25, no. 12, pp. 1547–1562, 1991.

[26] M. B. Linder, G. R. Szilvay, T. Nakari-Setälä, and M. E. Penttilä, "Hydrophobins: The protein-amphiphiles of filamentous fungi," *FEMS Microbiol. Rev.*, vol. 29, no. 5, pp. 877–896, 2005.

[27] D. Santhiya, Z. Burghard, C. Greiner, L. P. H. Jeurgens, T. Subkowski, and J. Bill, "Bioinspired deposition of TiO2 thin films induced by hydrophobins," *Langmuir*, vol. 26, no. 9, pp. 6494–6502, 2010.

[28] M. Reger, T. Sekine, T. Okamoto, and H. Hoffmann, "Unique emulsions based on biotechnically produced hydrophobins," *Soft Matter*, vol. 7, p. 8248, 2011.

[29] L. Espino-Rammer *et al.*, "Two novel class ii hydrophobins from Trichoderma spp. Stimulate enzymatic hydrolysis of poly(ethylene terephthalate) when expressed as fusion proteins," *Appl. Environ. Microbiol.*, vol. 79, no. 14, pp. 4230–4238, 2013.

[30] L. Chen *et al.*, "Specificity of O-glycosylation in enhancing the stability and cellulose binding affinity of Family 1 carbohydrate-binding modules," *Proc. Natl. Acad. Sci.*, vol. 111, no. 21, pp. 7612–7617, 2014.

[31] A. Biundo, D. Ribitsch, and G. M. Guebitz, "Surface engineering of polyester-degrading enzymes to improve efficiency and tune specificity," *Appl. Microbiol. Biotechnol.*, vol. 102, no. 8, pp. 3551–3559, 2018.

[32] D. Ribitsch *et al.*, "Enhanced cutinase-catalyzed hydrolysis of polyethylene terephthalate by covalent fusion to hydrophobins," *Appl. Environ. Microbiol.*, vol. 81, no. 11, pp. 3586–3592, 2015.

[33] U. Thumarat, R. Nakamura, T. Kawabata, H. Suzuki, and F. Kawai, "Biochemical and genetic analysis of a cutinase-type polyesterase from a thermophilic Thermobifida alba AHK119," *Appl. Microbiol. Biotechnol.*, vol. 95, no. 2, pp. 419–430, 2012.

[34] E. Herrero Acero *et al.*, "Enzymatic surface hydrolysis of PET: Effect of structural diversity on kinetic properties of cutinases from Thermobifida," *Macromolecules*,

vol. 44, no. 12, pp. 4632–4640, 2011.

[35] D. Ribitsch *et al.*, “Fusion of binding domains to Thermobifida cellulosilytica cutinase to tune sorption characteristics and enhancing PET hydrolysis,” *Biomacromolecules*, vol. 14, no. 6, pp. 1769–1776, 2013.

[36] A. Pellis, C. Gamerith, G. Ghazaryan, A. Ortner, E. Herrero Acero, and G. M. Guebitz, “Ultrasound-enhanced enzymatic hydrolysis of poly(ethylene terephthalate),” *Bioresour. Technol.*, vol. 218, pp. 1298–1302, 2016.

[37] E. Almansa, S. Heumann, A. Eberl, and F. Kaufmann, “Surface hydrolysis of polyamide with a new polyamidase from Beauveria brongniartii,” vol. 2422, 2009.

[38] R. Ara *et al.*, “Tailoring cutinase activity towards polyethylene terephthalate and polyamide 6 , 6 fibers,” vol. 128, pp. 849–857, 2007.

[39] V. A. Online, A. Biundo, R. Subagia, M. Maurer, D. Ribitsch, and G. M. Guebitz, “Switched reaction speci fi city in polyesterases towards amide bond hydrolysis by enzyme engineering †,” pp. 36217–36226, 2019.

[40] M. Fujisawa, H. Hirai, and T. Nishida, “Degradation of Polyethylene and Nylon-66 by the Laccase-Mediator System,” vol. 9, no. 3, pp. 103–108, 2002.

[41] F. Statistics, M. Academy, and S. F. Service, “World fire statistics,” 2006.

[42] J. Alongi, R. A. Carletto, A. Di Blasio, F. Carosio, F. Bosco, and G. Malucelli, “DNA: a novel, green, natural flame retardant and suppressant for cotton,” *J. Mater. Chem. A*, vol. 1, no. 15, p. 4779, 2013.

[43] J. G. Grote *et al.*, “DNA-based materials for electro-optic applications: current status,” vol. 5934, p. 593406, 2005.

[44] Z. H. Yang, Y. Xiao, G. M. Zeng, Z. Y. Xu, and Y. S. Liu, “Comparison of methods for total community DNA extraction and purification from compost,” *Appl. Microbiol. Biotechnol.*, vol. 74, no. 4, pp. 918–925, 2007.

[45] J. Alongi *et al.*, “Caseins and hydrophobins as novel green fl ame retardants for cotton fabrics,” *Polym. Degrad. Stab.*, vol. 99, pp. 111–117, 2014.

[46] K. S. Huang, C. H. Yang, S. L. Huang, C. Y. Chen, Y. Y. Lu, and Y. S. Lin, “Recent advances in antimicrobial polymers: A mini-review,” *Int. J. Mol. Sci.*, vol. 17, no. 9, 2016.

[47] S. Kalia, K. Thakur, A. Celli, M. A. Kiechel, and C. L. Schauer, “Surface modification of plant fibers using environment friendly methods for their application in polymer composites, textile industry and antimicrobial activities: A review,” *J. Environ. Chem. Eng.*, vol. 1, no. 3, pp. 97–112, 2013.

[48] J. Li *et al.*, “Recent advances in targeted nanoparticles drug delivery to melanoma,” *Nanomedicine Nanotechnology, Biol. Med.*, vol. 11, no. 3, pp. 769–794, 2015.

[49] L. P. Herrera Estrada and J. A. Champion, “Protein nanoparticles for therapeutic protein delivery,” *Biomater. Sci.*, vol. 3, no. 6, pp. 787–799, 2015.

[50] C. Tallian *et al.*, “Lysozyme-Responsive Spray-Dried Chitosan Particles for Early Detection of Wound Infection,” *ACS Appl. Bio Mater.*, vol. 2, no. 3, pp. 1331–1339, 2019.

[51] N. Lomis, S. Westfall, L. Farahdel, M. Malhotra, D. Shum-Tim, and S. Prakash, “Human serum albumin nanoparticles for use in cancer drug delivery: Process optimization and in vitro characterization,” *Nanomaterials*, vol. 6, no. 6, 2016.

[52] C. Tallian *et al.*, “Structural insights into pH-responsive drug release of self-assembling human serum albumin-silk fibroin nanocapsules,” *Eur. J. Pharm. Biopharm.*, vol. 133, pp. 176–187, Dec. 2018.

[53] A. Marchese *et al.*, “Antimicrobial activity of eugenol and essential oils containing eugenol: A mechanistic viewpoint,” *Crit. Rev. Microbiol.*, vol. 43, no. 6, pp. 668–689, 2017.

[54] F. Cucchiella, I. D’Adamo, and M. Gastaldi, “Sustainable management of waste-to-energy facilities,” *Renew. Sustain. Energy Rev.*, vol. 33, pp. 719–728, 2014.

[55] V. J. Boiten, S. L.-C. Han, and D. Tyler, “Circular economy stakeholder perspectives: Textile collection strategies to support material circularity,” *Resyntex*, 2017.

[56] F. Quartinello *et al.*, “Highly Selective Enzymatic Recovery of Building Blocks from Wool-Cotton-Polyester Textile Waste Blends,” no. 3, 2018.

[57] J. E. Plowman, “Proteomic database of wool components,” *J. Chromatogr. B Anal. Technol. Biomed. Life Sci.*, vol. 787, no. 1, pp. 63–76, 2003.

[58] Q. Wang, X. Fan, Y. Hu, J. Yuan, L. Cui, and P. Wang, “Antibacterial functionalization of wool fabric via immobilizing lysozymes,” *Bioprocess Biosyst. Eng.*, vol. 32, no. 5, pp. 633–639, 2009.

[59] J. Shen, M. Rushforth, A. Cavaco-Paulo, G. Guebitz, and H. Lenting, “Development and industrialisation of enzymatic shrink-resist process based on modified proteases for wool machine washability,” *Enzyme Microb. Technol.*, vol. 40, no. 7, pp. 1656–1661, 2007.

[60] H. B. M. Lenting, M. Schroeder, G. M. Guebitz, A. Cavaco-Paulo, and J. Shen, “New enzyme-based process direction to prevent wool shrinking without substantial tensile strength loss,” *Biotechnol. Lett.*, vol. 28, no. 10, pp. 711–716, 2006.

[61] C. G. Kumar and H. Takagi, “Microbial alkaline proteases: From a bioindustrial viewpoint,” *Biotechnol. Adv.*, vol. 17, no. 7, pp. 561–594, 1999.

[62] C. Betzel, S. Klupsch, G. Papendorf, S. Hastrup, S. Branner, and K. S. Wilson, “Crystal structure of the alkaline proteinase Savinase™from Bacillus lentus at 1.4 Å

resolution," *J. Mol. Biol.*, vol. 223, no. 2, pp. 427–445, 1992.

[63] G. Buschle-Diller, S. H. Zeronian, N. Pan, and M. Y. Yoon, "Enzymatic Hydrolysis of Cotton, Linen, Ramie, and Viscose Rayon Fabrics," *Text. Res. J.*, vol. 64, no. 5, pp. 270–279, 1994.

[64] S. Vecchiato *et al.*, "Enzymatic Recycling of High-Value Phosphor Flame-Retardant Pigment and Glucose from Rayon Fibers," *ACS Sustain. Chem. Eng.*, p. acssuschemeng.7b03840, 2017.

[65] M. Dimarogona, E. Topakas, and P. Christakopoulos, "Cellulose Degradation By Oxidative Enzymes," *Comput. Struct. Biotechnol. J.*, vol. 2, no. 3, p. e201209015, 2012.

[66] P. Bhavsar, M. Zoccola, A. Patrucco, A. Montarsolo, G. Rovero, and C. Tonin, "Comparative study on the effects of superheated water and high temperature alkaline hydrolysis on wool keratin," *Text. Res. J.*, vol. 87, no. 14, pp. 1696–1705, 2017.

[67] M. Zoccola, A. Aluigi, and C. Tonin, "Characterisation of keratin biomass from butchery and wool industry wastes," *J. Mol. Struct.*, vol. 938, no. 1–3, pp. 35–40, 2009.

[68] A. Shavandi, A. E. D. A. Bekhit, A. Carne, and A. Bekhit, "Evaluation of keratin extraction from wool by chemical methods for bio-polymer application," *J. Bioact. Compat. Polym.*, vol. 32, no. 2, pp. 163–177, 2017.

[69] N. Eslahi, F. Dadashian, and N. H. Nejad, "An investigation on keratin extraction from wool and feather waste by enzymatic hydrolysis," *Prep. Biochem. Biotechnol.*, vol. 43, no. 7, pp. 624–648, 2013.

[70] M. Volanti *et al.*, "Terephthalic acid from renewable sources: Early-stage sustainability analysis of a bio-PET precursor," *Green Chem.*, vol. 21, no. 4, pp. 885–896, 2019.

[71] C. Gamerith *et al.*, "Enzymatic recovery of polyester building blocks from polymer blends," *Process Biochem.*, vol. 59, pp. 58–64, 2017.

3

Increased flame retardancy of enzymatic functionalized PET and Nylon fabrics *via* DNA immobilization

Published in: Frontiers in Chemistry (2019)
DOI: 10.3389/fchem.2019.00685

Felice Quartinello, Klemens Kremser, Sara Vecchiato, Herta Schoen, Robert Vielnascher, Leon Ploszczanski, Alessandro Pellis and Georg M. Guebitz[1]

Abstract

Poly(ethylene terephthalate) (PET) and nylon find their main applications in working clothes, domestic furniture and as indoor decoration (curtains and carpets). The increasing attention on healthy lifestyle, together with protection and safety, gained a strong interest in today's society. In this context, reducing the flammability of textiles has

been tackled by designing flame retardants (FRs) able to suppress or delay the flame propagation. Commercially available FRs for textiles often consist of brominated,

chlorinated and organo-phosphorus compounds, which are considered a great concern for human health and for the environment. In this study, Deoxyribose Nucleic Acid (DNA) was investigated as a green and eco-friendly alternative to halogen-containing FRs. DNA is in fact able to provide flame retardant properties due to its intrinsically intumescent building blocks (deoxyribose, phosphoric-polyphosphoric acid and nitrogen-containing bases). In a first step, anchor groups (i.e. carboxyl groups) for subsequent coupling of DNA were introduced to PET and nylon-6 fabrics *via* limited surface hydrolysis with *Humicola insolens* cutinase (HiC). Released monomer/oligomers were measured *via* HPLC (1 mM of BHET for PET and 0.07 mM of caprolactam from nylon after 72 h). In a next step, DNA immobilization on the activated polymers was studied by using three different coupling systems, namely: EDC/NHS, dopamine and tyrosine. DNA coupling was confirmed *via* FT-IR that showed typical bands at 1220, 970 and 840 cm^{-1}. The tyrosine/DNA coupling on nylon fabrics resulted to be the most effective as certified by the lowest burning rate and total burning time (35 s, 150 mm and 4.3 $mm*s^{-1}$ for the blank and 3.5 s, 17.5 mm and 5 $mm* s^{-1}$ for nylon/tyrosine/DNA) which was also confirmed by FT-IR and ESEM/EDS measurements. Thermogravimetric analysis (TGA) further confirmed that tyrosine/DNA coated nylon showed a lower thermal degradation between 450-625 °C when compared to the untreated samples.

Increased flame retardancy of enzymatic functionalized PET and Nylon fabrics *via* DNA immobilization

Graphical abstract

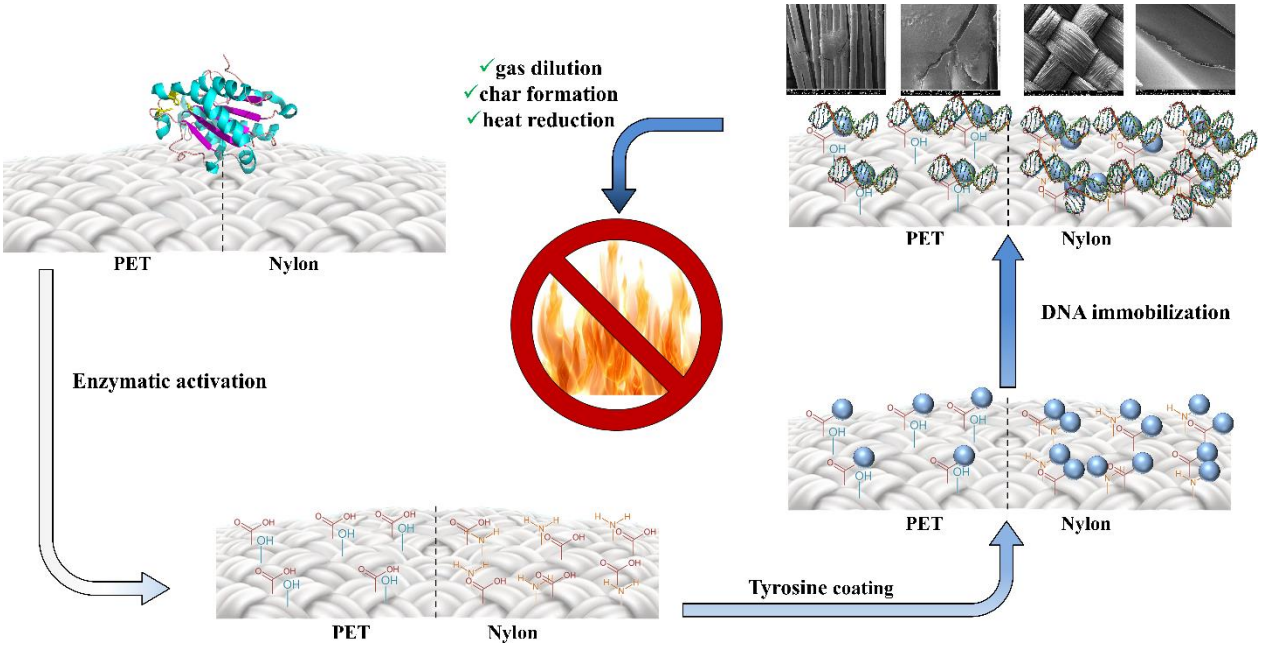

3.1 Introduction

Synthetic polymers, like poly(ethylene terephthalate) (PET) and nylon-6, are omnipresent in an average household (furniture, wall insulation, curtains, flooring, etc.) as well as in clothing. Within European fire brigade statistics, specially referring to these kinds of fibers and plastics, different studies confirmed that they greatly contribute to a quick flames spreading in case of fire, leading to major damages to humans and also high financial losses [1]. For this reason, flame retardant science gained a crucial role in textile and plastic manufacture in the last decades. Briefly, the application of Flame Retardant Compounds (FRC) prevent the ignition or lead to the self-extinguishing of the flame. FRC are added to the polymer surface as result of pretreatment or as post treatment [3]. The most widely used FRC are represented by inorganic or organic compounds, containing metal ions or halogenated atoms. Among the inorganic FRC, aluminum trihydrate (AlH_6O_3) and magnesium hydroxide ($Mg(OH)_2$) are the most prominently used in ceramic

surface treatment. During the fire propagation, these compounds have the property to release water during their endothermic degradation [4]. Within the class of halogenated flame retardants, chlorine and bromine-based compounds are the most widespread used because they are able to prevent the further heat propagation and thermal combustion. The last class of flame retardants comprises phosphorus-based flame retardants, often combined with nitrogen compounds. During the fire, these compounds release phosphoric acid (which leads to char formation) and ammonia (which causes a dilution in the gas phase) [5]. However, in the last years, several hazard impact studies of such FRC were reported, and together with the strict directives from EU community led to the ban of several halogenated FRC, since they show high toxicity for both human and animals [6]. As demonstrated by Watanabe [7],the major emission of brominated and chlorinated compounds occurs directly during production. Moreover, the amount of landfilled and incinerated textiles per years also constitutes a problem for the environment [8]. Most of the FRC are absorbed on surface material, therefore their leaching and consequently accumulation, cause major health risks also for marine environment and in the end also for human health due to their dietary.

The development of new and less toxic alternative FRC is definitively required. It has been demonstrated that natural compounds, like phytic acid and cyclo-dextrine [9], [10] may act as promising eco-friendly FRC for poly(lactic acid). Casein and hydrophobins have also shown FR potential, due to the their phosphoserine and cysteine content in their structures [11], releasing phosphoric acid, ammonia and sulfuric acid, which are able to reduce the fire spreading.

The DNA's double helix consists of two single strands of nucleotides. Each nucleotide contains one of the four nitrogen-containing bases adenine, guanine, cytosine or thymine. Together with a deoxyribose unit and a phosphate group they built up the sugar phosphate backbone of the DNA. The two antiparallel single strands are connected *via* hydrogen bonds to form the well-known α-helical structure with minor and major groove in between. Several studies have already proven the potential of DNA as flame retardant for example on cotton and wool fabrics using a layer by layer absorption [12]. By comparing DNA with the commercially available flame retardants, DNA provides all desired requirements to be

used as a flame-retardant compound. The nitrogen present in adenine, guanine, cytosine and thymine as well as deoxyribose units acting as carbon source, have the potential to release ammonia and carbon dioxide upon heating, which are non-combustible gases and can lead to self-extinguishing by displacing the oxygen. Furthermore, the sugar-phosphate backbone can release phosphoric acid during combustion, which leads to degradation and char formation and in further consequence to the barrier of the combustible material [12]. The availability of DNA has already become competitive to those of other chemicals as described by Grote and co-workers, which developed a large-scale method for the extraction of DNA out of salmon milt and roe sacks in waste products of japanese fishing industry [13]. Furthermore, alternative sources of waste like spend brewer's yeast [14] and vegetable waste [15] have been proven to be potential sources for DNA and can present a cheap and sustainable alternative to chemical flame retardants. Another advantage of using DNA is that a high purity is not necessary because also impurities like proteins can have positive effects due to their nitrogen content.

In this work, we investigated a covalent immobilization of DNA onto enzymatically activated PET and nylon-6. Therefore, after enzymatic, mild surface activation of both polymers, DNA was coupled using three different "natural-inspired" approaches, in order also to reduce the amount of chemical and biohazards compounds for human health and for the environment.

3.2 Materials and Methods

3.2.1 Chemicals, substrates and enzymes.

Poly(ethylene terephthalate) (PET) and polyamide 6 (nylon 6) fabrics, at thickness of 0.41±0.015 mm and weight of 240 ±12 g$(m^2)^{-1}$ were purchased from Goodfellow (Huntingdon, UK). All the other chemicals and solvents were purchased from Sigma-Aldrich (Vienna, Austria) at reagent grade and used without any further purification if not specified. The *Humicola insolens* cutinase (HiC) (CAS 9000-62-1) was purchased by Novozymes (Copenhagen, Denmark), and used without purification steps.

3.2.2 Biochemical characterization of HiC

Protein concentration was determined with the BIO-RAD Protein Assay Protocol (Bio-Rad Laboratories GmbH, Cat. No: 500-0006) using bovine serum albumin (BSA) as protein standard. Specifically, 10 µL of protein standard solution were added into the well of a 96 well plate (Greiner 96 well plate bottom transparent polystyrene). Afterwards, 200 µL of 1:5 diluted Bio-Rad reagent were added. The plate was incubated for 5 min at 21 °C and 300 rpm. The buffer (100 mM potassium phosphate pH 7) was used as blank. Relative protein absorption was measured at λ=595 nm, and the concentration was evaluated from the average of triplicates samples and blanks. Esterase activity assay was performed using *p*-nitrophenyl butyrate (*p*-NPB) as model substrate, as previously reported by Biundo et al. [16]. The increase of absorbance at 405 nm due to the releasing of *para*-nitrophenol was measured for 5 min, every 18 s with a plate reader (TECAN INFINITE M200). A blank was considered using 20 µL of buffer instead of enzyme solution. The activity was defined in unit (U), where 1 unit is considered as the amount of enzyme necessary to hydrolyze 1 µmol of substrate per minute under the given assay conditions.

3.2.3 Enzymatic functionalization of PET and nylon 6

3.2.3.1 Enzymatic functionalization

Prior to the enzymatic treatment, PET and nylon fabrics were cut into 1 cm^2 pieces with a hot wire and washed according to a commonly used washing protocol. Briefly, samples were washed with a Triton-X 100 solution (5 g/L w/v) followed by a washing step with Na_2CO_3 (100 mM) and mQ-H_2O as the last step. The complete washing procedure was performed at 60 °C, 30 min and 150 rpm on a thermo-shaker. Finally, samples were dried for 24 h at 21°C. Fabric samples were incubated in triplicates with three different concentrations of HiC (0.1, 0.25 and 0.5 mg/mL). The reaction was performed in 5 mL Eppendorf Tubes in a total volume of 4 mL potassium phosphate buffer (100 mM, pH 7). Enzymatic hydrolysis was performed for 24, 48 and 72 hours at 150 rpm and 60 °C. After

the incubation, samples were washed according to the washing protocol and dried for 24 h at 21 °C. For the upscale set up, samples with a size of 8 x 20 cm were incubated with an enzyme concentration of 0.25 mg/mL in a 2 L Erlenmeyer shaking flask for 72 h at 150 rpm at the same temperature.

To detect carboxyl (-COOH) and amino (-NH_2) groups on the surface of PET and nylon-6 fabrics after the enzymatic hydrolysis, a colorimetric method, using two different colour reagents, was tested. For the determination of -COOH groups, the basic dye Methylene Blue (MB) (**Figure S1A**) was used. Samples with the size of 1x1 cm were incubated with 1.5 mL MB (0.5 % in mQ-H_2O) at 80 °C for 60 min. After incubation, samples were washed according to the washing protocol and dried for 24 h at 21 °C [17].To detect -NH_2 groups on the surface of nylon, samples were treated with the acid dye Coomassie brilliant blue (CBB) (**Figure S1B**). The samples were incubated in 1.5 mL of CBB (0.5 mg/mL) in acid solution (mQ-H_2O/methanol/acetic acid 85:10:5 v/v, pH 2.2) for 5 minutes at 21 °C. To wash off the unbound dyes, samples were intensively rinsed with acid solution [18].
In order to determine the difference in colour intensity of the PET and nylon samples after the treatment with acid/basic dye, a ColorLite sph850 Spectrophotometer – Colour Measuring Instrument (Innovac, Germany) was used. This allows determination of the colour difference between the blank (no enzymatic treatment) and the treated samples using the L*, a* and b* coordinates. The interpretation of the measurement is based on the theory defined by the Commission Internationale de l`Eclairage (CIE), that two colours cannot be red and green or yellow and blue on the same time. The coordinates L*, a* and b* indicate the lightness, red/green and yellow/blue difference. Enzymatic treated PET and nylon samples were measured in triplicates (5 measurements per sample) against the non-treated blanks. To determine the colour difference, the delta (∆) L*, a* and b*should be calculated.

Equation 1

∆L^*=(L_sample^*-L_blank^*)

〖∆a〗^*=〖(a〗_sample^*-a_blank^*)

〖∆b〗^*=(b_sample^*-b_blank^*)

The values for ∆L*, a* and b* can be positive or negative. ∆L* indicates the difference in lightness (+ = lighter, - = darker), ∆a* the difference in red and green (+ = redder, - = greener) and ∆b* the difference in yellow and blue (+ = yellower, - = bluer).

3.2.3.2 High Performance Liquid Chromatography (HPLC)

The release products after enzymatic hydrolysis of PET and nylon were measured *via* HPLC. To remove protein impurities from the sample, a methanol precipitation step was performed with ice cold methanol (1:1 sample/methanol) [19]. Afterwards, samples were centrifuged at 12700 rpm for 15 min. at 4 °C (5920 R Centrifuge from Eppendorf) followed by an acidification step with 6 N HCl (6 µL per sample). Before pipetting the samples into the HPLC-vials, a filtration step with a 0.45 µM PA filter was performed. For the measurements of the PET released product (Ta), an Agilent LC-MS system was used with a Poroshell 120 column (InfinityLab Poroshell 120 EC-C18, 4.6 x 50 mm, 4 µM, Agilent), a flow of 0.35 mL/min and a non-linear gradient (**Table S1**). The released products were detected at 241 nm *via* UV-Vis spectroscopy. Caprolactam released from nylon-6 was measured using an Agilent LC-MS system with a phenomex® column (Aqua® 5 µm C18, 125 Å, LC Column, 250 x 4.6 mm) with an isocratic gradient (H_2O/MeOH, 60/40 [% v/v]) and flow of 0.5 mL/min for 50 min. Hydrolysates were measured at 210 nm *via* UV-Vis spectroscopy.

3.2.4 DNA immobilization on surface activated polymers

3.2.4.1 DNA characterization

To determine the length of the DNA molecules, an agarose gel electrophoresis was performed. A 3% agarose gel was produced by dissolving 1.2 g of agarose in 40 mL of 1x TAE-Buffer (50x Tris/Acetic Acid/EDTA (TAE), diluted with distilled deionized water) by heating in a microwave oven. For staining of the DNA, 4 µL nucleic acid gel stain were added to the gel. After casting the gel, it was allowed to solidify for 30 min and was put into a Mini-Sub cell GT cell from BIO RAD. For the preparation of the DNA samples, 5 µL

of a DNA loading dye were added to 25 µL of sample. 12 µL of the samples and 5 µL of Orange Ruler 10 bp DNA ladder (Thermo Fischer, USA) were pipetted on the gel and allowed to run for about 30 min at 120 V. Gels were afterwards imaged using a ChemiDocTM MP imaging system from BIO RAD. For the measurement of the DNA content, an Implen NanoPhotometer® was used. Therefore, the photometer was blanked, using only MES-buffer and afterwards the samples were measured in triplicates at 260 nm.

3.2.4.2 DNA cross-linking methods

To find the right concentration of DNA, DNA was dissolved in MES-Buffer (2-(N-morpholino)ethanesulfonic acid, 100 mM, pH 4.6) at 150 rpm and room temperature for 3 h, with 7% DNA solutions. The linkage between the salmon DNA and the pre-treated PET or nylon 6 samples was performed in three different ways using 1-Ethyl-3-(3-dimethylaminopropyl)carbodiimide (EDC)/N-Hydroxysuccinimide (NHS), dopamine or tyrosine as crosslinking agents (**Figure S2**).

<u>EDC/NHS cross-linking</u>

For the crosslinking of DNA using the EDC/NHS system, an EDC stock solution with 200 mg/mL and a NHS stock solution with 400 mg/mL were produced in MES-Buffer (100 mM, pH 4.6) [20]. Crosslinking reactions were performed in 12-well plates in a volume of 3 mL at 150 rpm and 21 °C. MES-Buffer, EDC, NHS and DNA stock solutions were added in suitable amounts to reach final concentrations in the reaction mixture of 50 mg/mL EDC, 100 mg/mL NHS and 7 % DNA. At first the right amount of MES buffer was added to the fabric, followed by 750 µL EDC stock solution. After 10 min, 750 µL NHS stock were added and after another 10 min incubation time, 1260 µL (7%) of DNA stock solution was pipetted to the reaction mixture. The DNA was allowed to bind for 24 h at 250 rpm and 21 °C. After incubation, samples were dried for 24 h at 21 °C.

Dopamine/tyrosine coupling

To use dopamine or tyrosine as crosslinking agents, a 2 mg/mL dopamine hydrochloride solution and a 2 mg/mL tyrosine solution were prepared in Tris/HCl buffer (100 mM, pH 8.5). For the coating with either dopamine or tyrosine, 3 mL of the solutions were pipetted to enzymatically treated PET and nylon-6 samples and incubated for 24 h at 250 rpm and 21 °C. After incubation, samples were washed by dipping them 3 times in mQ-H_2O. DNA immobilization reaction was performed with a 7% DNA solution (in MES-buffer) which was directly pipetted to the dopamine or tyrosine samples. The incubation with DNA was performed for 24 h at 250 rpm and 21 °C. After the incubation, the samples were dried for 24 h at room temperature [21].

3.2.5 Fourier-transformed Infrared Spectroscopy (FT-IR)

To measure changes on the surface of PET and nylon after enzymatic treatment and the different coating steps, a PerkinElmer Spectrum 100 FT-IR Spectrometer was used. Spectra were recorded from 4000-650 cm^{-1}. A total of 25 scans for each sample were recorded with a resolution of 2 cm^{-1}. Normalization of the recorded spectra was done at the band occurring in the 1410 cm^{-1} region (CH in plane bending and CC stretching), which has been already proven to be a suitable reference band [22]. The bands were assigned as follows: for PET, 1471 cm^{-1} (-CH_2 bending), 1410 cm^{-1} (-CH in plane bending and CC stretching), 1340 cm^{-1} (-CH_2 wagging), 1120 cm^{-1}(-O-CH_2 and ring CC stretching), 970 cm^{-1} (-O-CH_2 and C=O stretching), 847 cm^{-1}(bending of benzene rings. For nylon: 3300 cm^{-1} (-NH stretching and bending vibration of secondary amine), 1640 cm^{-1} (-NH bending of Amide I), 1540 cm^{-1} (-C=O stretching of Amide II), 1460 cm^{-1} (-CH_2 bending vibration), 1250 cm^{-1} (-C-N stretching vibration), 960 and 930 cm^{-1} (-CH out of plane bending). For DNA: 1680 cm^{-1} (P=O), 1220 and 1060 cm^{-1} (symmetric and asymmetric PO^{2-} vibration), 967 cm^{-1} (phosphodiester bond), 832 and 782 cm^{-1} (sugar-phosphate bond).

3.2.6 Environmental Scanning Electron Microscopy (ESEM)

For the SEM investigations a FEI Quanta 250 FEG (Thermo Fisher Scientific, Hillsboro, OR) was used under high vacuum condition and a variable high tension from 5-10 kV. The micrographs were recorded with the Everhart-Thornley-Detector in secondary electron (SE) mode. The fracture surface was sputter coated with a 10 nm thin layer of gold in order to provide sufficient electrical conductivity. The EDS measurements were performed for 60s, with 20 kV high tension and a Spotsize of 4,5 with a 10 mm^2 Apollo X Silicon Drift Detector by EDAX Ametek, NJ. USA, and Genesis Software V 6.53 from 21. September 2018.

3.2.7 Durability of washing

In order to confirm the covalent binding of DNA on fabrics a washing stability test was performed. Briefly DNA coated samples (8*20 cm) were washed in a solution containing 4 g/L of commercial detergent and the liquor ratio was 50:1. Each step was conducted at 40 °C for 5 min. After each wash, the fabric was removed, squeezed and rinsed with mQ-H_2O. The washing tests were repeated till 100 min were reached. After each washing step the DNA concentration present in solution was measured *via* Implen NanoPhotometer® as described above. The percentage of DNA was calculated from the initial (or previous) DNA content and compared with absorbed DNA on untreated and enzymatic treated fabrics.

3.2.8 Flame retardant assessment

3.2.8.1 Flammability test

Flammability tests were done according the ISO 6940 for the determination of ease of ignition of vertically oriented specimens. Samples were cut in the size of 8x20 cm and fixed in the apparatus (**Figure S3**) (Anon et al. 1989). For the ignition of the sample, the flame of the burner was set to a vertical height of 4 cm. Tests were performed in bottom edge ignition, in which the flame was applied to the sample to the shortest time to cause

ignition. The whole experiment was recorded on video and the time was measured from the time of ignition until self-extinguishing was reached or the sample completely burned. This test gives information about the burning time, burning length and the resulting burning rate. Furthermore, one can gain information about self-extinguishing, char-formation and the ease of ignition. An increase in flame-retardancy would result in longer burning time, a decrease of the burning length and a lower burning rate.

3.2.8.2 Thermogravimetric Analysis (TGA)

TGA was performed on a PL Thermal Sciences STA 625 thermal analyzer, using 10 mg of sample in an aluminum pan. The gas flow (N_2 or O_2) was set to 100 mL*min^{-1} and samples were heated from 30 to 625 °C at a heating rate of 10 °C*min^{-1}. The temperatures at 5 and 50 % mass loss (TD_5 and TD_{50}) were subsequently determined.

3.3 Results

3.3.1 Enzymatic functionalization

Polymer-degrading enzymes represent useful tools for specific but mild introduction of reactive chemical groups on polymer surfaces, retaining their bulk properties [24]. Different lipases and cutinases have demonstrated to be able to functionalize polyesters in a first instance [25], [26]. On the other hand, *Fusarium solani* cutinase was also applied for hydrolysis of polyamides [27] leading that cutinases are able also to partly modify nylon surfaces. *Humicola insolens* cutinase (HiC) had a protein concentration of 10 mg/mL and specific activity of 80 U/mg against *p*-PNB. To determine the optimal concentration of the enzyme for functionalization, different concentrations (0.1, 0.25 and 0.5 mg/mL) were incubated with 1 cm^2 fabric pieces (PET and nylon) at 60° C. For PET functionalization, the total amount of terephthalic acid released showed the highest concentration (0.05 mM) with 0.5 mg/mL of HiC after 72 h. On the other hand, the higher concentration of caprolactame (2.2 µM released from nylon) was obtained with 0.25 mg/mL of enzyme after 72 h. These optimal conditions were further used for the functionalization of 8*20 cm

stripes of both fabrics. The amounts of released products were 1.0 and 0.07 mM for terephthalic acid and caprolactam respectively (**Figure 1).**

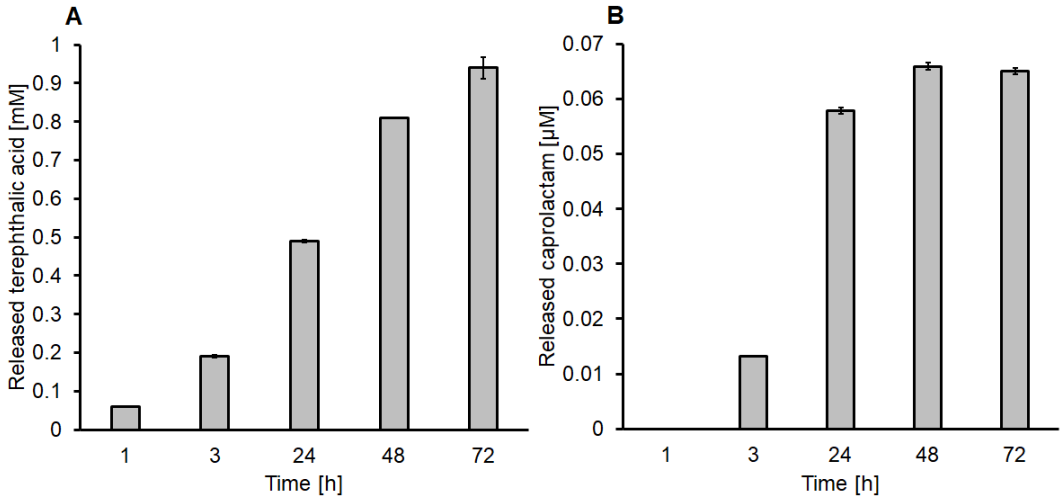

Figure 1. Determination of the released products after enzymatic hydrolysis *via* HPLC. A) terephthalic acid released from PET and (B) caprolactam released from nylon-6

The application of acid and basic dyes, confirmed the presence of newly formed functional groups on polymer surface, based on changes of L*, a*, b* and E* compared to the blanks (**Figure S4).** The delta (Δ) values of PET indicated that samples became darker, greener and bluer (**Table 1**). The same trend was found for polyamide, but with lower extent. This confirmed the HPLC results, with the lower amount of caprolactame released, but nevertheless more reactive groups were generated *via* enzymatic treatment.

Table 1. Color changes of PET and nylon surface before and after enzymatic treatment

Methylene blue (acid dye)				
	L*	**a***	**b***	**ΔE***
Untreated PET	134.15	8.75	31.70	0.06
PET_HiC	101.38	7	28.27	4.8
Delta (Δ)	-2.77	-1.75	-3.43	4.74
Comassie brilliant blue (basic dye)				

	L*	a*	b*	ΔE*
Untreated nylon	73.04	-1.31	-8.44	0.02
nylon_HiC	66.36	-1.42	-9.55	-8.59
Delta (Δ)	-6.68	-0.11	-1.11	8.57

Further proofs of the presence of more functional moieties were obtained *via* FT-IR measurements. The enzymatic hydrolysis of PET showed a reduction and a slight shift of the band at 1721 cm^{-1} (indicative of the carbonyl stretching group). Moreover, the band at 1240 cm^{-1} (C=O-O stretching and CC stretching) was lower, confirming that the enzyme cleaved some esters bonds within the PET fibers (**Figure 2A**).

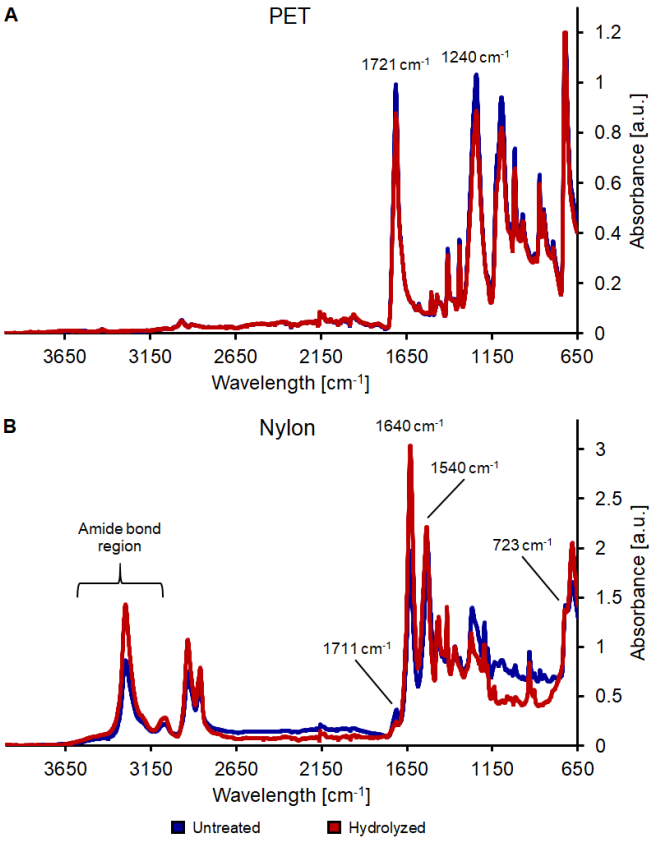

Figure 2. FT-IR analysis of untreated (blue line) and enzymatically hydrolyzed (red line) PET (A) and nylon-6 (B).

Nylon spectra show instead differences in the 3300-2800 cm^{-1} region, indicating partial breakage of amide bonds. Additionally, bands at 1640 and 1540 cm^{-1} decreased, while bands at 1711 cm^{-1} (C=O vibration) and 723 cm^{-1} (-NH_2 vibration) clearly indicated the formation of new carboxylic and amine groups (**Figure 2B**).

3.3.2 DNA immobilization

Low molecular weight Deoxyribose nucleic acid (DNA) from salmon sperm was used. Agarose gel defined that the length of DNA molecules were in the 20-30 bp size range (**Figure S5**). This size is suitable for immobilization applications since longer DNA fragments could hamper the reaction progression due to steric hindrance. As preliminary test, FT-IR of salmon DNA was recorded to discriminate DNA bands after the immobilization on PET and nylon-6. DNA characteristics bands resulted to be at 1680 cm^{-1} (P=O) with the presence of a small shoulder (C=O vibration of guanine, cytosine and thymine), 1220 and 1060 cm^{-1} (symmetric and asymmetric PO^{2-} vibration, and as well band at 967 cm^{-1} (phosphodiester) and 832, 782 cm^{-1} for sugar-phosphate bond (**Figure S6**).

EDC/NHS coupling system

The EDC/NHS coupling system is a multistep reaction able to link the carboxylic groups with primary amines. In a first step, EDC reacts with the obtained carboxylic groups on PET and nylon surface, leading the formation of acylisourea intermediate, which in a second step reacts with NHS to form an amino reactive sulfo-NHS ester. This last compound is then replaced by DNA molecule due to a stable amine bond with carboxylic acid group**.** Functionalized PET spectra after DNA immobilization using EDC/NHS as coupling system showed only minor changes: in particular, it was possible to observe an increase of the peak at 1710, 1230 and 1090 cm^{-1} characteristic from the DNA molecule (**Figure S7**). In enzymatically activated nylon-6, the band at 1630 cm^{-1} was intensified and shifted into the direction of P=O band of DNA. Moreover, changes in intensity of the peak in the area of 1060-960 cm^{-1} are typical from phosphate or phosphate ester moieties, indicating that the nucleic acid was immobilized in small extend (**Figure S8**).

Dopamine and tyrosine as cross-linkers

Dopamine is a small catecholamine, precursor of norepinephrine and epinephrine (brain neurotrasmettitors). In nature these compounds are used by mussels for the attachment to rock surfaces, mainly due to the ability to form thin polydopamine layers on surfaces [28]. FT-IR spectra of PET after dopamine coating were recorded, showing broad and intensified bands between 3600 and 2900 cm^{-1} due to hydrogen bonds which are formed between hydroxyl groups and amino groups from dopamine. Intensified bands in the 1650-1450 cm^{-1} area due to N-H bending vibrations and aromatic C-C stretching vibrations clearly confirm the presence of dopamine after coating [29]. Further characteristic peaks of dopamine are 1265 cm^{-1} (aromatic amine C-N stretching vibrations) and 1050 cm^{-1} (C-N bending vibrations between the benzene ring and the hydroxyl groups) that in the spectra are overlapping with bands characteristic for PET. In PET coated with dopamine/DNA, a new band at around 1680 cm^{-1} (P=O) appeared, as well an intensified and shifted bands at 1220 cm^{-1} and 1060 cm^{-1} (asymmetric and symmetric PO^{2-} vibrations), which clearly indicate the presence of immobilized DNA. This is also confirmed by intensified and shifted bands at 835 cm^{-1} and 780 cm^{-1} which contribute to C=C and C=N stretching modes of pyrimidines and purines (**Figure S9**) [12]. Dopamine coating of nylon samples showed changes in the FT-IR spectra, which correspond to the ones recorded for PET/Dopamine. Bands with a broader band within the range of 2800-3600 cm^{-1} indicate the formation of hydrogen bonds between the hydroxyl groups of dopamine. The band at 1493 cm^{-1}, characteristic for aromatic C-C stretching vibrations of dopamine, is overlaid by the amide II band of nylon but there is a shift into the direction of dopamine. A brighter and intensified peak at approximately 1265 cm^{-1} as well as a clearly visible peak at around 1050 cm^{-1} further confirms the presence of dopamine on the surface of nylon fabrics. Spectra of nylon/Dopamine/DNA samples showed an intensified, shifted peak which also forms a small shoulder at ~1540 cm^{-1}. Furthermore, a sharper and more intensified peak was recorded between 1470 – 1420 cm^{-1}. A shift of the band at ~1006 cm^{-1} and a broader bandwidth of the peak at around 835 cm^{-1} which are characteristic for C=C and C-N stretching modes, again

confirm that also the DNA immobilization on dopamine coated nylon fabric was performed (**Figure S10**). On the surface of nylon fabric, dopamine forms scurf-like particles which are attached to the fibers (**Figure S11**). There is no homogenous coating of DNA visible which is also confirmed by the FT-IR spectra, showing only low bands in the characteristic region of DNA. Imaging of PET after Dopamine/DNA coating showed again the scurf formation of dopamine on the fibre. In both fabrics, DNA coating was a non-homogenous layer (**Figure S11).**

L-tyrosine is a proteinogenic amino acid, also precursor of L-Dopa. Its chemical structure provides two reactive group (an amino and a carboxylic groups), which are suitable for cross-linking binding of macromolecules, such as DNA. In the spectrum from PET/tyrosine, bands at 3210 cm^{-1} and 3040 cm^{-1} (aromatic CH stretching), 1590 cm^{-1} (asymmetric stretching of NH_3^+) and 1450 cm^{-1} (scissoring vibration of tyrosine) are visible after the treatment [30]. By comparing the spectra of PET/tyrosine/DNA with the spectra of salmon DNA all peaks characteristic for DNA (1680, 1220, 1060, 967, 832 and 780 cm^{-1}) are clearly visible, which confirms the presence of DNA on the PET fabric. Due to the intense and clearness of the bands it was proven that DNA was immobilized on the polymer's surface (**Figure 3).**

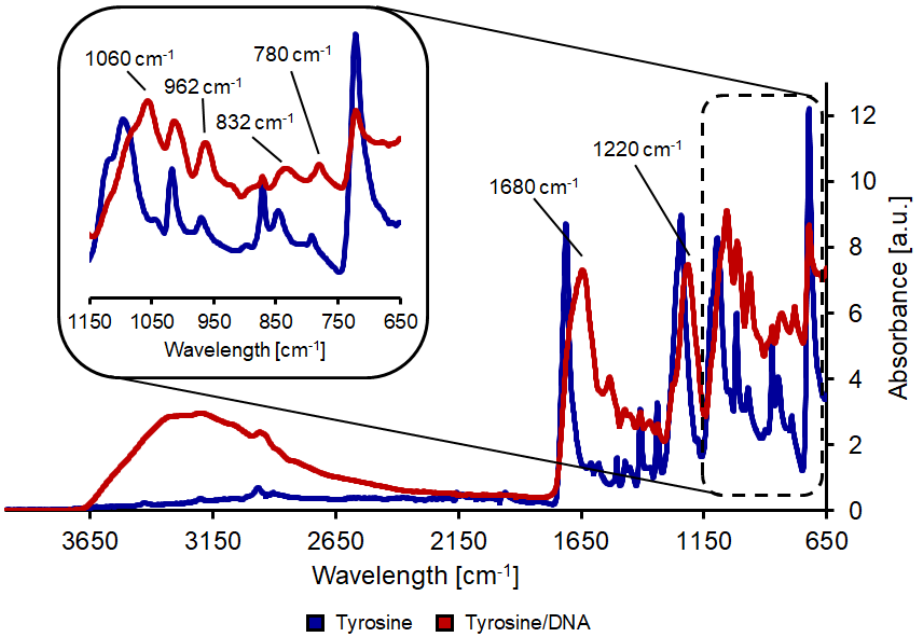

Figure 3. FT-IR analysis of hydrolyzed PET after coating with tyrosine (blue line) and after tyrosine/DNA coupling (red line).

The nylon/tyrosine reaction also showed distinct changes in the FT-IR spectra when compared to the blank. As described earlier, the reduction of the amide I and II bond (1657 and 1533 cm^{-1}) and the increase in the band at 1711 cm^{-1} is due to the hydrolysis of the polymer bonds which leads to an increase in carboxylic acid groups. This is also the reason for the intense band at ~1100 cm^{-1} which results from newly formed carboxyl groups. Nevertheless, tyrosine characteristic peaks were also visible in the case of nylon/tyrosine. These peaks are again located at 3040 cm^{-1}, 1590 cm^{-1} (overlaid by the amide II band) and 1330 cm^{-1}. Furthermore, there is a very strong and wide peak at 1250 cm^{-1} (OH in plane deformation coupled to C-O stretching) and together with the peak at 840 cm^{-1} the spectra clearly confirm that L-tyrosine is coupled to nylon fabric. The band at 1710 cm^{-1} was intensified and shifted towards the direction of the P=O bonding after the immobilization of DNA. Furthermore, bands at 1220 and 1060 cm^{-1} were further intensified and show a slight shift. At approximately 970 cm^{-1} the intensity of the band decreases which is due to ribose phosphate skeletal motions [12]. The shift of the bands at 1410 and 1340 cm^{-1} can be explained by the presence of purine and pyrimidine molecules (1470-1320 cm^{-1}) (**Figure 4**).

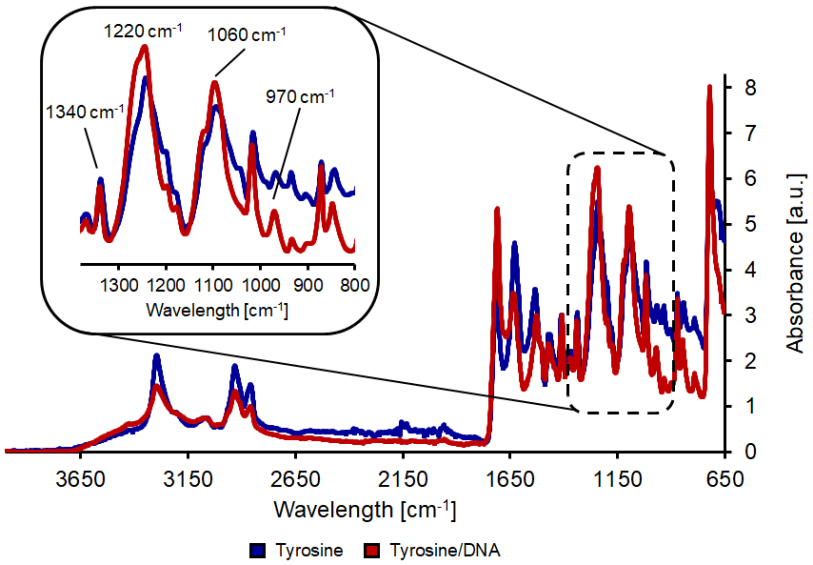

Figure 4. FT-IR analysis of hydrolyzed nylon-6 after coating with tyrosine (blue line) and after tyrosine/DNA coupling (red line).

Figure 6 shows the clear surface structure differences of tyrosine and DNA coated samples. For tyrosine coating, crystals were formed on the surface, while DNA covered the fibers homogeneously. This was confirmed by the EDS spectra, showing a newly formed and intense peak of phosphorus (**Figure S12)**. Compared to Nylon, the DNA-immobilization on PET was not homogenous, showing spots of DNA distributed on the surface of the sample. Furthermore, the EDS spectra showed a smaller peak for phosphorus compared to nylon/tyrosine/DNA (**Figure 5**).

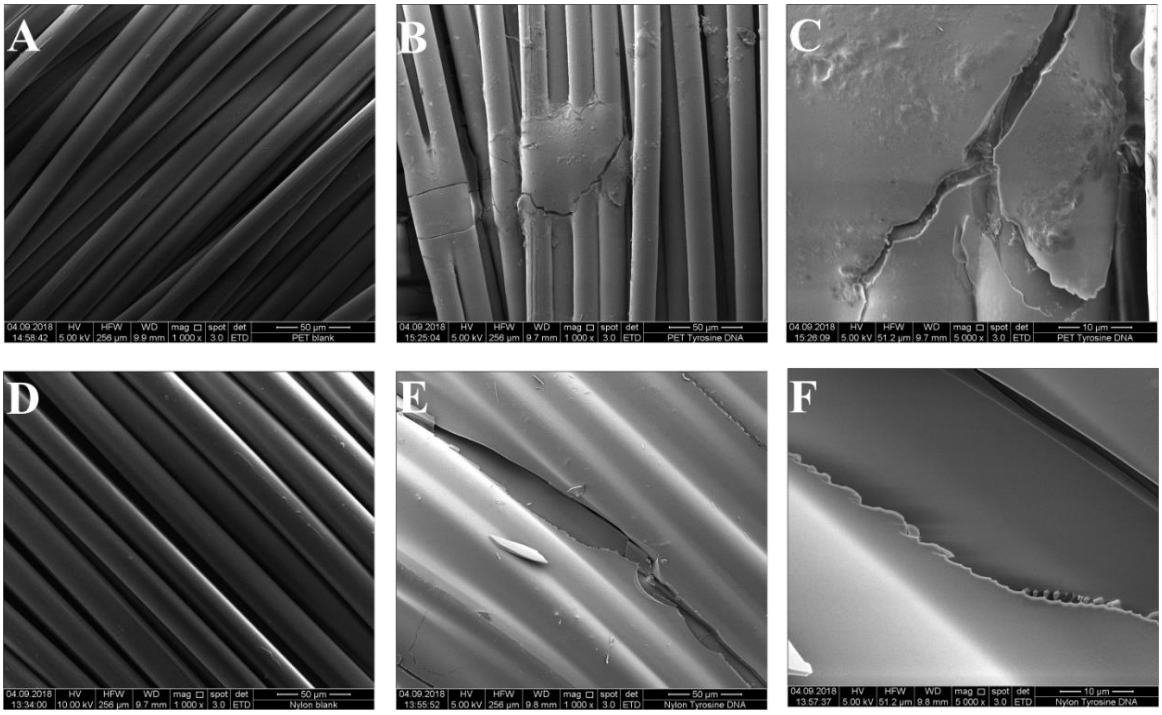

Figure 5. Scanning electron microscopy images of the samples. **A)** untreated PET 1000x magnification **B)** PET_tyrosine_DNA 1000x magnification **C)** PET_tyrosine_DNA 5000x magnification **D)** untreated nylon 1000x magnification **E)** nylon_tyrosine_DNA 1000x magnification **F)** nylon_tyrosine_DNA 5000x magnification.

The washing stability tests confirmed the previous results: the samples treated with EDC/NHS as cross-linking method showed the same DNA leaching trend as well the control samples, indicating that DNA was mostly absorbed. On the other hand, the dopamine and tyrosine coating systems demonstrated great covalent immobilization

stability; around 50% and 40% of DNA respectively were leached out after 45 min washing and stable (**Figure 6**).

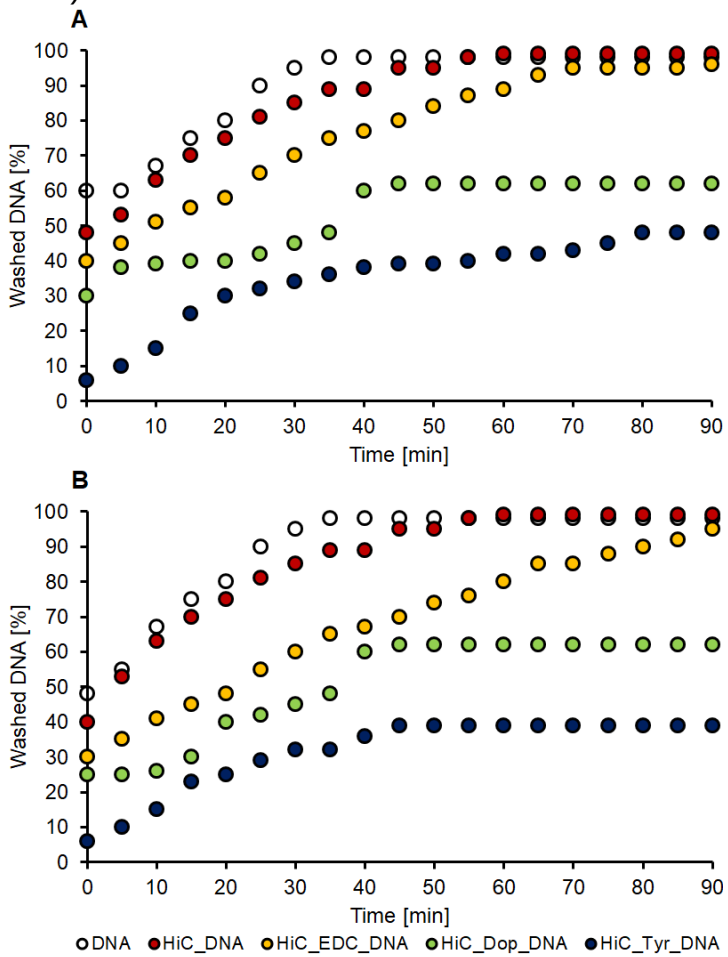

Figure 6. DNA washing stability. Washing of PET (A) and nylon (B) samples treated with DNA absorbed on untreated polymer (white dots), DNA absorbed on enzymatic treated polymer (red dots), and the three coupling conditions: EDC coupling (orange dots), dopamine coupling (green dots) and tyrosine coupling (blue dots).

Summarizing, FT-IR, SEM and washing step results, EDC/NHS coupling lead to a low for DNA immobilization of PET and nylon fabrics. Using Dopamine/DNA was not homogenously attached onto two polymer and moreover dopamine coating gave a dark brownish colour to both textiles, which can prohibit a potential textile application. Finally, tyrosine coating exhibited the optimal condition for DNA immobilization, stability, colour, and was therefore applied for further flame-retardant tests.

3.3.3 Flame retardant tests

For polyester, the three treatments showed a decrease in burning rate compared to the untreated (blank) and enzymatic treated (HiC) samples. The total burning time (TBT) increased as well as the length of the burned sample, showing that the immobilization of the DNA favors the flame-retardancy of PET fabrics (**Table 2**). Tyrosine/DNA treated PET samples resulted in a decreased burning rate and length of the burned specimen.

Table 2. Flammability of PET and nylon fabrics after enzymatic surface activation and coupling of DNA.

Sample	Total burning time [s]	Burning length [mm]	Burning rate [mm/s^{-1}]
PET Blank	6,75	57,5	8,5
PET_HiC	5	42,5	8,5
PET_HiC_tyrosine_DNA	11	68	6,2
nylon Blank	35	150	4,3
nylon_HiC	10	60	6,0
nylon_HiC_tyrosine_DNA	3,5	17,5	5,0

An increase in the char formation during burning of the tyrosine/DNA treated sample also indicates the presence of DNA (**Figure 7**). Compared to the untreated and enzymatically treated sample, it was possible to decrease the burning rate from 8.5 to 6.2 mm*s^{-1}, which further confirms that DNA provides flame retardant properties. Moreover, PET/blank showed a melting behavior of the fibres during combustion. In contrast, the tyrosine/DNA coated samples showed more intact fibres as well as char formation due to still attached DNA which serves as protection layer during thermal decomposition of the polymer.

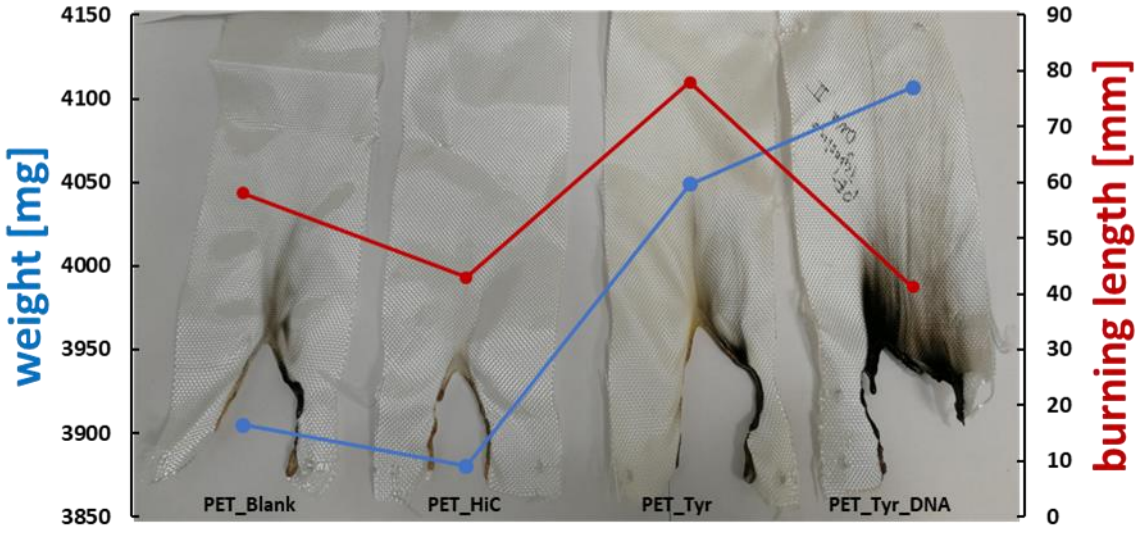

Figure 7. Results of flammability tests of enzymatically activated and tyrosine and tyrosine/DNA treated PET.

Nylon fabric showed different behavior compared to PET. Starting with the untreated nylon fabric which completely burned and did not manage to self-extinguish the flame (longest TBT), there is a clear trend in decreasing length of the burned sample visible throughout the different coating steps. In contrast, the enzymatic treated (nylon_HiC) fabric showed an about 1/3 reduced TBT and burning length. This may be explained by the newly formed amine groups after enzymatic hydrolysis, which can release ammonia during combustion, leading to a dilution in the gas phase and an extinguishing of the flame. Tyrosine/DNA seems to be the best treatment also for nylon fabric, due to the shortest TBT (few seconds) and burning length (~18 mm), furthermore, the flame was self-extinguished nearly immediately after the flame was applied to the fabric (**Figure 8**). After coating with tyrosine and immobilization of the DNA, the flame was immediately self-extinguished after ~18 mm and a few seconds. The brownish color of the burned parts, which results from sugars within the sugar-phosphate backbone of DNA, confirms the presence of DNA on the nylon fabric.

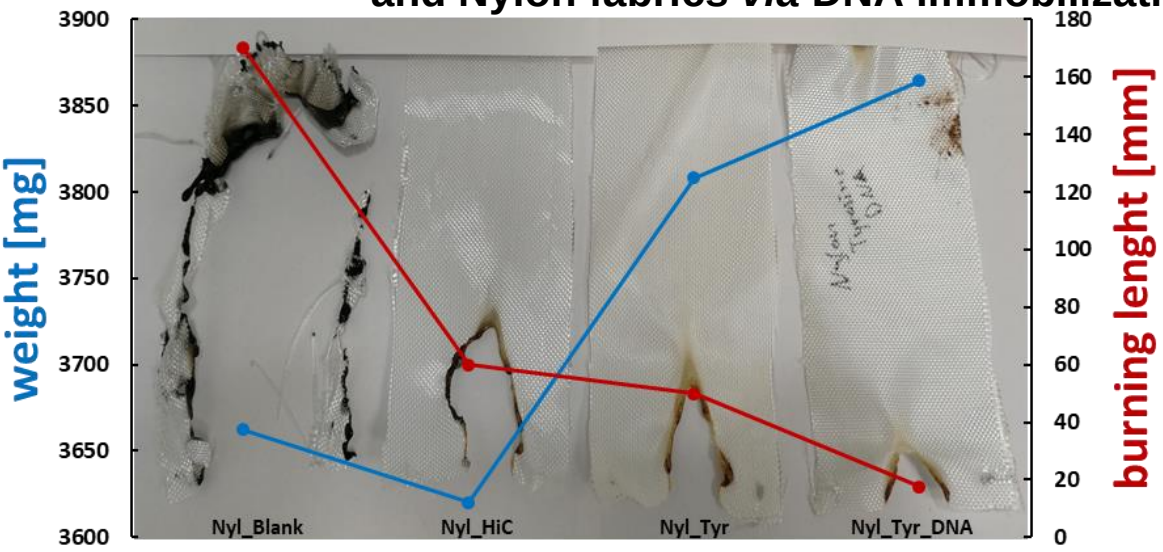

Figure 8. Results of flammability tests of enzymatically activated and Tyrosine and Tyrosine/DNA treated nylon.

In case of Tyrosine/DNA coated samples, the DNA seems to swell during combustion which indicates the release of non-combustible gases during thermal degradation of the DNA, leading to the very quick self-extinguishing of the flame. Beneath the DNA coating, nylon fibres are still intact and have not been attacked by the heat. PET/Blank showed a melting behavior of the fibres during combustion. In contrast, the tyrosine/DNA coated samples showed more intact fibres as well as char formation due to still attached DNA which serves as protection layer during thermal decomposition of the polymer. (**Figure 9).**

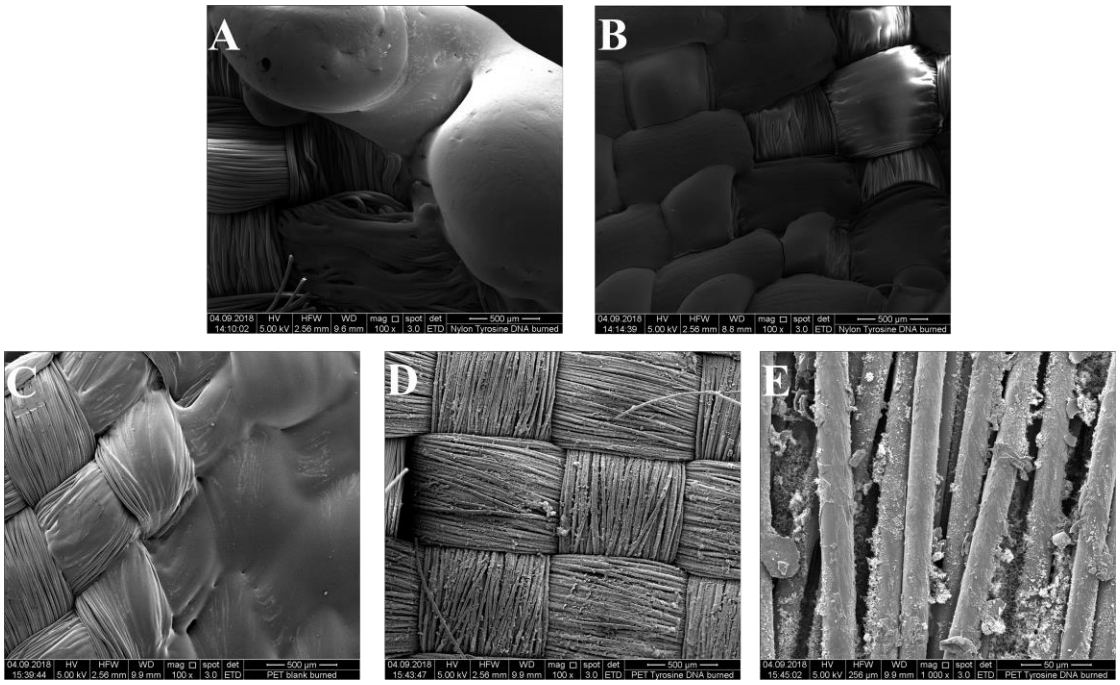

Figure 9 ESEM image of Nylon/Blank burned (100x) (A) and Nylon/tyrosine/DNA burned (100x) (B) in the upper part and PET/Blank burned (100x) (C) ,PET/tyrosine/DNA burned (100x) (D) and PET/tyrosine/DNA burned (1000x)

Thermogravimetric analysis performed under an air flow shows changes in thermo-oxidative behavior and thermal degradation while the same analysis performed under a N_2 flow didn't lead to any significative changes between the various samples. Tyrosine/DNA-coated PET showed a slower thermal degradation in the 500-600 °C region, indicating that DNA favors the flame-resistance (**Figure 10A**)

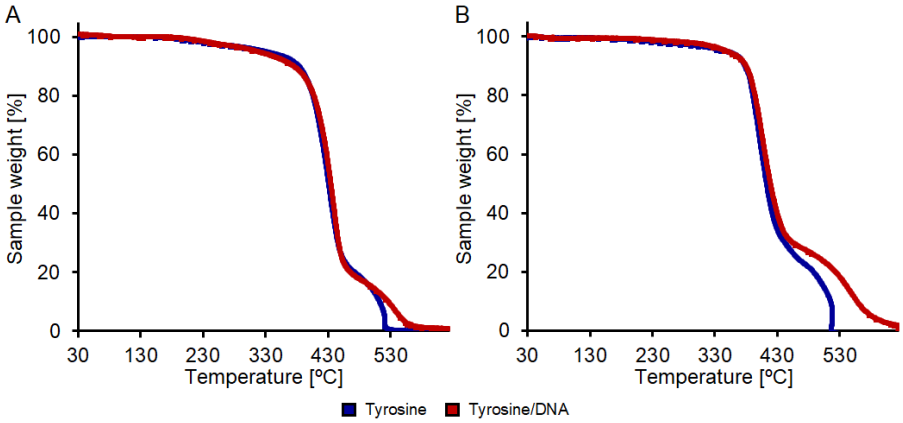

Figure 10. Thermal degradation analysis in air of PET (A) and nylon (B) samples. All samples were enzymatically hydrolyzed and coupled with only tyrosine (blue lines) or with tyrosine and DNA (red lines).

In the case of nylon, the coating with Tyrosine and DNA showed even higher effects in terms of thermal resistance. The weight-loss due to thermal degradation between 450-625 °C was significantly lower compared to the nylon sample treated with only tyrosine that shows a complete weight loss at 516 °C (**Figure 10B**). This further confirms that the DNA-immobilization on nylon was more successful if compared with the one performed on PET fabrics.

3.4 Conclusions

DNA provides all properties of a flame-retardant compound (temperature reduction by the release of water, release of inert gases and formation of a solid layer), has been investigated to be an eco-friendly alternative to commercial FR in terms of availability and the rather mild operation conditions. Enzymatic surface activation of PET and nylon prior to DNA coupling was successful *via Humicola insolens* cutinase, as confirmed by HPLC, dyes application and FT-IR. To immobilize DNA on the surface of PET and nylon, three different crosslinking agents have been applied (EDC/NHS, Dopamine and tyrosine), in which tyrosine has shown to be the most sufficient. This was also confirmed by the FT-IR spectra which present the most intense bands of DNA after the coating with L-tyrosine as well as the ESEM images showing homogeneous coating. These results were successfully proved with the flame retardant test, where this coating coated fabrics shown the lowest TBT and burning length.

Author Contributions

F.Q., K.K., H.S. and R.V performed the experiments. F.Q., A.P., S.V and G.M.G. planned the experiments. L.P. performed SEM measurements. F.Q. and A.P. wrote the manuscript. A.P. and G.M.G. supervised the work. All authors discussed the collected data and corrected the manuscript before submission.

ACKNOWLEDGMENTS

This project received funding from the European Union's Horizon 2020 research and innovation program under the grant agreement 641942 (Resyntex project). Alessandro Pellis thanks the FWF Erwin Schrödinger fellowship (grant agreement J 4014-N34) for financial support.

Conflicts of Interest: The authors declare no conflict of interest.

3.5 References

[1] F. Statistics, M. Academy, and S. F. Service, "World fire statistics," 2006.

[2] S. Vecchiato *et al.*, "Enzymatic Recycling of High-Value Phosphor Flame-Retardant Pigment and Glucose from Rayon Fibers," *ACS Sustain. Chem. Eng.*, p. acssuschemeng.7b03840, 2017.

[3] S. Chen, X. Li, Y. Li, J. Sun, and C. E. T. Al, "Intumescent Flame-Retardant and Coatings on Cotton Fabric," no. 4, pp. 4070–4076, 2015.

[4] Y. Wang *et al.*, "Core-shell expandable graphite @ aluminum hydroxide as a fl ame-retardant for rigid polyurethane foams," *Polym. Degrad. Stab.*, vol. 146, no. October, pp. 267–276, 2017.

[5] C. Wang, Z. Wang, and Z. Liu, "Flame - retardant rigid polyurethane foam with a phosphorus - nitrogen single intumescent flame retardant," no. May 2017, pp. 668–676, 2018.

[6] K. A. Salmeia, S. Gaan, and G. Malucelli, *Recent Advances for Flame Retardancy of Textiles Based on Phosphorus Chemistry*. 2016.

[7] I. Watanabe and S. Sakai, "Environmental release and behavior of brominated flame retardants," vol. 29, pp. 665–682, 2003.

[8] F. Quartinello *et al.*, "Highly Selective Enzymatic Recovery of Building Blocks from Wool-Cotton-Polyester Textile Waste Blends," no. 3, 2018.

[9] X. Cheng, J. Guan, R. Tang, and K. Liu, "Phytic acid as a bio-based phosphorus fl ame retardant for poly (lactic acid) nonwoven fabric," *J. Clean. Prod.*, vol. 124, pp. 114–119, 2016.

[10] J. Feng, S. Su, and J. Zhu, "An intumescent flame retardant system using b -

cyclodextrin as a carbon source in polylactic acid (PLA),” no. April, 2011.

[11] J. Alongi *et al.*, “Caseins and hydrophobins as novel green fl ame retardants for cotton fabrics,” *Polym. Degrad. Stab.*, vol. 99, pp. 111–117, 2014.

[12] J. Alongi, R. A. Carletto, A. Di Blasio, F. Carosio, F. Bosco, and G. Malucelli, “DNA: a novel, green, natural flame retardant and suppressant for cotton,” *J. Mater. Chem. A*, vol. 1, no. 15, p. 4779, 2013.

[13] J. G. Grote *et al.*, “DNA-based materials for electro-optic applications: current status,” vol. 5934, p. 593406, 2005.

[14] I. M. P. L. V. O. Ferreira, O. Pinho, E. Vieira, and J. G. Tavarela, “Brewer’s Saccharomyces yeast biomass: characteristics and potential applications,” *Trends Food Sci. Technol.*, vol. 21, no. 2, pp. 77–84, 2010.

[15] Z. H. Yang, Y. Xiao, G. M. Zeng, Z. Y. Xu, and Y. S. Liu, “Comparison of methods for total community DNA extraction and purification from compost,” *Appl. Microbiol. Biotechnol.*, vol. 74, no. 4, pp. 918–925, 2007.

[16] A. Biundo *et al.*, “Characterization of a poly(butylene adipate-co-terephthalate)-hydrolyzing lipase from Pelosinus fermentans,” *Appl. Microbiol. Biotechnol.*, vol. 100, no. 4, pp. 1753–1764, 2016.

[17] J. E. Song and H. R. Kim, “Improvement in nylon fabrics ’ reactivity via enzymatic functionalization,” *J. Text. Inst.*, vol. 5000, p. 0, 2017.

[18] S. Noel, B. Liberelle, L. Robitaille, G. De Crescenzo, and C. Hc, “Quantification of Primary Amine Groups Available for Subsequent Biofunctionalization of Polymer Surfaces,” pp. 1690–1699, 2011.

[19] F. Quartinello *et al.*, “Synergistic chemo-enzymatic hydrolysis of poly(ethylene terephthalate) from textile waste,” *Microb. Biotechnol.*, vol. 10, no. 6, pp. 1376–1383, 2017.

[20] J. S. Pieper, T. Hafmans, J. H. Veerkamp, and T. H. Van Kuppevelt, “Development of tailor-made collagen } glycosaminoglycan matrices : EDC / NHS crosslinking , and ultrastructural aspects,” vol. 21, pp. 581–593, 2000.

[21] B. H. Lee, J. Rho, and P. B. Messersmith, “Facile Conjugation of Biomolecules onto Surfaces via Mussel Adhesive Protein Inspired Coatings,” pp. 431–434, 2009.

[22] I. Donelli, P. Taddei, P. F. Smet, D. Poelman, V. A. Nierstrasz, and G. Freddi, “Enzymatic surface modification and functionalization of PET: A water contact angle, FTIR, and fluorescence spectroscopy study,” *Biotechnol. Bioeng.*, vol. 103, no. 5, pp. 845–856, 2009.

[23] “Flammability and Flame retardancy of leather Ryszard Kozlowski, Bozena

Mieleniak, Malgorzata Muzyczek and Ryszard Fiedorow," vol. 1989, pp. 1–9, 1989.

[24] A. Pellis, E. Herrero Acero, V. Ferrario, D. Ribitsch, G. M. Guebitz, and L. Gardossi, "The Closure of the Cycle: Enzymatic Synthesis and Functionalization of Bio-Based Polyesters," *Trends Biotechnol.*, vol. 34, no. 4, pp. 316–328, 2016.

[25] C. Gamerith, M. Gajda, A. Ortner, E. H. Acero, G. M. Guebitz, and M. Ulbricht, "Enzymatic hydrolysis of poly(ethyleneterephthalate) used for and analysed by pore modification of track-etched membranes," *N. Biotechnol.*, vol. 39, pp. 42–50, 2017.

[26] A. Ortner *et al.*, "activated poly (lactic acid) surfaces †," pp. 816–822, 2017.

[27] C. Silva, R. Ara, M. Casal, M. G. Georg, and A. Cavaco-paulo, "Influence of mechanical agitation on cutinases and protease activity towards polyamide substrates," vol. 40, pp. 1678–1685, 2007.

[28] A. Rollett *et al.*, "RSC Advances conjugate for targeted drug delivery using tyrosinase from Agaricus bisporus," pp. 1460–1467, 2013.

[29] B. Luo, X. Wang, Y. Wang, and L. Li, "Fabrication, characterization, properties and theoretical analysis of ceramic/PVDF composite flexible films with high dielectric constant and low dielectric loss," *J. Mater. Chem. A*, vol. 2, no. 2, pp. 510–519, 2014.

[30] Y. Wang, Y. Chang, L. Yin, Y. Xue, Z. Li, and C. Xue, "A Novel Technological Process of Extracting l-Tyrosine with Low Fluorine Content from Defatted Antarctic Krill (Euphausia superba) By-product by Enzymatic Hydrolysis," *Food Bioprocess Technol.*, vol. 9, no. 4, pp. 621–627, 2016.

3.6 Supporting information

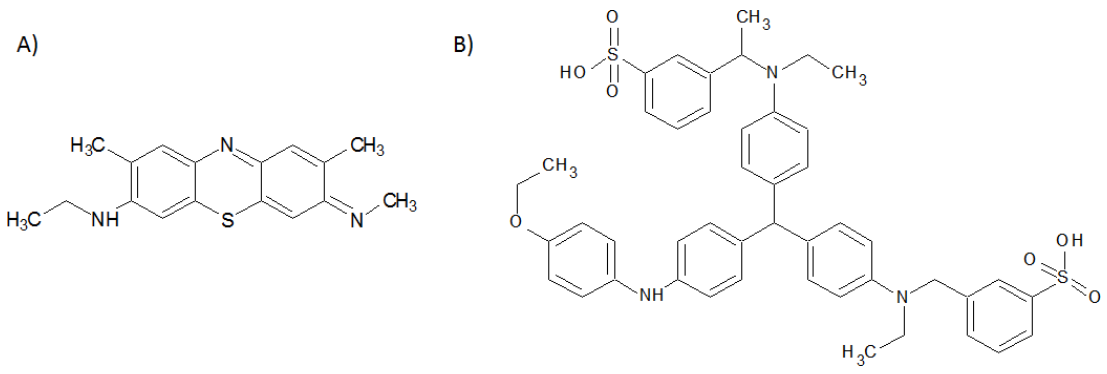

Figure S1: Chemical structure of Methylene Blue a) and Coomassie Brilliant Blue

Table S1: HPLC gradient for the measurement of PET hydrolysates

Time [min]	A (H_2O + 0.1 % Formic Acid) [% v/v]	B (MeOH + 0.1 % Formic Acid) [% v/v]
2	50	50
9	0	100
12	0	100
14	70	30

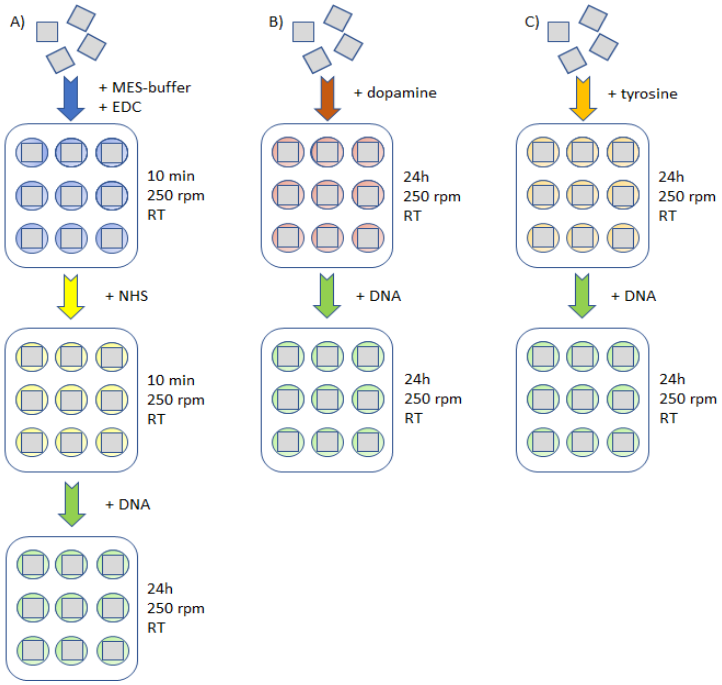

Figure S2: Schematization of DNA immobilization reactions

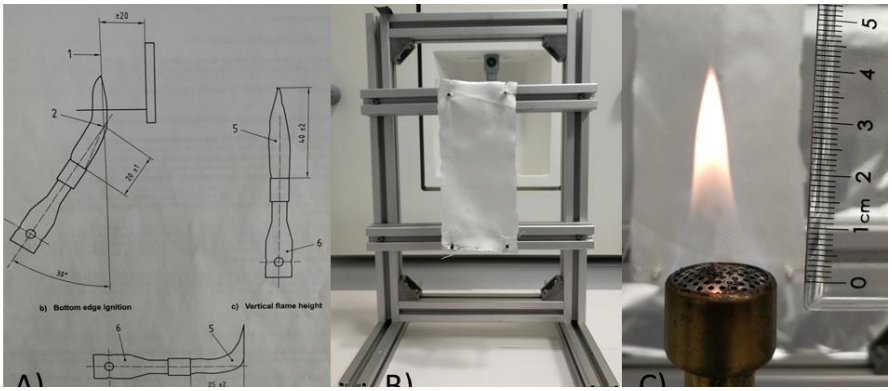

Figure S13 Flame position during bottom edge ignition, B) fixed fabric sample in the apparatus and C) flame of the burner set to a height of 4 cm

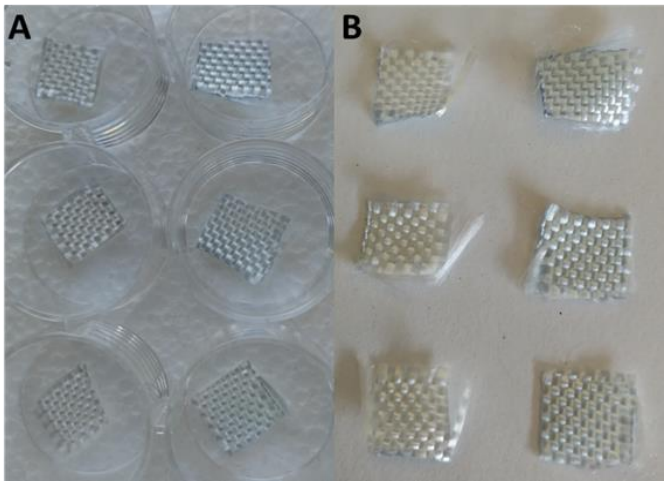

Figure S4 Samples after the treatment with acid and basic dye: A) PET blank (left) and enzymatic treated (right) after staining with Methylene blue; B) Nylon-6 blank (left) and enzymatic treated (right) after Comassie Brillant blue staining

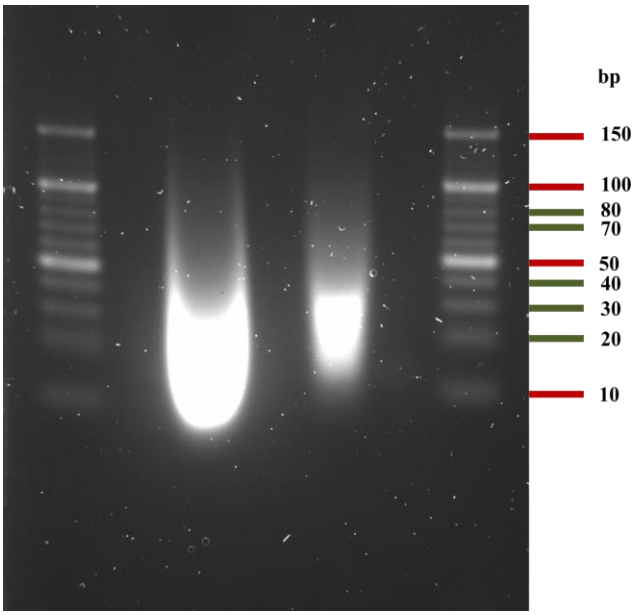

Figure S5 Agarose gel.

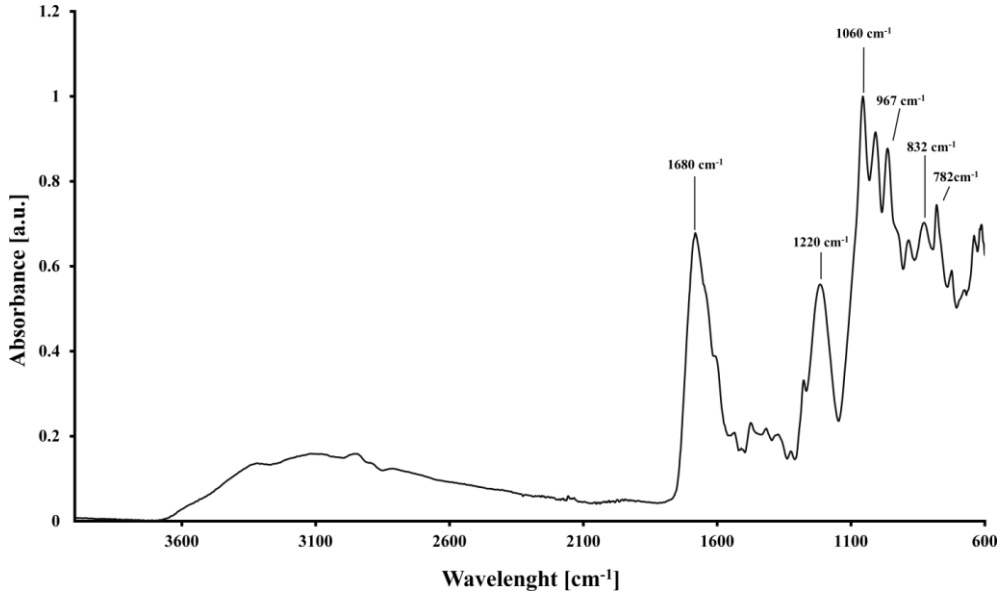

Figure S6 FT-IR DNA from salmon sperm

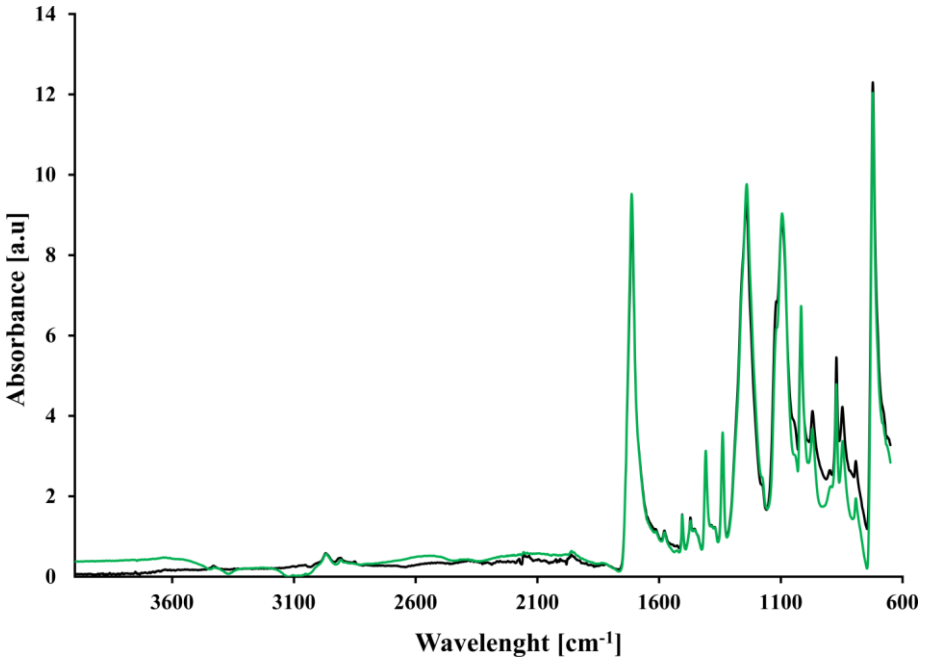

Figure S14 enzymatic treated PET (black line) and enzymatic treated PET coated with DNA via EDC/NHS (green line)

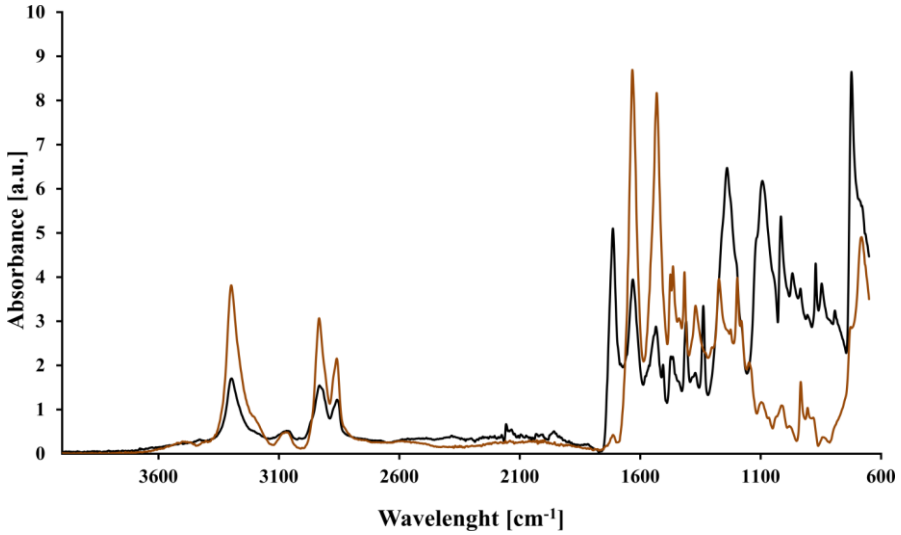

Figure S8 enzymatic treated Nylon (black line) and enzymatic treated Nylon coated with DNA via EDC/NHS (orange line)

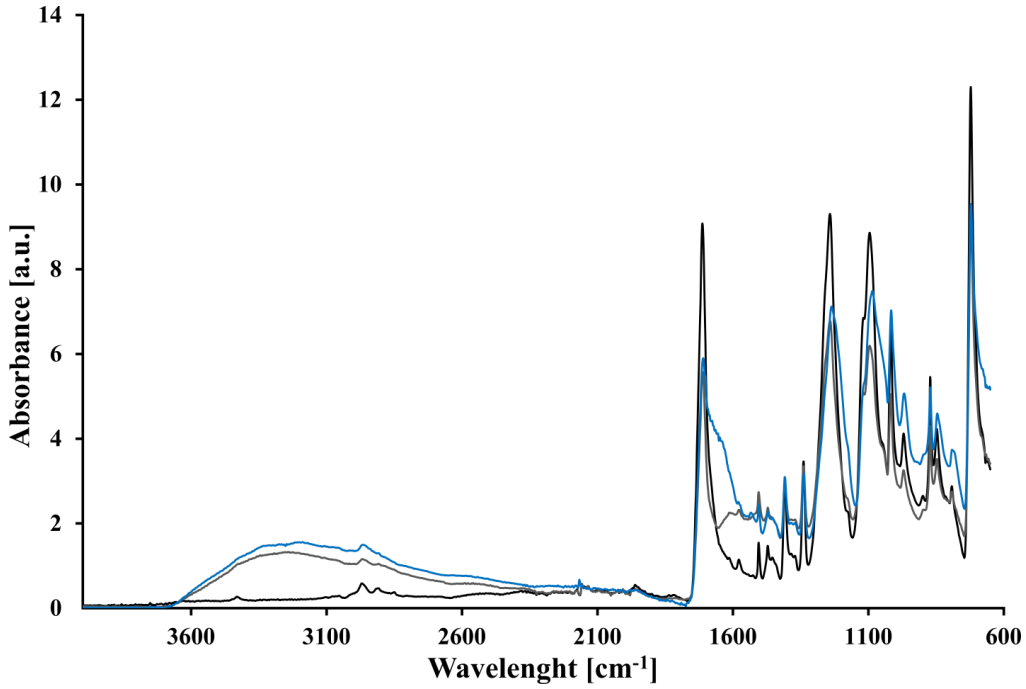

Figure S9 enzymatic treated PET (black line) and enzymatic treated PET coated with dopamine (grey line) and enzymatic treated PET coated with dopamine/DNA

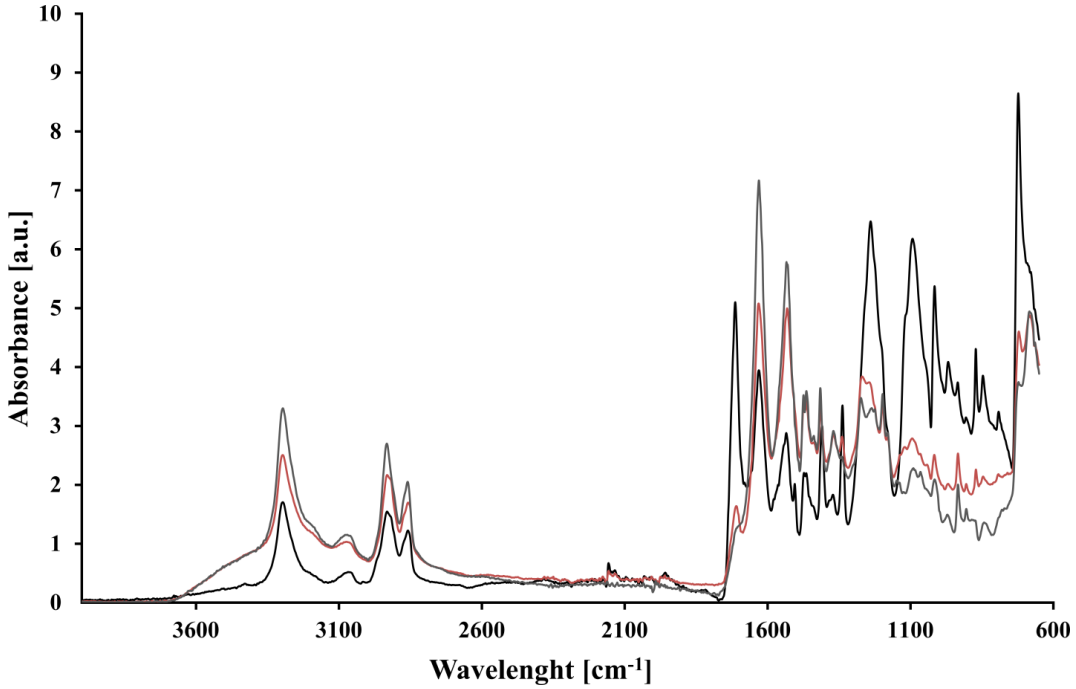

Figure S10 enzymatic treated Nylon (black line) and enzymatic treated Nylon coated with dopamine (grey line) and enzymatic treated nylon coated with dopamine/DNA

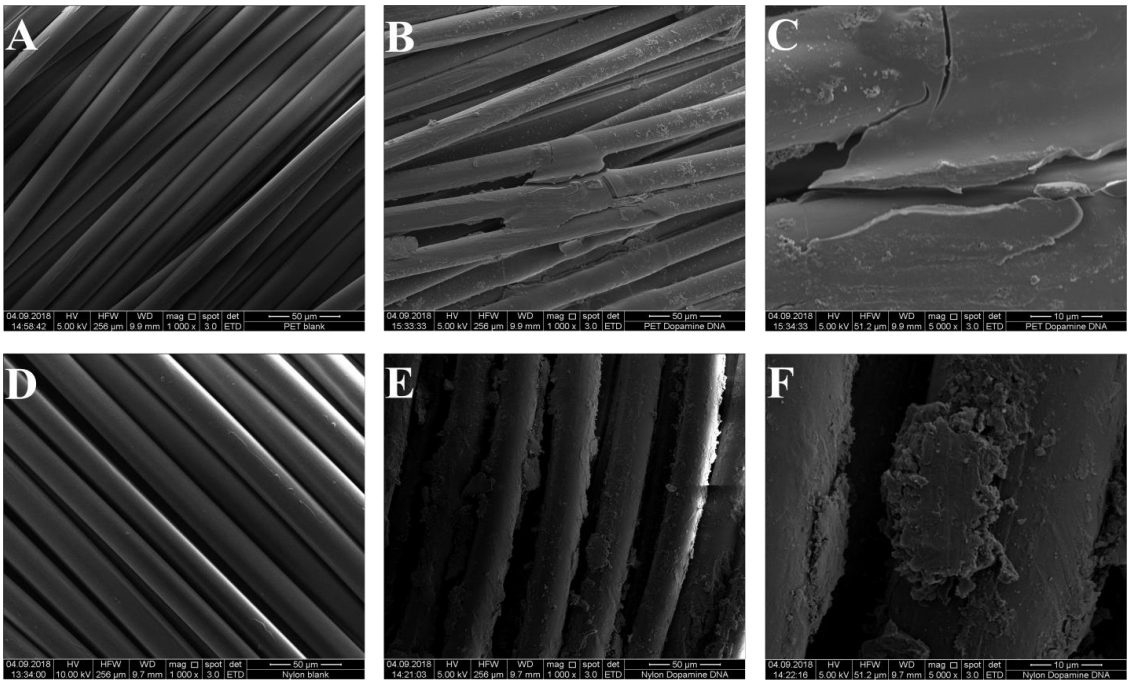

Figure S11 A) untreated PET 1000x magnification **B)** PET_dopamine_DNA 1000x magnification **C)** PET_dopamine_DNA 5000x magnification **D)** untreated Nylon 1000x magnification **E)** Nylon_dopamine_DNA 1000x magnification **F)** Nylon_dopamine_DNA 5000x magnification

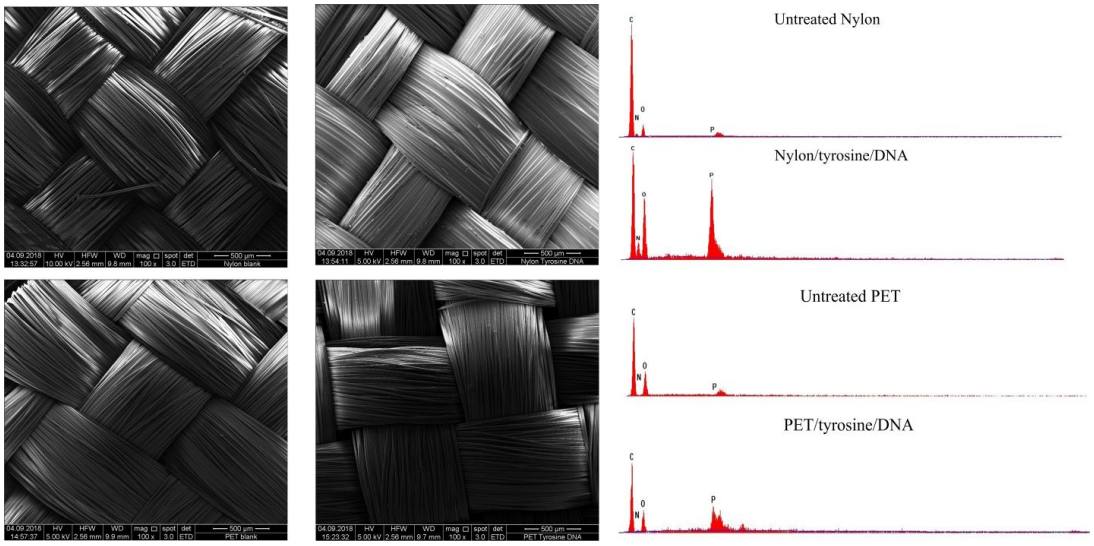

Figure S12 A) untreated Nylon 100x magnification **B)** PET_tyrosine_DNA 100x magnification **C)** PET 100x magnification **D)** Nylon_tyrosine_DNA 100x magnification **E)** EDS results

4

Smart Textiles in Wound Care: Functionalization of Cotton/PET Blends with Antimicrobial Nanocapsules

Published in: Journal of Materials Chemistry B (2019)
DOI: 10.1039/c9tb01474h

Felice Quartinello , Claudia Tallian , Julia Auer , Herta Schön , Robert Vielnascher, Simone Weinberger , Karin Wieland , Anna M. Weihs , Alexandra Herrero-Rollett, Bernhard Lendl , Andreas H. Teuschl , Alessandro Pellis and Georg M. Guebitz

Abstract

Management of infected wounds became one of the most cost-intensive procedures in the health sector. Hereby, burn wounds are of significant importance due to the high infection risk, possible leading to severe consequences such as sepsis. However, in the last decade antibiotic wound treatments caused a rising number of antibiotic resistances in bacteria leading to a strong need for alternative strategies. Therefore, the development of new antimicrobial wound dressings is focused in this study by the immobilization of pH-responsive human serum albumin/silk fibroin nanocapsules onto cotton/PET blends

loaded with the phenylpropanoid eugenol. Ultrasound-assisted production of eugenol loaded nanocapsules resulted in particle sizes (hydrodynamic radii) between 319.73 ± 17.50 and 574.00 ± 92.76 nm and zeta potentials ranging from -10.39 ± 1.99 mV to -12.11 ± 0.59 mV. Release studies of eugenol were conducted in different artificial sweats varying in pH, due to recent discoveries on sweat gland contribution in wound reepithelialisation. Formulations containing 10% of silk fibroin with lower degradation degree showed the highest release of 41% at pH 6.0. After immobilization, antimicrobial activity of functionalized cotton/PET blends was tested resulting in 81% inhibition for *Staphylococcus aureus* and 33% inhibition for *Escherichia coli*. Particle uniformity, silk fibroin concentration and high surface area to volume ratio of the produced nanocapsules were identified as the contributing factors leading to high antimicrobial activities against both strains. Therefore, the successful presented production of antimicrobial textiles using nanocapsules loaded with an active natural compound is seen as a potential future alternative for commercially available antiseptic wound dressings overcoming the issue of antibiotic resistance development

Smart Textiles in Wound Care: Functionalization of Cotton/PET Blends with Antimicrobial Nanocapsules

4.1 Introduction

Acute wound infections, as well as chronic infected wounds, are a severe complication worldwide with wound management that became one of the most cost-intensive sectors in health care. In Europe, the average cost of a wound is 6.650 € for leg ulcers and about 1.000 € in case of foot ulcers, which sums up to 2-4% of the total healthcare budget. In general, it is estimated that 1-1.5% of people are suffering from wound infection once in their life time[1], [2]. In case of burn wounds, infection remains the most common cause of patient's morbidity and mortality until now. However, patients suffering from burn wounds have a particularly elevated risk to develop infection and wound sepsis [3]. In general, wound healing consist of four overlapping phases: haemostasis, inflammation, proliferation and remodelling, whereby the development of an infection is independent of the wound status.[4], [5] If the host defence is not any longer capable of overcoming the bacterial burden, an infection takes place causing delayed wound healing and in the worst case sepsis, followed by possible patient's mortality.[4],[6].Therefore, the development of effective wound treatment and management strategies are needed. Approaches using topical antiseptics in wound care of infected wounds are already described to be a successful alternative to antibiotics. In this regard, the prevention of the development of possible antibiotic resistances in the wound colonizing bacteria can be overcome.[7] In general, extensive abuse of antibiotics in wound care led to new virus occurrence and the prevalence of multi-resistance bacteria such as vancomycin-resistant *Enterococcus* (VRE) or methicillin-resistant *Staphylococcus aureus* (MRSA)[8]. These occurrences have triggered new research approaches for antimicrobial textiles. In this context, the aim of the use of natural components as antimicrobial and antiseptic agents in wound care has grown steadily. Eugenol, a phenylpropanoid, which can be extracted from essential oils of e.g. clove oil, nutmeg, cinnamon or bay leaf, is one of these known substances with antimicrobial activity [9], [10]. The antibacterial activity against gram-positive and gram-negative bacteria has been demonstrated in various studies using either plant extracts of clove (*Caryophyllus aromaticus*) [11], basil (*Ocimun basilucum*)[11], cinnamon bark (*Cinnamomum zeylanicum*)[10] or eugenol as pure phytochemical[11], [12]. Hereby,

minimum inhibiting concentrations (MIC) between 0.5 and 1.0 mg mL^{-1} for *S. typhimurium* and *E. coli* and MIC over 1.0 mg mL-1 for *L. monocytogenes* were found [12]. Furthermore, Yoo et al. reported that eugenol from clove inhibits cancerous cells' proliferation [13]. In general, the functionalization of textiles with antimicrobial agents is of great interest [14]. The combination of textile fiber functionalization and nanotechnology to achieve antiseptic and antimicrobial properties was previously investigated by the application of metal-based nanoparticles. Hereby, either silver [15]–[18] or zinc oxide[19]–[21] nanoparticles or a combination of both particle species [22] were used to provide antimicrobial properties against gram-positive and gram-negative bacteria. Biopolymer-based approaches were reported to combine alginate [23] with silver or titan dioxide[24] nanoparticles, chitosan with zinc oxide or to functionalize silk fibers with lysozyme[25]. However, the functionalization of textile blends with protein-based stimuli responsive antimicrobial nanoparticles has not yet been reported.

In this study, this new approach was investigated by combing eugenol loaded HSA/SF nanocapsules with enzyme functionalized cotton/PET blends to achieve microbial growth inhibition for both gram-positive and gram-negative bacteria. As a new published study by Rittié et al. revealed the beneficial influence of sweat glands on reepithelialisation in wounds [26] release behaviour of eugenol loaded HSA/SF nanocapsules were tested in-vitro in different artificial sweats.

4.2 Material and Methods

4.2.1 Materials, Chemicals and Enzymes.

The used enzymes, Cellic CTec3® as cellulase cocktail and *Humicola insolens* cutinase (HiC) were purchased from Novozymes (Copenhagen, Denmark), and used without prior purification steps. Medical tissue (130 thread count, cotton/poly(ethylene terephthalate (PET) blends, 50%) were purchased from Sobaks Home medical supply, Inc. (Owosso, Michigan, USA). Cocoons of the silk worm *Bombyx mori* were purchased from the Academy of Agricultural Sciences, Sericulture and Agriculture Experiment Station (Vratsa,

Bulgaria). Human serum albumin (HSA) and 2-Methoxy-4-(2-propenyl)phenol (Eugenol) were purchased from Sigma Aldrich (Saint Louis, US). Spectra/Por 3 Dialysis Membranes (Spectra/Por 3 Standard RC Tubing MWCO 3.5 kDa) were purchased from Spectrumlabs (US). All other chemicals were of analytical grade and used as received.

4.2.2 Biochemical characterization of enzymes.

Protein concentration determination was accomplished according to the Bradford protein assay (Bio-Rad Laboratories GmbH, Vienna, Austria, Catalyst No.: 500-0006), which was carried out as previously described [9]. Cutinase activity assay was performed with p-NP-butyrate (*p*-NPB), as described by Pellis *et al*. [10]. The filter paper assay (FPA) was used as recommended by IUPAC for the measurement of cellulase activity. Rolled filter paper (7.5 × 75 mm2, around 50 mg each) was submerged in a glass tube with 1 mL 50 mM sodium citrate buffer pH 4.8. Therefore, 100 µL of cellulase enzyme cocktail (diluted 1:1000) was added to the substrate. The reaction was stopped at different time points (0, 5, 10, 20, 40, 60 min) by adding 500 µL of 1 M NaOH. Specifically, for the first time point at 0 min NaOH was added before the enzyme and this reaction was considered as blank. Afterwards, 3,5-dinitrosalicylic acid (DNS) reagent was added and the sample was boiled for 5 min, followed by the addition of 1 mL of ultrapure water [11]. 200 µL of each sample were transferred in a 96 well-plate and the absorbance was measured at 540 nm. All measurements were conducted in triplicates.

4.2.3 Enzymatic treatment of cotton/PET blends.

Textile samples were cut into 2 x 2 cm; afterwards they were washed in three steps. First, 100 mL of 5 g L^{-1} Triton solution were added and then mixed for 30 min at 60 °C and 150 rpm. In the second step, the solution was removed and 100 mL of 0.1 M sodium carbonate solution (Na_2CO_3) were added and mixed at the same conditions. In the last step, the Na2CO3 solution was removed and about 100 mL ultrapure water was added and again mixed with the same conditions. After the last washing step, the solution was removed, and the samples were dried under the fume hood for 12 h. In order to functionalize cotton components within the blended textiles to obtain functional groups

(OH)[11], the washed samples were incubated with different solutions of Cellic CTec3® (1, 2.5 and 5%) in 100 mM citric acid buffer pH 4.8 and incubated at 60 °C and 150 rpm. On the other hand, PET components within the blended textiles were functionalized to obtain -COOH moieties [12] *via* incubation with HiC, with the same concentration and conditions as the cellulase cocktail, in 100 mM potassium phosphate buffer pH 7. The enzymatic incubations were performed for 24, 48 and 72 h. Thereafter, samples were washed as previously described. The percentage of weight loss caused by the enzymes was determined after the washing/drying steps of the samples.

4.2.4 High-Performance Liquid Chromatography (HPLC).

After enzymatic treatment of the cotton/PET fabrics, the biocatalysts ware precipitated. In case of cutinase incubation, methanol precipitation was used. 500 µL of samples were diluted with 500 µL of cold methanol, then centrifuged (Centrifuge Beckman JU-MI) at 14000 rpm at 0 °C for 15 min. The supernatant was acidified by adding 10 µL of 6 M HCl and then transferred into HPLC vials. For HPLC (Agilent Technologies, 1260 Infinity, Palo Alto, CA, USA) measurements, a reversed phase column C18 (Poroshell 120 EC-C18 2,7 µm 3.0x150 mm) was used. Analyses were carried out using a H_2O/MeOH/HCOOH gradient (Tab. S1). The flow rate was set to 0.8 mL min^{-1} with a constant temperature of 40 °C. The injection volume was 10 µL. For PET functionalization studies, a terephthalic acid calibration curve was prepared to quantify the amount of monomer released. On the other hand, after the enzymatic incubation, the products from cotton degradation were treated using Carrez-precipitation [13]. Therefore, 20 µL of 2% of K4[Fe(CN)6] $3H_2O$ solution were added to the samples, after vortexing and incubation for 1 min, 20 µL 2% of $ZnSO_4$ $7H_2O$ solution were added. After vortexing and incubation for 5 min, the samples were centrifuged (30 min, 14000 rpm, 25 °C). The supernatants were filtered into glass vials. HPLC-RI (1100 series, Agilent Technologies, Palo Alto, CA) was used for separation equipped with an ICSep-ION300 column (Transgenomic Organic, San Jose, CA) of 300 mm by 7.8 mm and 7 µm particle diameter. As mobile phase, 0.01 N H_2SO_4 was used with a flow rate of 0.325 mL/min at 45 °C. A 40 µL sample was injected, and the runtime was 45 min. A glucose calibration (10-250 mM) curve was prepared.

4.2.5 Surface analysis using attenuated total reflection Fourier transform infrared spectroscopy and scanning electron microscopy.

After the enzymatic functionalization, ATR-FTIR analysis using a Spectrum GX spectrometer (Perkin Elmer, USA) with diamond ATR accessory (Spec Ltd., UK) was performed. A total of 30 scans for each sample were taken with a resolution of 1 cm^{-1} and normalized in the range of 2500-2000 cm^{-1} before any data processing. The bands were assigned as follows: 3300 cm^{-1} –OH groups from cellulosic fiber , 870 cm^{-1} C–H out of plane bending, 1720 cm^{-1} ν(C=O), 1590 cm^{-1} ν(C=C), 1250 cm^{-1} ν(C–O–C)[14].

4.2.6 Extraction of silk fibroin from *Bombyx mori* cocoons.

Silk fibroin (SF) extraction was slightly modified from the published protocol of Rockwood *et al.*[15]. In brief, cut silk cocoons were degummed by boiling in 0.02 M sodium carbonate solution for 30 min (30 mb) or 60 min (60 mb), resulting in two different degradation degrees of SF fibers. Resulting SF fibers were washed three times with ultrapure water and dried overnight. Further, 20% w v-1 SF fibers were dissolved in a 9.3 M lithium bromide solution at 50 °C for 5 h. Subsequently, the resulting SF solution was dialyzed against ultrapure water for 3 days. The SF solution was then purified by two centrifugation steps and stored at 4 °C until further use.

4.2.7 HSA/SF nanocapsules production and encapsulation of eugenol.

HSA/SF nanocapsules production (unloaded and eugenol loaded) was based on the ultrasound induced self-assembling approach published by Tallian *et al.*[16], whereby the method was modified regarding maximum eugenol encapsulation. Protein solutions (HSA and SF in ultrapure water) in different concentrations (0-75 % SF in two different degradation degrees, e.g. 30 mb or 60 mb) were added to 2 mL of 100 mM potassium phosphate buffer pH 8.0 to obtain a total protein concentration of 4.2 mg (**Table S2**). Subsequently, 1.3 mL of n-dodecane were added as organic phase for unloaded nanocapsules and the mixtures were sonicated using a Branson Sonifier 250 (Emerson, Saint Louise Missouri, US) equipped with a disruptor horn (13 mm diameter). The

sonication time was set to 2 min with a pulse on time of 1 sec followed by a pulse off phase for 2 sec with a constant amplitude of 10%. The amplitude was chosen based on initial experiments testing nanocapsules formation at different amplitude settings, whereby no significant impact on was obtained (Figure S6). For eugenol loaded HSA/SF nanocapsules 1 mg mL^{-1} (1%) of eugenol was added to the organic phase before sonication. After sonication, the mixtures were stored at 4 °C for 12 h for phase separation. Thereafter, the organic phase was removed, performing 5 washing steps with 100 mM sodium phosphate buffer with pH 7.4. Briefly, samples were centrifuged at 4 °C and the supernatants were removed after each step and replaced with new buffer. After completion, the obtained nanocapsules dispersions were stored at 4 °C until further use or analysis.

Determination of the hydrodynamic radii. The size of unloaded and eugenol loaded HSA/SF nanocapsules was analysed using a Dynapro Nanostar (Wyatt Technology Europe, Germany) system. A total measurement time of 30 min at 21 °C with 20 acquisitions and an acquisition time of 2 sec each was used. Data were evaluated using a baseline limit (+/-) data filter set at 0.05 and maximum SOS filter limit of 200. The obtained average hydrodynamic radius (RH) of each sample was evaluated for three measurement periods, i.e. 0-10 min, 10-30 min and 0-30 min, to evaluate nanocapsules dispersion properties. Temperature induced fluctuations in RH were analysed in a temperature range between 25 and 75 °C with similar measurement and data evaluation settings.

Zeta potential determination using laser-Doppler velocimetry. Zeta potential measurements of unloaded HSA/SF nanocapsules for the evaluation of colloidal stability were performed using a Zetasizer Nano ZS (Malvern Instruments GmbH, Germany). Samples were diluted (15x) and analysed in 100 mM sodium phosphate buffer with pH 7.4 three times in automatic mode. Obtained results were averaged and outlier identification was performed using a modified Thompson tau test.

Secondary structure analysis using attenuated total reflection Fourier transform infrared spectroscopy. ATR FT-IR analysis was accomplished of lyophilized unloaded and loaded HSA/SF nanocapsules using a Spectrum GX spectrometer (Perkin Elmer, USA) with diamond ATR accessory (Spec Ltd., UK). The obtained spectra, which were recorded in the range of 650-4000 cm^{-1} with a spectral resolution of 1 cm^{-1} were normalized between 650 and 1200 cm^{-1} and baseline corrected[16]. For each sample three single spectra with each 15 scans were performed and averaged. For cross-linking confirmation the ratios of different secondary structures (α-helix and β-sheet) were evaluated similar to the method published by Tallian *et al.*[16].

Scanning electron microscopy (SEM). Morphology of eugenol loaded HSA and HSA/SF nanocapsules was investigated using a Hitachi 3030TM instrument (Metrohm INULA GmbH) equipped with a cryo chamber (-20 °C) working at energy-dispersive X-ray spectrometry (EDX) acceleration voltage. All images were acquired by collecting secondary electrons during the measurement.

Determination of the encapsulation efficiency. Encapsulation efficiency of eugenol during HSA/SF nanocapsules production was determined by collecting the washing solutions of the five washing steps. Experiments were performed in triplicates and samples were filtered (0.2 µm Nylon) prior to the analysis. Eugenol concentration was determined using a 1260 HPLC system equipped a Poroshell 120 EC-C18 4.0 µm (4.6*5 mm, 120 Å) guard column coupled to a Poroshell 120 EC-C18 4.0 µm (4.6*50 mm, 120 Å) column (Agilent Technologies, US). For detection a G7117A DAD detector (Agilent Technologies, US) was used and the DAD signals were monitored at 280 nm. The injection volume was set to 10 µL. The mobile phase was a 40/60 mixture of ultrapure water and acetonitrile. External calibration, including the limit of detection, limit of determination and the limit of quantification determined based on DIN32645, was performed using a standard dilution series in methanol with concentrations of between 1.0 and 0.0001 mg mL^{-1}. Calculation of the encapsulation efficiency (EE) was performed using equation 1.

Equation (1): $EE[\%] = \left(\frac{c_I - c_E}{c_I}\right) * 100$

EE: Encapsulation efficiency

c_I: Initial concentration of eugenol (1 mg L^{-1})

c_E: Concentration of encapsulated eugenol (mg L^{-1})

pH-responsive release studies. pH-responsive release was studied in three simple standardized artificial sweat solutions (**Table 1**) of various pH, which were prepared as described in the paper of Callewaert *et al*.[17].

Table 1. Compositions and pH-values of artificial sweats (ISO pH 5.5, ISO pH 8.0 and EN pH 6.5) published by Callewaert *et al.*[17]. used for the release studies of HSA/SF nanocapsules loaded with eugenol. All artificial sweats were sterilized by filtration before use, pH was adjusted using 1 M HCl or 1 M NaOH.

Composition	**Concentration [% w v^{-1}]**		
	ISO pH 5.5	**ISO pH 8.0**	**EN pH 6.5**
Sodium chloride	0.50	0.50	1.08
Urea	-	-	0.12
Lactic acid (88%)	-	-	0.13

For each sample of eugenol loaded HSA/SF nanocapsules release experiments were performed in triplicates. Hence, 200 µL of nanocapsules dispersions were incubated in 1 mL of the different artificial sweats at 37 °C and 150 rpm for 168 h to mimic skin environment and mechanical stress. Samples were taken after 1, 3, 6, 24, 48, 120, 144

and 168 h, whereby the artificial sweats were separated from the HSA/SF nanocapsules and replaced with 1 mL of fresh artificial sweats and the incubation was prolonged until the next sampling time point. The eugenol concentration was determined using the described HPLC-DAD method (see section “Determination of the encapsulation efficiency”). Thereafter, the cumulative release over 168 h was calculated based on the obtained HPLC-DAD data for each formulation and artificial sweat. All data were tested and corrected for outliers.

Cytotoxicity studies of eugenol loaded and unloaded HSA/SF nanocapsules. Cytotoxicity studies were performed according to the method previously published by Tallian *et al.*[16]. Briefly, THP-1 cells (human acute monocytic leukaemia cell line) were cultivated in 10% FBS, 1% L-glutamine, 1% penicillin-streptomycin (Lonza, Switzerland) and 0.05 mM 2-mer- captoethanol (Sigma Aldrich, US) containing PRMI 1640 cell culture media in humidified atmosphere (5 % CO_2) at 37 °C. Cytotoxicity of unloaded and eugenol loaded HSA/SF nanocapsules were analysed using a commercial MTT assay (3-(4,5-dimethylthiazol-2-yl)-2,5-diphe- nyltetrazolium bromide; Sigma Aldrich, US). Hereby, THP-1 monocytes were incubated with nanocapsules formulations (1 mg mL^{-1}, 250 µg mL^{-1} and 62.5 µg mL^{-1}) for 24 h. Negative and positive control groups were included as previously published[16]. After completing the incubation time, MTT reagent was added to the incubated cells (650 µg mL^{-1}) and the incubation was prolonged for 1 h at similar conditions. Subsequently, cell culture suspensions were centrifuged at 250 g for 5 min, the supernatant was removed and DMSO was added. Afterwards, the plate was incubated on a mechanical shaker at 200 rpm in the dark for 20 min, which was followed by an absorbance measurement at 540 nm using a Tecan Sunrise plate reader (Tecan Trading AG, Switzerland). All obtained results are presented as mean ± standard deviation (SD) of the performed triplicates, whereby a Kruskal-Wallis test with Dunn’s multiple comparison test was used for group comparisons (p-values≤0.05).

4.2.8 Immobilization of loaded HSA/SF nanocapsules.

For the attachment of nanocapsules to the enzymatically functionalized textile fabric samples using the EDC/NHS system (see sample description in **Table 2**), an EDC stock solution with 200 mg mL^{-1} and an NHS stock solution with 400 mg mL^{-1} were produced in MES-Buffer (0.1 M, pH 4.6). Crosslinking reactions were performed in 12-well plates using a final volume of 3 mL at 150 rpm and 21 °C. MES-Buffer, EDC and NHS were added in suitable amounts to reach final concentrations in the reaction mixture of 50 mg mL^{-1} EDC and 100 mg mL^{-1} NHS. The according amount of MES buffer (to a total reaction volume of 5 mL) was added to the fabric, followed by 750 µL EDC stock solution. After 10 min, 750 µL of the NHS stock solution were added and after another 10 min incubation time 250 µL of nanocapsules solution were added. The latters were allowed to bind for 24 h at 150 rpm and 21 °C. For a control sample without nanocapsules 750 µL EDC solution, 750 µL NHS solution and 500 µL MES buffer were added. After incubation, samples were washed 4 times with ultrapure water and dried overnight at 21 °C.

Table 2. Sample ID for immobilization studies including the blank reactions (I-IV) and the immobilized nanocapsules (NCs) containing different ratios of HSA and SF.

ID	Sample information
I	Fabric
II	Fabric + EDC
III	Fabric + NHS
IV	Fabric + EDC + NHS
V	Fabric + EDC + NHS + Eugenol loaded HSA NCs
VI	Fabric + EDC + NHS + Eugenol loaded 3010 NCs
VII	Fabric + EDC + NHS + Eugenol loaded 3025 NCs

VIII	Fabric + EDC + NHS + Eugenol loaded 3050 NCs

Morphology analysis of nanocapsules functionalized cotton/PET blends. In order to confirm the successful coupling of eugenol loaded HSA/SF nanocapsules to the textile surface of cotton/PET blends, SEM analysis were performed using the method described in section “Scanning electron microscopy (SEM)”.

Antimicrobial studies.

Overlay method. 50 mL of the Mueller Hinton (MH) medium were pipetted into a shaking flask and inoculated with a colony of *Staphylococcus aureus*. In the same way, a colony of *Escherichia coli* was incubated in 50 mL of LB medium. MH and LB media were chosen, as they are suggested by the distributor as optimum growth media. Both overnight-cultures (ONCs) were incubated for 12 h overnight at 37 °C and 150 rpm. Afterwards, the optical density (OD) was measured at 600 nm and the amount of colony forming units (CFU) mL^{-1} was calculated[18]. The textile samples and the blanks (triplicate of each) were placed in the middle of petri dishes containing MH and LB soft agar. The MH and LB soft agar were prepared, cooled down to 45 °C and inoculated with the ONC to reach a final concentration of 105 CFU mL^{-1}. 2.5 mL of the soft agar were pipetted into every petri dish to cover the textile fabric samples completely. Then, they were incubated for 24 h at 37 °C in a static incubator. The diameter of the area of growth inhibition was measured at two points and the average was taken to determine the antimicrobial activity of the crosslinked nanocapsules.

Saline method. The samples and the blanks (triplicate of each) were placed in 12-well-plates and 2 mL of the physiological saline solution (containing 0.85% NaCl) were pipetted into the sample or blank containing wells. The residual saline solution was inoculated with the ONC to reach a final of 7.3 x 105 CFU mL^{-1} [19]. The well-plates were incubated for 24 h at 37 °C and 150 rpm. 50 µL of every well were pipetted and spread into a petri dish, filled with agar media (LB and MH). The petri dishes were placed in a static incubator for

24 h at 37 °C. The CFUs on every petri dish were counted to determine the antimicrobial effect of the crosslinked nanocapsules.

4.3 Results

In this study, the coupling of antimicrobial HSA/SF nanocapsules onto cotton/PET textile blends was investigated (schematic overview, see ESI, Figure S5). To allow the attachment of the protein-based nanocapsules onto the polyester surface via EDC/NHS chemistry, the number of carboxyl groups was increased via limited enzymatic hydrolysis. Since the material was composed of 50% PET/Cotton, we tested the possibility to functionalize cotton, using oxidases in the enzyme cocktail mixture, whereby -COOH groups can be generated. Furthermore, PET was activated by HiC to directly generate -COOH groups.

4.3.1 Enzymatic surface activation of cotton/PET blends.

Enzymatic functionalization benefits from the milder reaction conditions[20], high specificity/selectivity and less damages over the physical and chemical methods[21]–[23]. Therefore, fabric samples were incubated with cellulase cocktails and cutinase to determine, which enzymatic treatment leads to higher functionalization and less fiber damages. Briefly, cellulase treatment demonstrated 15% of weight loss already after 24 h of incubation and with the lowest amount of enzymes (1% v/v) (Figure 1A). On the other hand, the incubation with cutinase demonstrated a lower weight loss profile, obtaining approximately 7% of weight loss with the lower concentration of enzyme (1% v/v) after 48 h (Figure 1B). Incubation with 2.5% and 5% of HiC resulted in similar results compared to the lowest concentration. HPLC results confirmed that the amount of glucose (cotton degradation product) obtained, were much higher than the terephthalic acid released from PET (Figure 1C & D). Consequently, the incubation for 24 h with 1% HiC was preferred to the other incubation conditions.

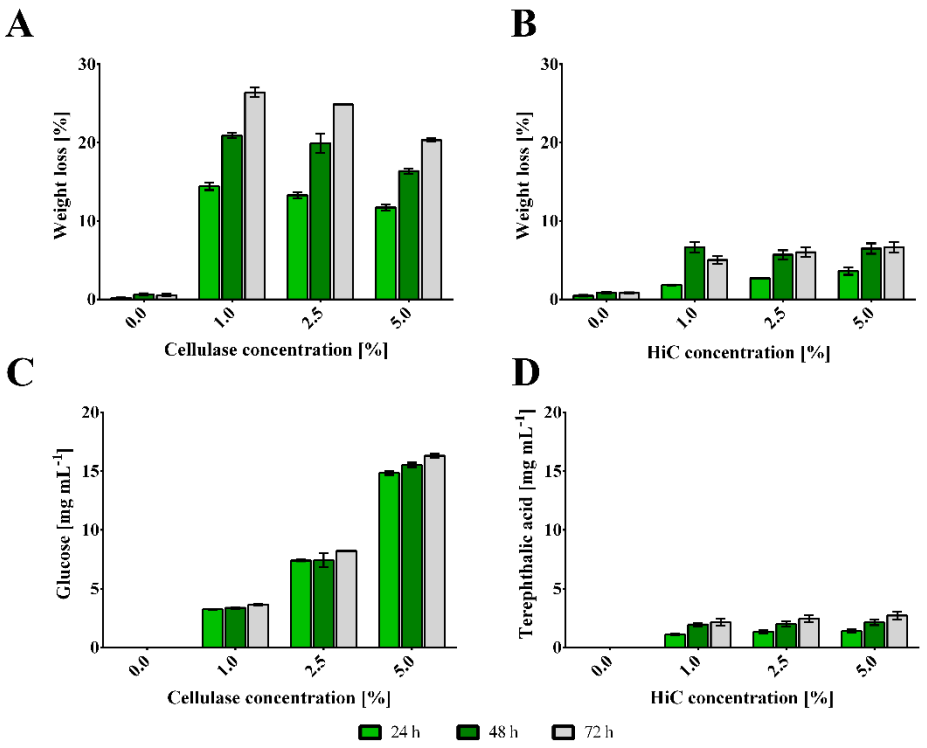

Figure 1. (A) Cotton/polyester blend weight loss with different concentrations of cellulase cocktail (1-5%) after 24, 48 and 72 h (B) Cotton/polyester blend weight loss with different concentrations of *Humicola insolens* (1-5%) cutinase after 24, 48 and 72 h (C) Glucose (cotton monomer)concentration released with cellulase cocktail incubations (1-5%) after 24, 48 and 72 h (D) Terephthalic acid (PET monomer) concentration released with HiC incubations (1-5%) after 24, 48 and 72 h. All experiments were performed in triplicates.

This result was further confirmed by FT-IR analysis. The intensity of the band at 1720 cm^{-1}, which represent the carbonyl stretching vibration, was reduced after such incubation condition. Furthermore, the band at 1240 cm^{-1} (C(=O)-O stretching and CC stretching) showed lower intensity after hydrolysis (Figure 2). The change of shape and intensity of the bands at 1240 cm^{-1} and 1100 cm^{-1} confirmed that the enzyme could cleave the ester bonds within the PET structure, while modifying the cellulose structure leading to the reactive surface for the subsequent nanocapsules functionalization.

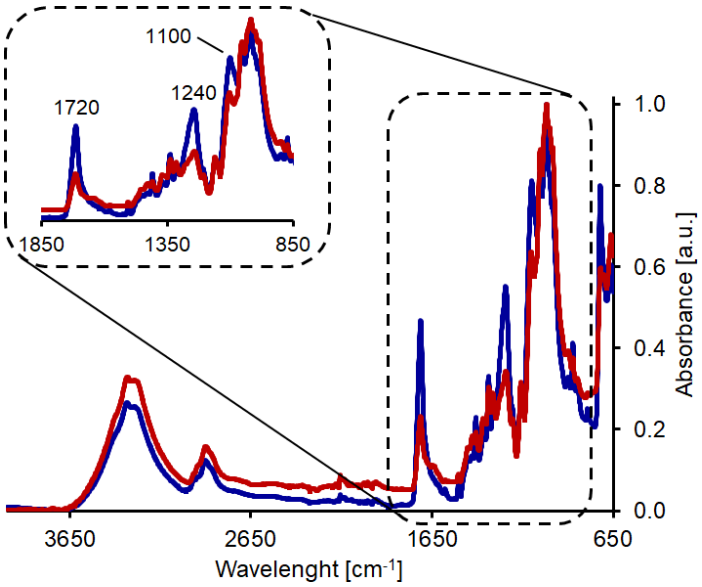

Figure 2. FT-IR spectroscopy of cotton/polyester blends. Untreated sample (blue line) and sample after incubation with 1% HiC 48 h (red line). Spectra were baseline corrected and normalized in the range of 2500-2000 cm^{-1}.

4.3.2 HSA/SF nanocapsules production and formulation properties

For the production of antimicrobial textiles via the immobilization of HSA/SF nanocapsules, eugenol was encapsulated during particle production. Hereby, the successful self-assembly based on ultrasound induced formation of crystalline β-sheets and the liked enhanced stability due to the physical crosslinkingwas investigated using ATR-FTIR spectroscopy and compared to data published by *Tallian et al* (**Figure 3C**) [16]. Previous studies have proven micelle formation by the interaction of the hydrophobic sequence motives of SF (GAGAGS) with the organic solvent during ultrasound treament. In this study, eugenol was added in the organic phase before sonication, resulting in a slight decrease of the β/α ratios for all tested formulations (HSA, HSA/SF with two different degradation degrees and various percentages of SF). Direct comparison of 30 mb eugenol loaded HSA/SF nanocapsules with 60 mb formulations showed no significant difference in crosslinking efficiency for formulations of ident SF concentration. Thus, the addition of eugenol in the organic phase (n-dodecane) can be directly linked to the decrease in crosslinking efficiency. This effect can be caused by the slight change in solvent viscosity

(n-dodecane <0.002 Pa*s, eugenol 0.007817 Pa*s) which directly influences solvent dispersion, ultrasound wave propagation and cavitation effects such as formation, growth and implosion of the obtained microbubbles. This hypothesis is supported by studies published by Cheng et al.[40], Lévêque et al and Hemwimol et al that investigated the influence of solvent properties on cavitation effects in ultrasound-assisted extraction and dispersion approaches. The impact on the cross-linking efficiency can therefore be directly linked to the concentration of SF in the formulations, which is further supported by physical parameters such as hydrodynamic radius, colloidal stability (**Figure 3A-B**) and morphology were assessed.

Size analysis using DLS resulted in hydrodynamic particle radii of eugenol filled HSA/SF nanocapsules ranging between 303.77 ± 0.75 nm (6050) and 574.00 ± 92.76 nm (3010) (**Figure 3A** and **Table S3**). Hereby, the hypothesized trend of increasing nanocapsules sizes of HSA/SF nanocapsules with increasing SF concentration could not be applied on eugenol loaded HSA/SF published data of Tallian *et al.*[16]. To ensure nanocapsules stability, size, and uniformity, of the chemical and nanocapsules, as the addition of eugenol led to an inverted effect on nanocapsules size. Viscosity related influences on cavitation effects, solvent dispersion and during capsule formation are hypothesized to be the triggering factors for these observations. Distortions are therefore correlating with the concentration of SF in the formulations. However, both in DLS based time dependent (**Figure 3A** and **Table S3**) and temperature dependent (**Figure S1**) stability studies revealed high variations in the initial third of the measurement time due to directed movement, i.e. floating caused by the hydrophobic core.

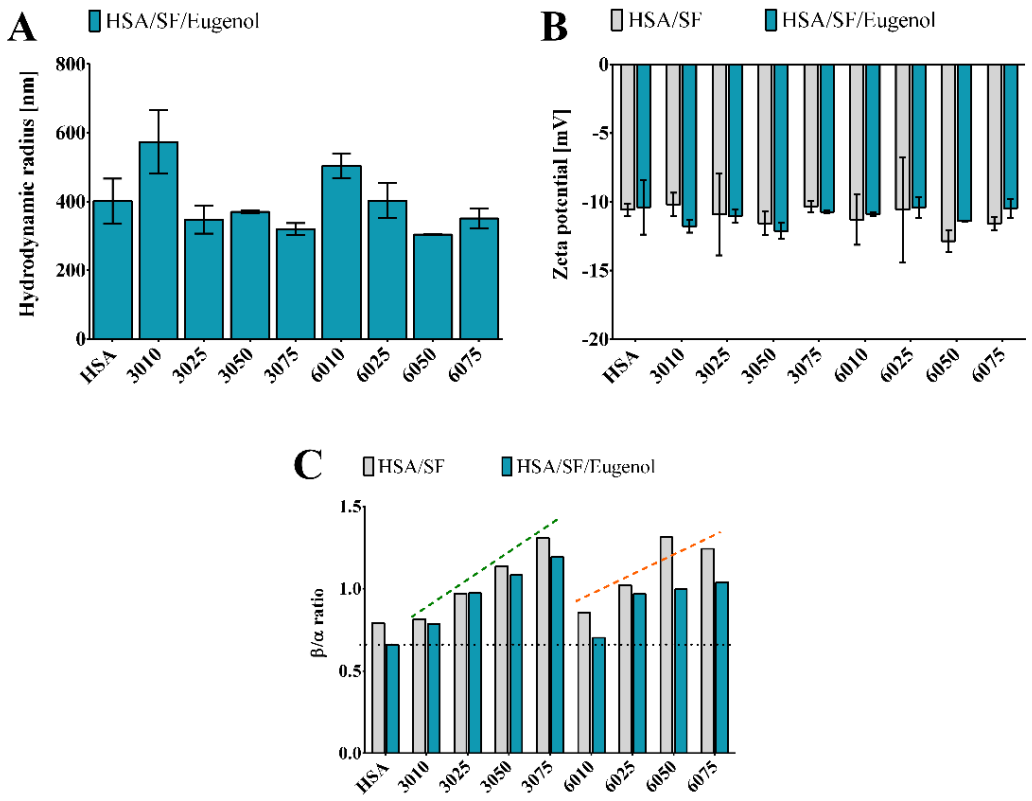

Figure 3. Characterization of monodisperse eugenol filled HSA/SF nanocapsules composed of different percentages of SF (10-75%) and two different degradation degrees (30 or 60 mb). (A) Dynamic light scattering based hydrodynamic radii in nm. (B) Zeta potential in mV compared to unloaded HSA/SF nanocapsules with ident protein concentrations. (C) Secondary structure ratios (β/α ratios) calculated from ATR-FTIR spectra of unloaded and eugenol loaded HSA/SF nanocapsules for the amid I bands (β: 1626 cm^{-1}; α: 1648 cm^{-1}), whereby the increase in β-sheets structures is separately indicated for nanocapsules containing 30 or 60 mb SF by dashed lines

After an analysis time of 10 min all formulations showed high stability, e.g. no fluctuations or temperature induced disruption up to 75 °C. Furthermore, colloidal stability was investigated using laser Doppler-velocimetry. Zeta potential values (**Figure 3B**) were obtained ranging from -10.18 ± 0.84 mV to -12.86 ± 0.82 mV for unloaded and ranging from -10.39 ± 1.99 mV to -12.11 ± 0.59 mV for eugenol loaded HSA/SF nanocapsules. For all formulations the addition of eugenol during nanocapsules formulation showed no significant impact on colloidal stability, confirming that eugenol was encapsulated in the nanocapsules cores. In general, particles/capsules with zeta potential values between -

10 to -20 mV are considered as relatively stable [24], whereby aggregation behaviour was further investigated in combination with nanocapsules morphology. Particle morphology and size, as well as the corresponding surface area to volume ratio are crucial parameters for enhanced targeted release properties [25]. Scanning electron microscopy images of eugenol loaded HSA/SF nanocapsules showed spherically shaped structures, however analysis influenced the nanocapsules size due to sample freezing related expansion of the nanocapsules cores (**Figure S2**). Additionally, all samples showed high uniformity and stability without the tendency for aggregation.To ensure a maximum eugenol encapsulation during particle production, and achieve a high antimicrobial activity, the encapsulation efficiency was determined. Enhanced efficiencies are of high importance as drug encapsulation allows a decrease in therapeutics loss, reduction of substance amount used during production and the guarantee of prolonged release rates [26]. HPLC-DAD analysis of eugenol evaluated based on DIN32645 showed values below the limit of detection indicating a complete encapsulation of eugenol for all formulations tested. Based on these results, *in-vitro* release studies were performed to ensure the release of eugenol for antimicrobial activity. In this context, release studies were designed to mimic possible future applications, whereby nanocapsules will be immobilized on cotton/PET textile blends possibly used in wound treatment. Rittié *et al*. revealed the benefiting influence of sweat glands on re-epithelialization in wounds [27], hence release kinetics were tested in artificial sweats of various pH and compositions (**Table 1**). Thus, the interaction between sweat (e.g. beneath a wound dressing for burn wound treatment, if sweat glands are intact) and the benefiting release properties for antimicrobial activity could be accessed for the produced eugenol loaded HSA/SF nanocapsules system.

The pH of open wounds is reported to range from 6.5 to 8.5 and for burn wounds ranging between pH 5.3 and 8.4, which is significantly elevated compared to the average pH of 5.5 of intact skin (range: 4.8-6.0) [28]. Thus, the pH values of the artificial sweats were chosen to cover these ranges. Generally, due to enzyme activity wound pH should not fall below 4 as the acidic pH permanently inactivates proteases and therefore healing activity is disabled [28]. Cumulative release of HSA/SF nanocapsules containing 60 mb SF

showed generally similar release values as for nanocapsules containing 30 mb SF (ISO pH 5.5: 35.27% for 3010 and 37.86% for 6010), indicating that the release of eugenol is independent of the degradation degree of SF.

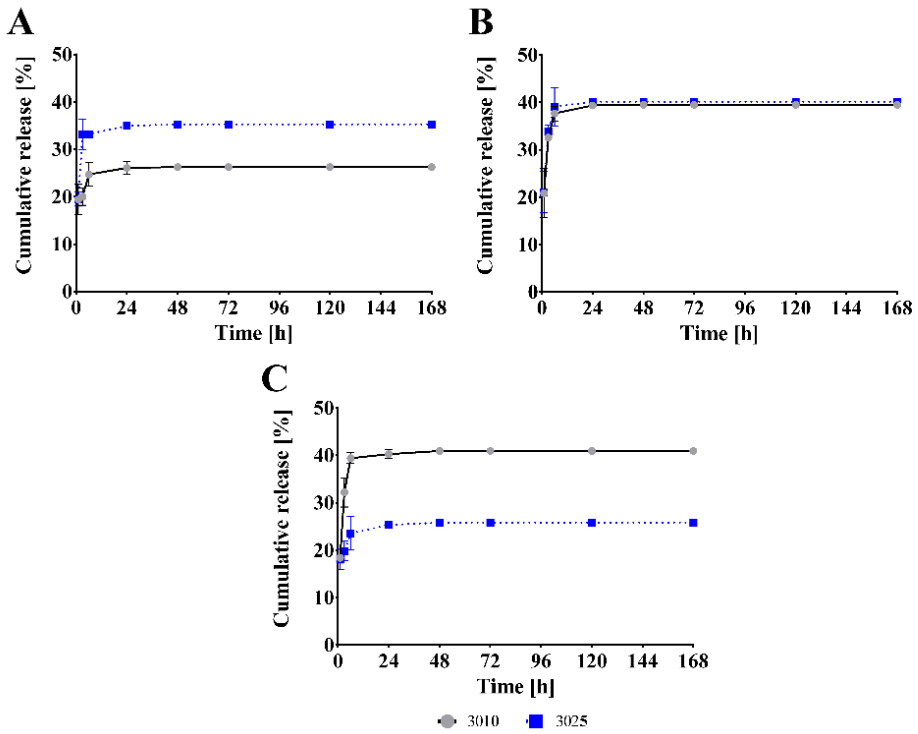

Figure 4. Average cumulative release of eugenol from HSA/SF nanocapsules with lower degradation degree (30 mb) and 10 or 25% SF over a time period of 168 h in artificial sweats prepared as previously described by Callewaert *et al.* [17]. (A) ISO pH 5.5, (B) ISO pH 8.0 and (C) EN pH 6.0. All time points were measured in triplicates.

Maximum eugenol release could be obtained with the formulations 3010 (40.93% at pH 6.0) and 3025 (40.11% at pH 8.0), whereby SF containing formulations showed a faster release kinetic compared to HSA (**Figure 4** and **Figure S2**). Compared to previous studies a correlation of decreases in cumulative release with increasing pH could be confirmed (**Figure 4C**), however for all pH values a maximum release of approximately 40% could be obtained depending on the used formulation.

Cytotoxicity tests.

To ensure the safety of the produced unloaded and eugenol loaded HSA/SF nanocapsules, cytotoxicity studies on human THP-1 monocyte cells were performed similar to the method published by Tallian *et al.*[16] (**Figure 5**). Eugenol loaded HSA/SF nanocapsules formulation showed slightly decreased cell viability If applied in higher concentrations of 250 µg mL^{-1} and 1 mg mL^{-1}, whereby the cytotoxic effect decreased with increasing percentage of silk fibroin in the formulations for both unloaded and loaded HSA/SF nanocapsules at these higher concentrations. At the lowest tested concentration, i.e. 62.5 µg mL^{-1} no significant decrease in cell viability compared to the control group could be detected, indicating that eugenol loaded HSA/SF nanocapsules applied in this concentration are not affecting healthy human cells. These data correlate with previous published studies of Martins *et al.*[29], Sharma *et al.* [30] and Gerosa *et al.* [31], whereby generally the studies indicated that eugenol/eugenol derivatives showed no cytotoxic effect on normal cell lines, but selectively killed microorganism cells [29].

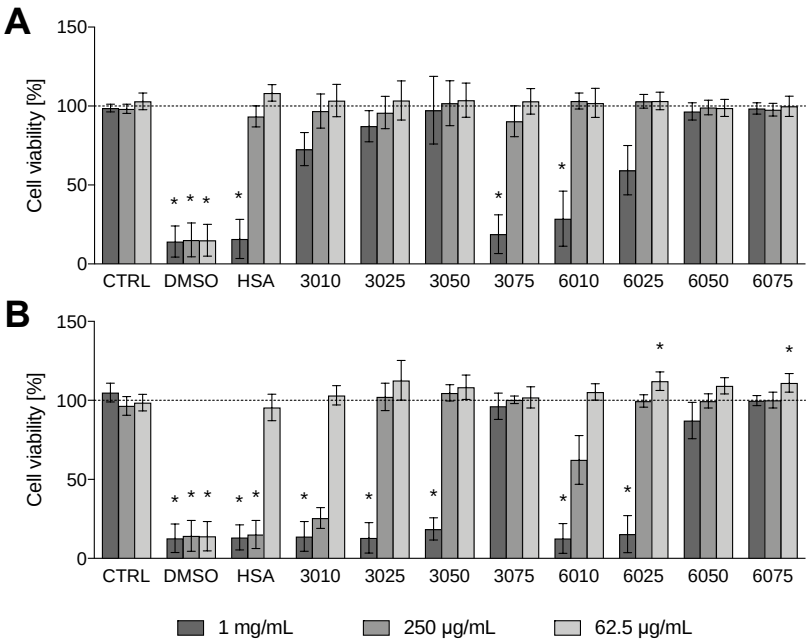

Figure 5. Effect of SF content, concentration of HSA and HSA/SF nanocapsules on cell viability of human THP-1 monocyte cells. (A) unloaded and (B) eugenol loaded particles of indicated formulations and at final concentrations of 1 mg mL^{-1}, 250 µg mL^{-1} or 62.5 µg mL^{-1} were incubated with THP-1 monocytes for 24 hours. Cell viability was determined via MTT assay and normalized to untreated control cells (CTRL; 100% viability). DMSO was used at 30% final concentration to obtain a cytotoxicity control (DMSO). (n=4; mean ± SD; Kruskal-Wallis test with Dunn's multiple comparison test; all samples were compared to corresponding untreated control (CTRL); difference of p-values is statistically not different to control, except from bars marked with *,p≤0.05).

4.4 HSA/SF nanocapsules immobilization on cotton/PET textiles and antimicrobial activity.

Based on nanocapsules characteristics, e.g. high crosslinking efficiency, low hydrodynamic radius, low zeta potential and maximum cumulative release, formulations containing 30 mb SF were hypothesized to show enhanced antimicrobial activity and therefore immobilized onto the enzymatic (with 1% HiC, 24 h at 50° C) activated cotton/PET blend. As shown in Figure 6, the different types of 30 mb SF nanocapsules were immobilized after EDC/NHS coupling reaction (**Figure S4**). Typical signals of amide bonds appear as shoulders in the 1648/1626 cm^{-1} area (amide I band) and the 1539/1516 cm^{-1} region (amide II band). The presence of nanocapsules was further confirmed by the shoulders/bands at 3070 cm^{-1}, due to the secondary –NH groups.

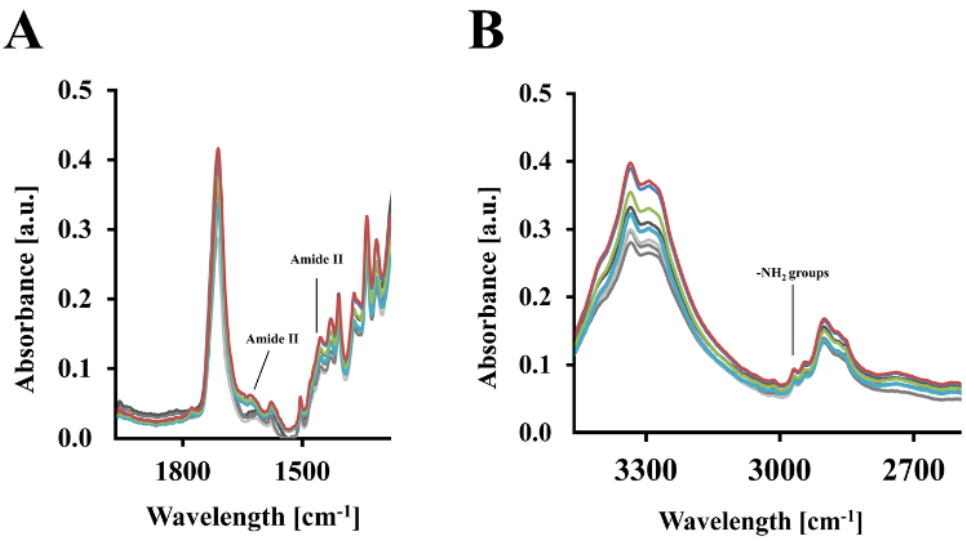

Figure 6. FTIR spectroscopy of cotton/polyester blend with immobilized HSA/SF nanocapsules. Reaction I (black line); Reaction II (grey line); Reaction III (dark grey dash line); Reaction IV (dark grey dash line); Reaction V (cyano dash line); Reaction VI (green line); Reaction VII (blue line); Reaction VIII (red line). Spectra were baseline corrected and normalized in the range of 2500-2000 cm^{-1}. (A) Amide I and II peaks identification (B) $-NH_2$ signal identification.

Additionally, SEM analysis were performed to investigate the successful immobilization of eugenol loaded HSA/SF nanocapsules on the cotton/PET blends (**Figure 7**). In the images obtained from these analyses, the nanocapsules are visible at 1000x and 3000x magnification as nanocapsules clusters attached to the cotton/PET fibers proving successful immobilization.

Spices have traditionally been used for food preservation as well as to enhance flavour and health. Eugenol, as extract from essential oils of e.g. clove oil, nutmeg, cinnamon or bay leaf [32], [33] is known for its antimicrobial activity due to the substituted aromatic structure. It has been shown that it is able to inhibit microbial growth in different levels: changes of cell membrane permeability or in the ion transport system and ATP generation inhibitions [34], [35].

In Figure 8, cotton/PET blends functionalized with different formulations of eugenol loaded HSA/SF nanocapsules have shown higher inhibition against *S. aureus* (81% inhibition, **Figure 7B**) and lower against *E. coli* (33% inhibition, **Figure 7B**). In both studies (overlay and saline methods), the eugenol loaded formulation 3010 demonstrated the highest microbial inhibition, which is in according with the fastest release, obtained during kinetic study performed with artificial sweat solution at pH 6.0.

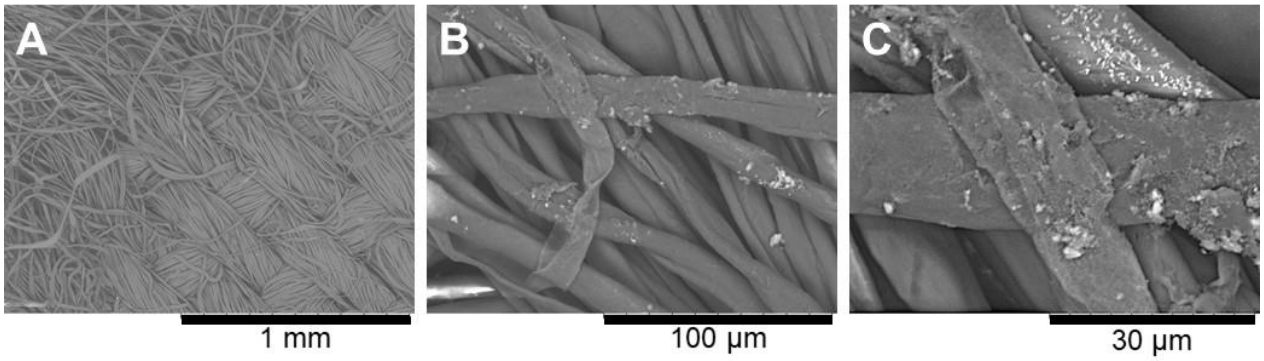

Figure 7. Scanning electron microscopy images of immobilized eugenol loaded HSA/SF nanocapsules (reaction VII, 3025) on cotton/PET blends (50%) with a magnification of (A) 100x, (B) 1000x and (C) 3000x.

A possible explanation for the higher inhibition against *S. aureus*, could be the different membrane composition, whereby gram+ seems to be more susceptible to eugenol. Generally, in gram+ bacteria the presence of eugenol leads to the damage of the bacterial membrane, possibly due to its charge and interaction with lipids. Gram- bacteria instead are not affected as gram+, they still are susceptible of eugenol presence but in minor relevance. In the work of Hemaiswarya & Doble [36], they explained that gram- microorganisms are used synergistically with antibiotics to improve the treatment effects of eugenol. Most infection cases in hospitals are due to gram+ microorganisms (e.g. *Pseudomonas aeruginosa*)[37].Therefore, the high inhibition values are seen as benefitting for the possible later application in wound dressings. Compared to the inhibition by 81% against gram+ bacteria, 33% inhibition for gram- microorganisms is not seen as high inhibition but it can reduce and prevent the possible infection from such bacteria.

This effect is additionally visible for the tested formulations containing immobilized nanocapsules 3025 followed by nanocapsules 3050, which can be further correlated with

the release studies and the cross-linking information obtained for nanocapsules production. As the cross-linking efficiency can be directly linked to the SF concentration, this can lead together with the obtained high release rates in the tested artificial sweats to the hypothesis that eugenol can be released faster due to lower cross-linking efficiencies during nanocapsules production. Hence, resulting in the desired higher antimicrobial activity. Nanocapsules uniformity and the high surface area to volume ratio are contributing to this effect, as the eugenol release can be facilitated due to increased chemical reactivity of SF. Enhanced chemical reactivity of nanoparticles was previously described in different publications by Biener *et al.* [25] and Stark *et al*. [38]. pH-induced changes in SF crystallinity where also subject of intensive research [39], which additionally confirmed the obtained results for enhanced antimicrobial activity due to higher chemical reactivity at lower pH (pH 6.0, formulation 3010). Additionally, the obtained cytotoxic effect supports presented the cytotoxicity results and the correlating studies of Martins *et al.*[29] showing that the cytotoxic effect of eugenol is limited to microorganisms cell types.

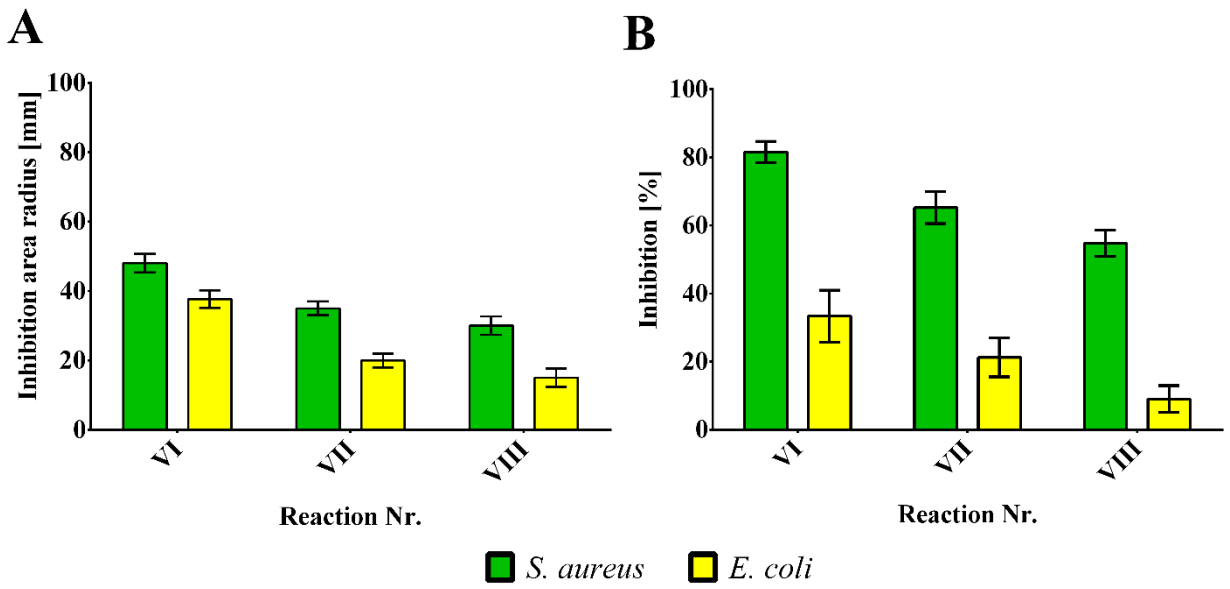

Figure 8. Antimicrobial effect of fabrics functionalised with antimicrobial nanocapsules against *S. aureus* (green bars) and *E. coli* (yellow bars). (A) Overlay method (B) saline method. All the experiments were performed in triplicates. Reaction numbers I to V are not displayed as no inhibition was obtained.

4.5 Conclusions

Antimicrobial wound dressings are of high need due to the rising numbers of antibiotic resistances. The use of immobilized pH-responsive HSA/SF nanocapsules loaded with eugenol, a phenylpropanoid, showing high antimicrobial activity, on cotton/PET blends was successfully presented as a possible future alternative for commercially available antiseptic wound dressings. Nanocapsules containing SF in a lower degradation degree with hydrodynamic radii between 319.73 ± 17.50 and 574.00 ± 92.76 nm and zeta potentials ranging from -10.39 ± 1.99 mV to -12.11 ± 0.59 mV were evaluated regarding their release properties of eugenol. In this context, formulations containing 10% of SF with lower degradation degree (3010) showed the highest release of 40.93% at pH 6.0 in artificial sweat. After immobilization, particle uniformity, SF concentration and high surface area to volume ratio of the produced nanocapsules led to high antimicrobial activities against strains of *Staphylococcus aureus* and *Escherichia coli*, with both tested methods (saline and overlay method). The simplicity of the eugenol loading process via ultrasound-assisted nanocapsules production, of the enzymatic functionalization and of the chemical immobilization, as well as the obtained high antimicrobial activity suggest that this antimicrobial textile system has an interesting potential as wound dressing for possible future wound treatment applications and to prevent bacterial migration in hospital bed sheets and other tissues of medical use.

4.6 Conflicts of interest

The authors declare no competing financial interest.

Acknowledgements

The work performed has received financial funding from the European Union H2020 Programme (H2020-NMP-PILOTS-2015) under the grant agreement FOLSMART [grant number 683356] and from the NÖ Forschungs- und Bildungsges.m.b.H. (NFB) and the provincial government of Lower Austria through the Science Calls (Project ID: SC16-024).

Alessandro Pellis thanks the FWF Erwin Schrödinger fellowship (grant agreement J 4014-N34) for financial support.

4.7 References

[1] F. Gottrup, J. Apelqvist, P. Price, and European Wound Management Association Patient Outcome Group, “Outcomes in controlled and comparative studies on non-healing wounds: recommendations to improve the quality of evidence in wound management,” *J. Wound Care*, vol. 19, no. 6, pp. 237–268, Jun. 2010.

[2] K. F. Cutting and K. G. Harding, “Criteria for identifying wound infection,” *J. Wound Care*, vol. 3, no. 4, pp. 198–201, Jun. 1994.

[3] D. Church, S. Elsayed, O. Reid, B. Winston, and R. Lindsay, “Burn wound infections.,” *Clin. Microbiol. Rev.*, vol. 19, no. 2, pp. 403–34, Apr. 2006.

[4] A. Kawasumi, N. Sagawa, S. Hayashi, H. Yokoyama, and K. Tamura, “Wound Healing in Mammals and Amphibians: Toward Limb Regeneration in Mammals,” *Curr. Top. Microbiol. Immunol.*, vol. 367, pp. 33–49, 2012.

[5] G. Tegl, D. Schiffer, E. Sigl, A. Heinzle, and G. M. Guebitz, “Biomarkers for infection: enzymes, microbes, and metabolites,” *Appl. Microbiol. Biotechnol.*, vol. 99, no. 11, pp. 4595–4614, Jun. 2015.

[6] G. Tegl, A. Rollett, J. Dopplinger, C. Gamerith, and G. M. Guebitz, “Chitosan based substrates for wound infection detection based on increased lysozyme activity,” *Carbohydr. Polym.*, vol. 151, pp. 260–267, Oct. 2016.

[7] B. Allegranzi *et al.*, “New WHO recommendations on intraoperative and postoperative measures for surgical site infection prevention: an evidence-based global perspective,” *Lancet Infect. Dis.*, vol. 16, no. 12, pp. e288–e303, Dec. 2016.

[8] T. Ristić *et al.*, “Antimicrobial efficiency of functionalized cellulose fibres as potential medical textiles,” *Sci. against Microb. Pathog. Commun. Curr. Res. Technol. Adv.*, pp. 36–51, 2011.

[9] A. Biundo *et al.*, “Characterization of a poly(butylene adipate-co-terephthalate)-hydrolyzing lipase from Pelosinus fermentans,” *Appl. Microbiol. Biotechnol.*, vol. 100, no. 4, pp. 1753–1764, 2016.

[10] S. Weinberger *et al.*, “Enzymatic surface hydrolysis of poly(ethylene furanoate) thin films of various crystallinities,” *Green Chem.*, vol. 19, no. 22, pp. 5381–5384, 2017.

[11] S. Vecchiato *et al.*, “Enzymatic Recycling of High-Value Phosphor Flame-Retardant Pigment and Glucose from Rayon Fibers,” *ACS Sustain. Chem. Eng.*, p. acssuschemeng.7b03840, 2017.

[12] F. Quartinello *et al.*, “Synergistic chemo-enzymatic hydrolysis of poly(ethylene terephthalate) from textile waste.,” *Microb. Biotechnol.*, vol. 10, no. 6, pp. 1376–1383, 2017.

[13] A. Pellis *et al.*, “Biocatalyzed approach for the surface functionalization of poly(L-lactic acid) films using hydrolytic enzymes,” *Biotechnol. J.*, vol. 10, no. 11, pp. 1739–1749, 2015.

[14] F. Quartinello *et al.*, “Highly Selective Enzymatic Recovery of Building Blocks from Wool-Cotton-Polyester Textile Waste Blends,” *Polymers (Basel).*, vol. 10, no. 10, p. 1107, Oct. 2018.

[15] D. N. Rockwood, R. C. Preda, T. Yucel, X. Wang, M. L. Lovett, and D. L. Kaplan, “Materials fabrication from Bombyx mori silk fibroin,” *Nat. Protoc.*, vol. 6, no. 10, pp. 1612–1631, 2011.

[16] C. Tallian *et al.*, “Structural insights into pH-responsive drug release of self-assembling human serum albumin-silk fibroin nanocapsules,” *Eur. J. Pharm. Biopharm.*, vol. 133, pp. 176–187, Dec. 2018.

[17] C. Callewaert, B. Buysschaert, E. Vossen, V. Fievez, T. Van de Wiele, and N. Boon, “Artificial sweat composition to grow and sustain a mixed human axillary microbiome,” *J. Microbiol. Methods*, vol. 103, pp. 6–8, Aug. 2014.

[18] M. Balouiri, M. Sadiki, and S. K. Ibnsouda, “Methods for in vitro evaluating antimicrobial activity : A review $,” *J. Pharm. Anal.*, vol. 6, no. 2, pp. 71–79, 2016.

[19] B. Thallinger *et al.*, “International Journal of Antimicrobial Agents Preventing microbial colonisation of catheters : Antimicrobial and antibiofilm activities of cellobiose dehydrogenase,” *Int. J. Antimicrob. Agents*, vol. 44, no. 5, pp. 402–408, 2014.

[20] G. M. Guebitz and A. Cavaco-Paulo, “Enzymes go big: surface hydrolysis and functionalisation of synthetic polymers,” *Trends Biotechnol.*, vol. 26, no. 1, pp. 32–38, 2008.

[21] C.-M. Chan, T.-M. Ko, and H. Hiraoka, “Polymer surface modification by plasmas and photons,” *Surf. Sci. Rep.*, vol. 24, no. 1–2, pp. 1–54, 1996.

[22] M. Rahman and G. C. East, “Titanium Dioxide Particle-induced Alkaline Degradation of Poly(ethylene Terephthalate): Application to Medical Textiles,” *Text. Res. J.*, vol. 79, no. 8, pp. 728–736, 2009.

[23] L. Azfarniam and M. Norouzi, “Multifunctional Polyester Fabric Using a Multicomponent Treatment,” vol. 17, no. 2, pp. 298–304, 2016.

[24] S. Bhattacharjee, “DLS and zeta potential – What they are and what they are not?,” *J. Control. Release*, vol. 235, pp. 337–351, Aug. 2016.

[25] J. Biener, A. Wittstock, T. Baumann, J. Weissmüller, M. Bäumer, and A. Hamza, “Surface Chemistry in Nanoscale Materials,” *Materials (Basel).*, vol. 2, no. 4, pp. 2404–2428, Dec. 2009.

[26] E. Wenk, A. J. Wandrey, H. P. Merkle, and L. Meinel, “Silk fibroin spheres as a platform for controlled drug delivery,” *J. Control. Release*, vol. 132, no. 1, pp. 26–34, 2008.

[27] L. Rittié, D. L. Sachs, J. S. Orringer, J. J. Voorhees, and G. J. Fisher, “Eccrine Sweat Glands are Major Contributors to Reepithelialization of Human Wounds,” *Am. J. Pathol.*, vol. 182, no. 1, pp. 163–171, Jan. 2013.

[28] B. Greener, A. A. Hughes, N. P. Bannister, and J. Douglass, “Proteases and pH in chronic wounds,” *J. Wound Care*, vol. 14, no. 2, pp. 59–61, Feb. 2005.

[29] R. M. Martins, M. D. Farias, F. Nedel, C. M. P. de Pereira, C. Lencina, and R. G. Lund, “Antimicrobial and cytotoxic evaluation of eugenol derivatives,” *Med. Chem. Res.*, vol. 25, no. 10, pp. 2360–2367, Oct. 2016.

[30] A. Kumar Sharma, A. Gupta, and R. Kumar, “Pharmacological activities of cinnamaldehyde and eugenol: antioxidant, cytotoxic and anti-leishmanial studies,” *Cell. Mol. Biol.*, vol. 63, no. 6, pp. 73–78, 2017.

[31] R. Gerosa, M. Borin, G. Menegazzi, M. Puttini, and G. Cavalleri, “In vitro evaluation of the cytotoxicity of pure eugenol,” *J. Endod.*, vol. 22, no. 10, pp. 532–534, Oct. 1996.

[32] S. M. Ali *et al.*, “Antimicrobial activities of Eugenol and Cinnamaldehyde against the human gastric pathogen Helicobacter pylori,” *Ann. Clin. Microbiol. Antimicrob.*, vol. 4, no. 1, p. 20, Dec. 2005.

[33] S. F. Nabavi, A. Di Lorenzo, M. Izadi, E. Sobarzo-Sánchez, M. Daglia, and S. M. Nabavi, “Antibacterial Effects of Cinnamon: From Farm to Food, Cosmetic and Pharmaceutical Industries.,” *Nutrients*, vol. 7, no. 9, pp. 7729–48, Sep. 2015.

[34] A. Rao, Y. Zhang, S. Muend, and R. Rao, “Mechanism of Antifungal Activity of Terpenoid Phenols Resembles Calcium Stress and Inhibition of the TOR Pathway □,” vol. 54, no. 12, pp. 5062–5069, 2010.

[35] F. Nazzaro, F. Fratianni, and L. De Martino, “Effect of Essential Oils on Pathogenic Bacteria,” pp. 1451–1474, 2013.

[36] S. Hemaiswarya and M. Doble, “Synergistic interaction of eugenol with antibiotics against Gram negative bacteria,” *Phytomedicine*, vol. 16, no. 11, pp. 997–1005, Nov. 2009.

[37] P. G. Bowler, B. I. Duerden, and D. G. Armstrong, “Wound microbiology and associated approaches to wound management.,” *Clin. Microbiol. Rev.*, vol. 14, no.

2, pp. 244–69, Apr. 2001.

[38] W. J. Stark, P. R. Stoessel, W. Wohlleben, and A. Hafner, “Industrial applications of nanoparticles,” *Chem. Soc. Rev.*, vol. 44, no. 16, pp. 5793–5805, Aug. 2015.

[39] A. S. Lammel, X. Hu, S.-H. Park, D. L. Kaplan, and T. R. Scheibel, “Controlling silk fibroin particle features for drug delivery,” *Biomaterials*, vol. 31, no. 16, pp. 4583–4591, 2010.

4.6 Supporting information

Table S1. HPLC gradient for determination of glucose, where A is water, B is methanol and C is formic acid.

Time [min]	A [%]	B [%]	C [%]	Flow (mL min^{-1})	Pressure (bar)
1	80	10	10	0.75	600
8	40	50	10	0.75	600
10	0	90	10	0.75	600
15	0	90	10	0.75	600

Table S2. Ratio of HSA to SF in nanoparticle formulations with two different degradation degrees of SF (30 and 60 mb) before sonication, edited from Tallian et al.[16]

ID[1]	Degradation degree of SF[2] [mb]	% SF
HSA	**none**	**0**
3010	**30**	**10**
3025	**30**	**25**
3050	**30**	**50**
3075	**30**	**75**
6010	**60**	**10**
6025	**60**	**25**

6050	**60**	**50**
6075	**60**	**75**

[1] ID composed of the combination of the degradation degree and the % of silk fibroin in the formulation e.g. 3050 with 30 mb SF and 50% HSA/SF ratio, HSA refers to formulations containing no silk fibroin

[2] Refers to the minutes of boiling (30 minutes or 60 minutes)

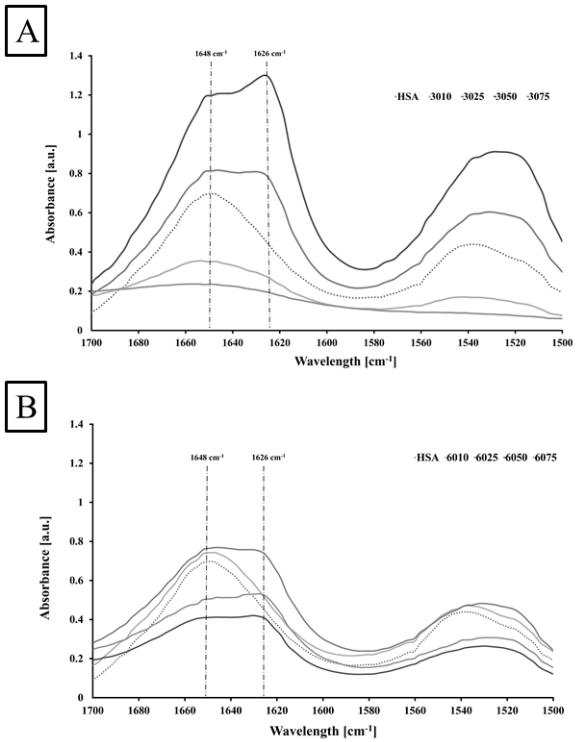

Figure S1: ATR-FTIR spectra of the amide I region (β: 1626 cm^{-1}; α: 1648 cm^{-1}) of eugenol loaded HSA and HSA/SF nanocapsules normalized between 650 and 1200 cm^{-1} and baseline corrected[36].

Table S3. Dynamic light scattering based hydrodynamic radius data in nm over time for a measurement period of 30 min of eugenol loaded HSA/SF nanocapsules consisting of two different degradation degrees of SF (30 or 60 mb) and different concentrations of SF (10-75%) evaluated for the initial 10 min (t1), the measurement time between 10-30 min (monodisperse phase, t2) and the complete measurement time (t3).

	t_1		t_2		t_3	
	$\bar{x}$	σ	$\bar{x}$	σ	$\bar{x}$	σ
	[nm]					
HSA	328.78	46.79	400.92	65.86	438.62	108.70
3010	1120.71	44.15	574.00	92.76	796.63	5.60
3025	677.67	65.56	347.75	40.95	448.71	23.15
3050	762.92	39.05	369.97	3.64	499.01	28.69
3075	378.85	14.34	319.73	17.50	345.03	17.95
6010	1277.90	156.18	504.41	35.91	845.10	201.19
6025	655.15	78.53	403.11	50.36	447.87	85.24
6050	477.74	4.29	303.77	0.75	341.51	31.73
6075	401.87	25.95	350.76	28.81	365.16	35.18

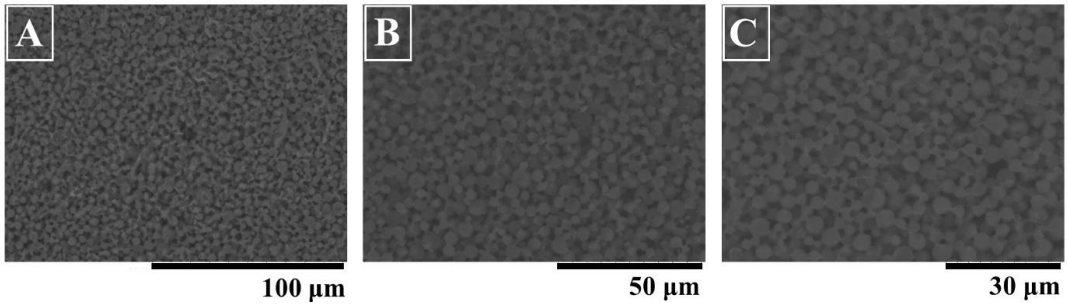

Figure S2: Scanning electron microscope images of eugenol loaded HSA/SF nanocapsules consisting of 25% SF with lower degradation degree of 30 mb (3025) with (A) 1000x (B) 1500x (C) 2000x magnifications obtained with a SEM equipped with a cryo chamber at -20 °C.

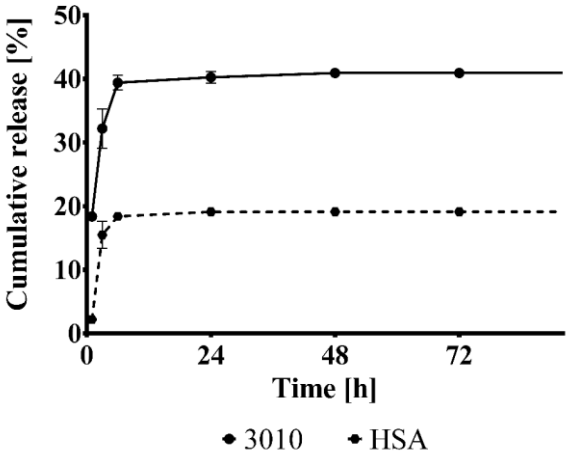

Figure S3. Cummulative release of eugenol from HSA and HSA/SF nanocapsules with lower degradation degree (30 mb) and 10 SF over a time period of 168 h in artificial salivas prepared as described in the paper of Callewaert *et al.*[17] (EN pH 6.0).

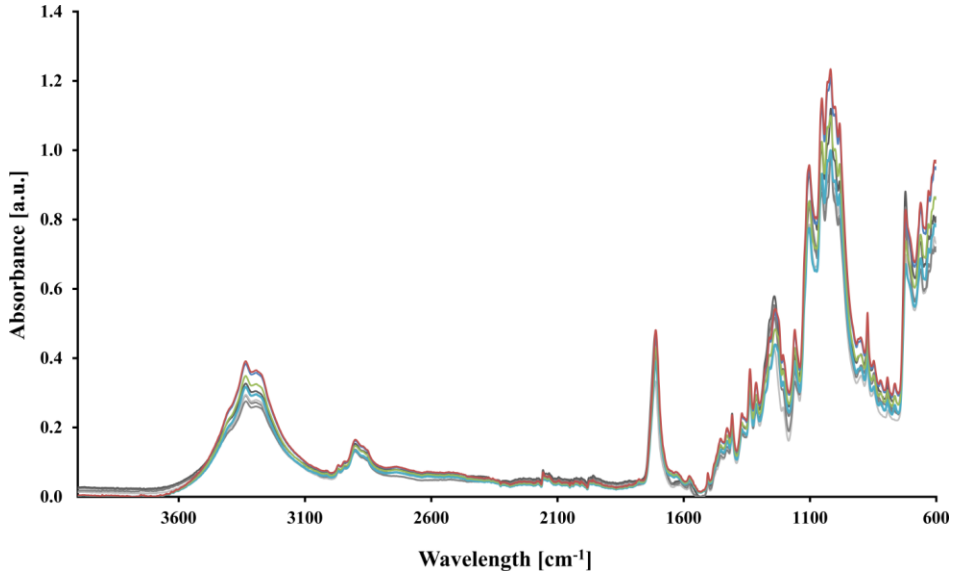

Figure S4. FTIR spectroscopy of cotton/polyester blend with immobilized HSA/SF nanocapsules. Reaction I (black line); Reaction II (grey line); Reaction III (dark grey dash line); Reaction IV (dark grey dash line); Reaction V (cyano dash line); Reaction VI (green line); Reaction VII (blue line); Reaction VIII (red line).Spectra were baseline corrected and normalized in the range of 2500-2000 cm^{-1}.

5

Highly selective enzymatic recovery of building blocks from wool-cotton-polyester textile waste blends

Published in: Polymers (2018)

DOI: 10.3390/polym10101107

F. Quartinello, S. Vecchiato, S. Weinberger , K. Kremenser, L. Skopek , A. Pellis, G. M. Guebitz

Abstract

In Europe, most of the discarded and un-wearable textiles are incinerated or landfilled. In this study we present an enzyme-based strategy for the recovery of valuable building blocks from mixed textile waste and blends as a circular economy concept. Therefore, model and real textile waste were sequentially incubated with 1) protease for the extraction of amino-acids from wool components (95% efficiency) and 2) cellulases for the recovery of glucose from cotton and rayon constituents (85% efficiency). The purity of the

remaining poly(ethylene terephthalate) (PET) unaltered by the enzymatic treatments was assessed *via* Fourier-transformed infrared spectroscopy and NMR. Amino acids recovered from wool were characterized *via* elementary and molecular size analysis, while the glucose resulting from the cotton hydrolysis was successfully converted into ethanol by fermentation with *Saccharomyces cerevisiae*. This work demonstrated that the step-wise application of enzymes can be used for the recovery of pure building blocks and their further reuse in fermentative processes (glucose).

Graphical Abstract

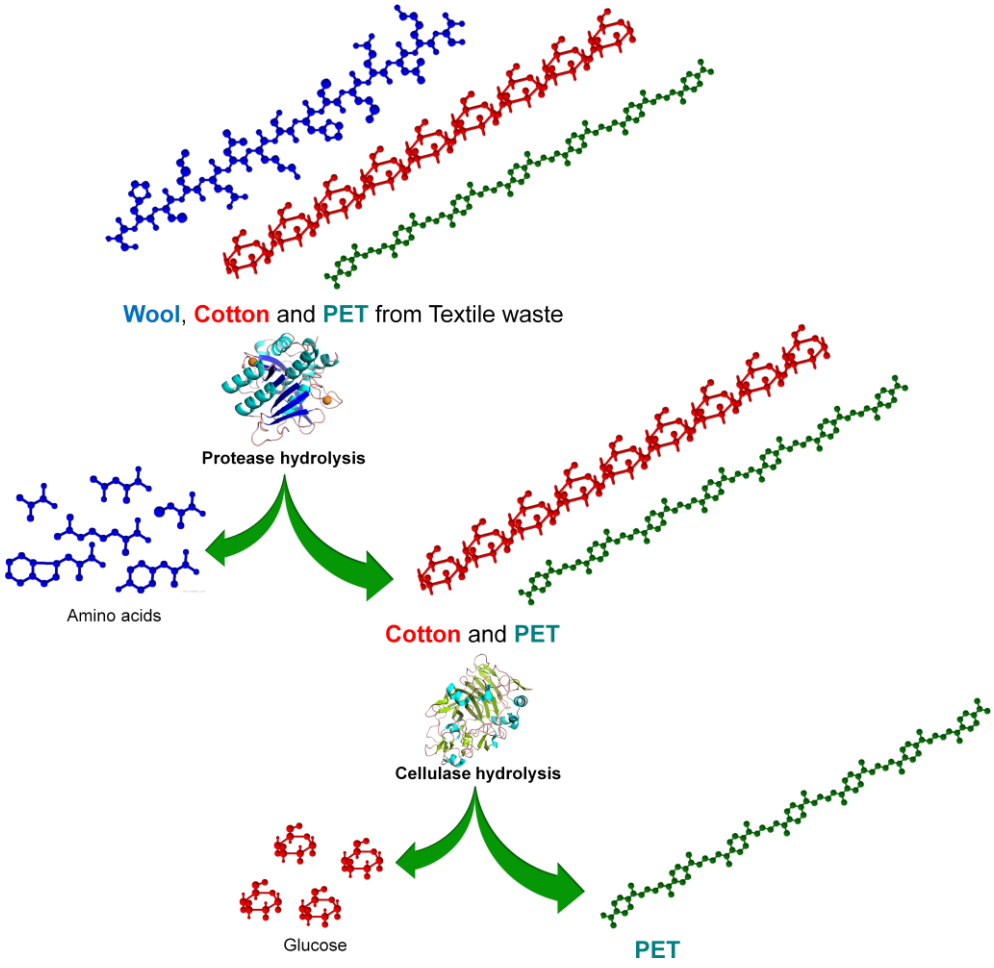

Highly selective enzymatic recovery of building blocks from wool-cotton-polyester textile waste blends

5.1 Introduction

In the last decades the production of textiles, especially for clothing, is exponentially increasing mostly due to the globalization phenomena [1]–[3]. This intensive production is responsible for the decreases in prices leading the consumers to consider clothes as disposable materials. From the estimation provided by Hollins (based on an extrapolation of data provided by nine textile sorters in EU countries), 80.000 tons of textile waste are generated per year[4]. Like it is the case for other solid wastes, textile waste comprise three types of streams: 1) pre-consumer (obtained from fiber processing and manufacturing); 2) post-consumer (all the textiles that the consumers discard either because damaged or gone out of fashion) and 3) post-industrial, which is generated from commercial and industrial applications[5]. The end-life of such material is landfilling which, together with soil pollution, represent also a global warming challenge due the production of gases[6],[7]. For example only 18% of this kind of waste in the last years was used for energy recovery[8]. Furthermore, considering the material composition, the discarded textiles still contains valuable polymers that could be reused. Resource depletion, climate changes and rising consumer awareness are providing challenges to the governments and the industrial systems to find new solutions towards improved and environmentally-friendly waste management systems and treatments. Most of the collected items could be exported separated in wearable and un-wearable textiles. Therefore , such un-wearable fabrics can be used for recycling therefore lowering the environmental impact of clothing waste therefore matching the most recent environmental legislations[9]. Textile waste recycling could save around 4.2 trillion gallons of water, 17 million tons of CO_2 and 7.5 million cubic yards of landfilled space[10].

Textiles are composed from both natural and synthetic materials. Natural fibers include cellulose-based materials (cotton, viscose, linen or hemp) or to a lower extend protein-based materials like wool and silk[11]. On the other hand, polyester is the most common synthetic polymer and is used also blended with the above listed materials [1], [12], [13].

Highly selective enzymatic recovery of building blocks from wool-cotton-polyester textile waste blends

Blended materials, like cotton-polyester, wool-polyester and cotton-wool, allow tuning properties to the fabrics such as wettability or softness and in parallel representing a reduction in the production costs. However, blends represent a challenge in terms of separation and recycling; due to the interconnection of the fibers, a separation method (mechanical or chemical) as pretreatment is required. Similarly, mixed textile waste is difficult to separate. Enzymes, due to their high specificity, would allow step-wise recovery of the components of blended materials under environmentally friendly conditions [14],[15]. Although, enzymatic hydrolysis of individual components has been demonstrated by our and other groups [16]–[19], the potential of enzymes for stepwise recovery of building blocks from blends has not been demonstrated so far. Hence, in this study step-wise enzymatic hydrolysis of cellulose/wool/polyester blends was investigated. In this work, a stepwise enzymatic process which can specifically separate the three different polymers present in textile waste was developed. Moreover, the enzymatic treatment achieved the preservation of the functional properties of the relative hydrolyzed products, which are suitable as secondary value-added products for different industrial applications.

5.2 Materials and Methods

5.2.1 Chemicals, substrates and enzymes.

Different samples of cellulose, wool, polyester and their blends were provided from the SOEX group (Hamburg, Germany). All the other chemicals and solvents were purchased from Sigma-Aldrich (Vienna, Austria) at reagent grade and used without any purification if not specified. The used enzymes, Cellic CTec3® and Savinase 12T® were kindly provided by Novozymes (Copenhagen, Denmark), and used without prior purification steps.

5.2.2 Enzymatic hydrolysis

The mixed samples consisted of pure cellulosic material (61%), pure polyester (11%), cellulose/PET blends (18 %), wool and wool blends (2 %), polyamide and other materials (8 %) according to figure 1.

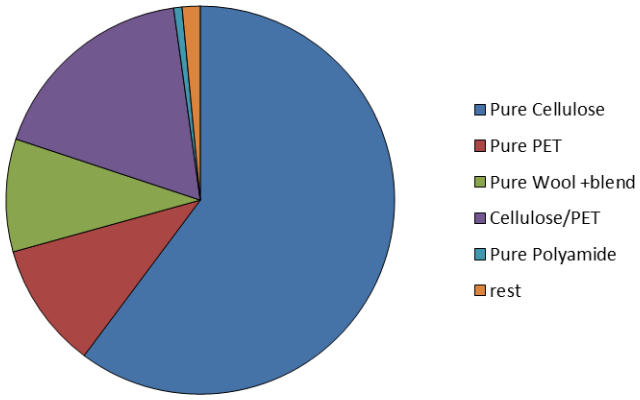

Figure 1 Composition of mixed textile waste, data provided from the SOEX Group (Hamburg, Germany)

On the other hand, different mixtures of pure cellulose, polyester and wool textiles were prepared (**Table1**).

Table 2 Composition of artificial blended textile samples in weight percentage.

	cotton (%)	**wool (%)**	**PET (%)**
CWP_90/5/5	90	5	5
CWP_80/5/10	80	5	15
CWP_80/10/10	80	10	10
CWP_70/10/20	70	10	20

CWP_60/10/30	60	10	30
CWP_50/10/40	50	10	40

All the samples were grinded to a size of 1 mm, in order to increase the available area for the enzymatic treatment and improve the mass transfer[20]. The artificial blends were washed in MQ-water heated up at boiling temperature for 30 min and subsequently dried at 105 °C for 6 hours. The same treatment was performed for the real samples from textile waste. 1 g of each sample was weighted and incubated with 75 mL of 50 mM Tris-HCl buffer pH 9 (containing 1 g L^{-1} of SDS and 6 g L^{-1} of sodium bisulfite) containing 8 U mL^{-1} (ratio with solid matter) of protease for two days at 50 °C and stirred at 400 rpm on a magnetic stirrer[21]. Afterwards, samples were vacuum-filtered with PES 0.2 µM filter (Millipore, Austria), added into 75 mL of MQ-H_2O, stirring for 30 min at 400 rpm. Later, samples were again filtered and dried at 105 °C for 6 hours. Subsequently, 75 mL of 50 mM sodium citric buffer pH 4.8 with 2750 U mL^{-1}% of cellulase cocktail were incubated for 5 days at 400 rpm and 50 °C[22]. After the hydrolysis of the cellulose moieties, each sample was filtered and dried as described above. Before and after each step (hydrolysis and washing step), the samples weighted. All measurements were performed in triplicates. The yield of the hydrolysis treatment was calculated using the following equation.

Equation (1):

$$Yield = \frac{W_a - W_b}{W_a} * 100$$

W_a = weight of the initial (or previous) step

W_b = weight after the step of interest

5.2.3 Protein hydrolysate characterization

5.2.3.1 Protease activity and thermal stability assay

The activity of the protease was determined at different pH levels of the buffer (8, 9 and 10), with and without of SDS and Sodium bisulfite using the azocasein-assay[22],[23]. In order to start enzymatic hydrolysis, 75 µL of enzyme solution (1% w/w) were mixed with 125 µL of a 2% azocasein solution. Pure buffer without the enzyme was used for the determination of the blank. After 30 minutes of incubation at 37 °C and shaking at 300 rpm, the reaction was stopped by adding 600 µL TCA (10%). Afterwards the solution was incubated for 15 minutes at 25 °C. The samples were then centrifuged for 5 minutes at 20 °C and 13000 rpm in order to precipitate the not hydrolyzed casein. Then 600 µL of the supernatant were mixed with 700 µL of NaOH (1 M) subsequently 220 µL of the mixture was transferred into a 96 well plate and the absorbance was measured at 440 nm using an Infinite M 200 plate reader. The determination of the absorbance was performed in triplicates. The thermal stability of the enzyme was determined using the same azocasein assay as described above. Briefly, the enzyme solution was incubated at 50 °C and 300 rpm. The aliquots were taken at 0, 3, 6, 24 and 48 h after the beginning of the degradation process and the remaining enzymatic activity was evaluated.

5.2.3.2 Chemical analysis

Total Carbon (TC), Total inorganic Carbon (TiC) and total nitrogen (TN) were determined on a Shimadzu System composed of a TOC-VCPH total organic carbon analyzer and a TNM-1 nitrogen measurement unit, equipped with ASI-V auto sampler unit. The measurement range of TC was 10 to 1000 mg L^{-1}, of TIC 10 to 100 mg L^{-1} and TN 20 to 200 mg L^{-1}. If necessary, samples were diluted accordingly with ultrapure water. Determination limits were determined according to DIN32645 as 4.45 mg L^{-1} for TC, 5 mg L^{-1} for IC and 4.39 mg L^{-1} for TN. TOC was calculated as difference of TC and TIC.

5.3.2.3 Molecular weight distribution of keratin hydrolysis

The keratin extraction during the enzyme treatment was followed *via* SDS-PAGE analysis. A volume of 20 µL of each sample obtained from the different textile waste hydrolysates were mixed with 20 µL of Laemmli buffer and heated for 5 min. Afterwards, 12 µL of solution were transferred into a precast polyacrylamide gel (4-15%), using 5 µL of protein marker IV (10-170 KDa, 10 bands). Moreover, 1 g of untreated pure wool was stirred with a 10 mL solution of 50 mM Tris-HCl pH 8.5, containing 2-mercaptoethanol (1.5 M), urea (8 M) and SDS (0.25 M)[24]. Then 20 µL of this solution were run in SDS-PAGE as described before.

5.3.2.4 Amino acid determination

In order to determine the amino groups present in supernatant after protease treatment the ninhydrin assay was performed. Therefore, a ninhydrin reagent, consisting of 75 mL od dimethylsulfoxide (DMSO), 300 mg hydrindantin, 2 gr of ninhydrin and 25 mL of 4 M sodium acetate (pH 5.2). Standard samples (0-200 µM) were prepared from a 10 mM stock solution of glycine in mQ-H_2O. A volume of 100 µL of sample (or standard) were incubated with 75 µL of ninhydrin reagent and incubated for 30 min at 80° C. Thereafter, samples were cooled down and 100 µL of stabilizing solution (50% of ethanol in water) were added. The absorbance was determined at 570 nm using an Infinite 200 Pro spectrophometer (Tecan, Switzerland).

5.2.4 Cellulose hydrolysis

5.2.4.1 Total cellulose assay.

The Filter paper assay (FPA) was used as recommended by IUPAC was used[25]. Rolled filter paper (7.5*75 mm, around 50 mg each) was submerged in glass tube with 1 mL 50 mM sodium citrate buffer pH 4.8. Therefore 100 µL of enzyme (diluted 1:1000) were added to the substrate. The reaction was stopped at different time points (0, 5, 10, 20, 40,

60 min) by adding 500 µL of 1 M NaOH. Specifically, for the first time point at 0 min NaOH was added before the enzyme and considered that reaction as blank. Afterwards, 3,5 dinitrosalicylic acid (DNS)[26] reagent was added and then the sample boiled for 5 min, followed by the addition of 1 mL of mQ-H_2O. 200 µL of each sample were transferred in a 96 well-plate and the absorbance was measured at 540 nm. All measurements were conducted in triplicates.

5.2.4.2 Quantification of glucose *via* HPLC.

Carrez precipitation was performed with the supernatant obtained from hydrolyzed cellulosic materials to separate the soluble sugars from the proteins. Briefly, to 960 µL of supernatant were added 20µL of 2% $K_4[Fe(CN)_6]$*3 H_2O and 20 µL of 2% $ZnSO_4$* 7 H_2O solutions. Samples were centrifuged at 14.000 rpm at 4 °C for 15 min and filtered through 0.2 µm nylon filter into HPLC vials for measurements. Agilent technologies 1260 Infinity II HPLC, with Transgenomic IC SEP-ION-300 coupled with refractive index detector was performed with H_2SO_4 with flow rate of 0.325 mL min^{-1} at 45 °C.

5.2.4.3 Bio-Ethanol production.

After the enzymatic hydrolysis, the supernatant was ultra-filtered through a VivaFlow membrane (5000 MWCO) (Sartorious, Germany), in order to remove impurities. Afterwards, the glucose was passed through a 0.1 µm sterile vacuum filter (EMD, Millipore, Austria). The amount of glucose after the filtration was determined as described above via HPLC and stored at 4 °C until further use.The glucose released from enzymatic hydrolysis of cellulose was used for ethanol production from *Saccharomyces cerevisiae*. An overnight pre-culture was incubated at 28 °C and 150 rpm in YPD media (1% yeast extract, 2% peptone, 2% d-glucose)[19]. Then, the pre-culture as collected by centrifugation washed 3 times and re-suspended in 10 mL of mQ-water. The yeast was re-inoculated to an Optical Density (OD_{600}) of 0.1. In this case the culture media was prepared containing YPD (1% yeast extract, 2% peptone and 2% of $_D$-glucose) for the control and in the end YPGc (1% extract, 2% peptone and 2% glucose obtained from the

textile degradation). The growth of *S. cerevisiae* was monitored by measuring the OD_{600} after 0, 3, 6, 18, 24 hours. During the same time points, different samples were collected for quantification of glucose and ethanol *via* HPLC as described before.

5.2.5 Poly(ethylene terephthalate) characterization

After step-wise enzymatic "extraction" of protein and cellulose based materials FT-IR spectra of the residual materials were recorded. PET fabric from GoodFellow was used as standard in order to determine the purity of the PET obtained after the different enzymatic processes. A second blank with grinded pure cotton was measured in order to discriminate the signals from cellulose material to PET peaks. A total of 25 scans for each samples were taken with a resolution of 2 cm^{-1} and normalized before any data processing. The bands were assigned as follows: 3300 cm^{-1} (-OH groups from cellulosic fiber) 870 cm^{-1} (C-H out of plane bending), 1720 cm^{-1} ν(C=O), 1590 cm^{-1} ν(C=C), 1250 cm^{-1} ν(C-O-C). Enzymatic hydrolysis of residual PET was performed using 5 µM of *Humicola insolens* cutinase (HiC) (Novozyme, Denmark). Therefore, weight loss of PET samples after the enzymatic treatment was quantified as described for protein and cellulose based materials.

5.3. Results

5.3.1 Step-wise enzymatic extraction of textile building blocks

To assess the impact of the material composition on enzymatic hydrolysis, protease and cellulase activities and incubation times were chosen in a way to reach about 90 % conversion based on preliminary experiments with pure materials.In a first step, building-blocks of protein-based textile waste components, namely wool was recovered by protease treatment. About 90 % of the protein content of both pure wool and model mixtures were recovered in the solution after protease treatment. For the real textile waste sample, a slightly lower recovery of 85 % was measured (**Figure 2**). Furthermore, no

glucose (or oligosaccharides) was detected after protease treatment, indicating specificity of the protease. In a second step, recovery of cellulose building blocks (i.e. glucose) from cotton and man-made cellulose fibres was investigated. Higher yields were seen for those samples with higher cellulose content (**Figure 2**, Samples CWP_90/5/5- CWP_80/10/10), which decreased to 50% when the polyester increased to 40% (Figure 2, Sample CWP_50/10/40). However, almost 80 % of the cellulose fiber building blocks were recovered from real textile waste after cellulase treatment. The washing steps, performed between the enzymatic processes, did not significantly improve yields, i.e. only a slight increase below 1 % was seen. (**Figure S1**). Regarding the recovery from real textile waste, the yield was 5-10% lower when compared to the model mixture with similar cellulose content, probably due to the intimate connections of the fibers present in the artificial blends.

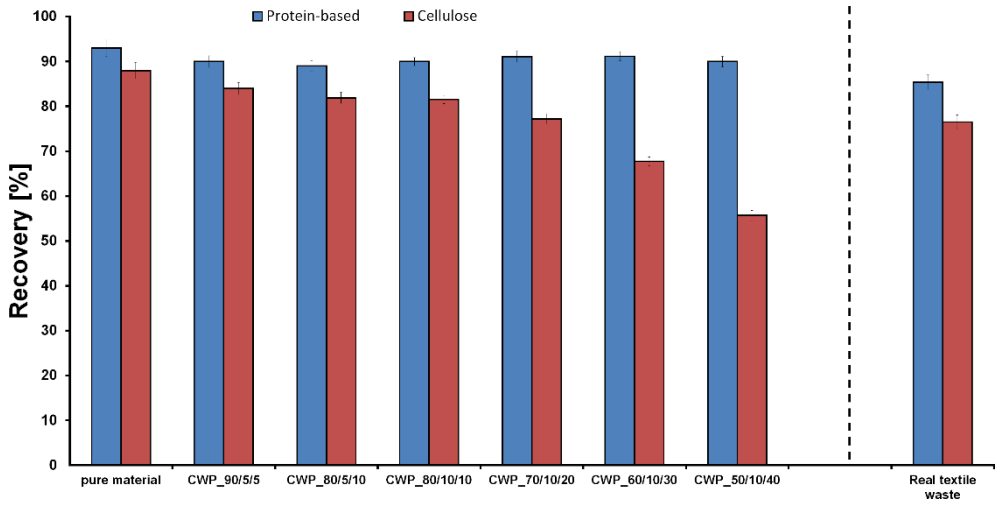

Figure 2 Recovery of protein and cellulose fibre building blocks after sequential treatment of textile waste and model mixtures with proteases and cellulases, respectively depending on cellulose (C), wool (W) and polyester (P) content. The data are given in (%) related to weight loss from the starting material (test performed in triplicates).

5.3.2 Protein hydrolysate characterization

Wool is a protein fiber composed of 95% by weight of keratin which consists of 18 amino acids with a relatively high proportion of cysteine (10-15 %)[27], [28]. Keratin has high number of disulphide bonds which are responsible for a high stability to the wool protein structure. The main morphological element, the cortex, is protected by the cuticle. The cortex consists of shaped cortical cells of lower-sulphur content intermediate filaments (IFP) with an average of 40-65 KDa. These proteins form α-helical structure, named microfibril. These proteins are embedded in a matrix of β-keratin sheets which comprise keratin associated proteins (KAP). The KAPs contain two non-filamentous proteins rich in cysteine (11-26 KDa) and protein with high glycine, serine and tyrosine content (6-9 KDa). Savinase 12T® is secreted by the alkalophilic bacterium *Bacillus lentus* and is a representative of the subtilisin enzymes with high enzymatic activity in the pH range 8-12[29]. The activity and the thermal stability of the enzyme was positively influenced by the presence of SDS as surfactant, due to better dissolution of the enzyme from the granulate powder. Furthermore, sodium bisulphite (which is needed for breaking disulphide bonds in wool) was not affecting the enzyme catalysis (**Figure S2**). Protease activity was slightly higher at pH 9 and pH 10 when compared to pH 8 but but the enzyme was no longer stable at pH 10 (**Figure S3**).The enzymatic solubilization of wool was also quantified based on total organic carbon and the total nitrogen analysis in the solution after removal of the solids. The amounts released correlated well with the initial wool content and the weight loss measured (Figure 3). The carbon/nitrogen ratio was 3:1 in agreement with published values [24] for wool hydrolysates applied for germination application[30], [31] or as phenolic compound replacement[32]–[34]. In the hydrolysate of real textile waste, we observed a similar C/N ratio (**Figure 3**).

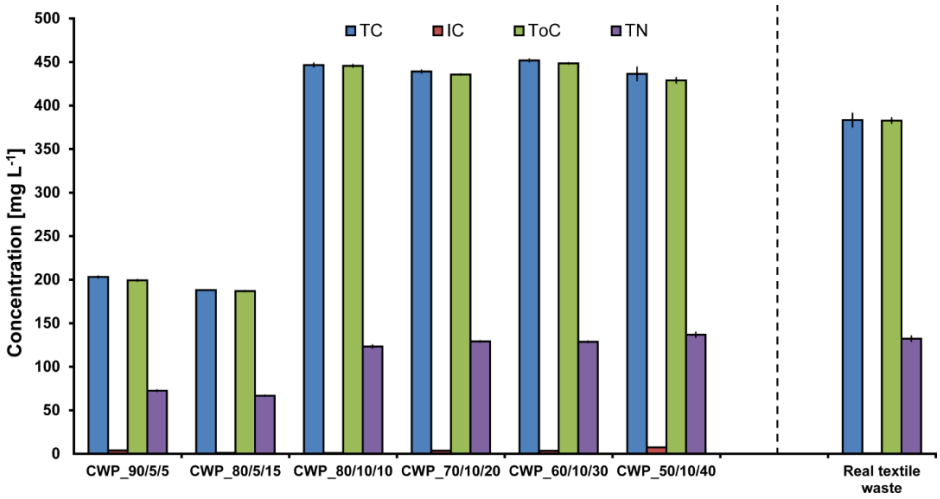

Figure 3 Determination of Total Carbon (TC), Inorganic Carbon (IC), Total organic carbon (ToC) and Total nitrogen of textile fibre sample hydrolysates after the protease treatment. Blank values from TC, IC, ToC and TN were subtracted.

Peptides released upon protease treatment had a molecular weight lower than 10 KDa according to SDS-Page analysis (**Figure S4**). Furthermore, amino groups of the peptides/amino acids in the hydrolysates were quantified by using the ninhydrin assay. Also in this case, the corresponding amount of these moieties is correlated by the initial amount of protein based material, showing the same trend as well the ToC and TN (**Figure S5**).

5.3.3 Cellulose based material hydrolysis and ethanol production.

The cellulase preparation used for the hydrolysis of cellulose fibres present in textile waste comprised a complete cellulose degrading enzyme system including endoglucanases, cellobiohydrolyses, polysaccharide monooxygenases and beta-glucosidases allowing synergistic hydrolysis yielding glucose[35]. Glucose is a perfect carbon source for biotechnological production of platform chemicals and biofuels. Moreover, when recovered from waste streams there is no ethic concerns related to competition to food production. However, impurities potentially contained in textile waste might inhibit growth of microorganisms. Hence, production of bioethanol of recovered glucose was exemplary

investigated in this study and used as carbon source for *S.cerevisiae* in comparison to commercial glucose. The amount of glucose released after hydrolysis of the textile waste samples by cellulases depended on the initial cellulose content. The highest amount was obtained (2.9 g/L) in Sample CWP_90/5/5 (**Figure 4**). Inversely, samples with lower amount of such material has shown slightly lower amount of released sugar. This can be explained by the presence of higher oligosaccharides as previously reported by Vecchiato *et al*[19].

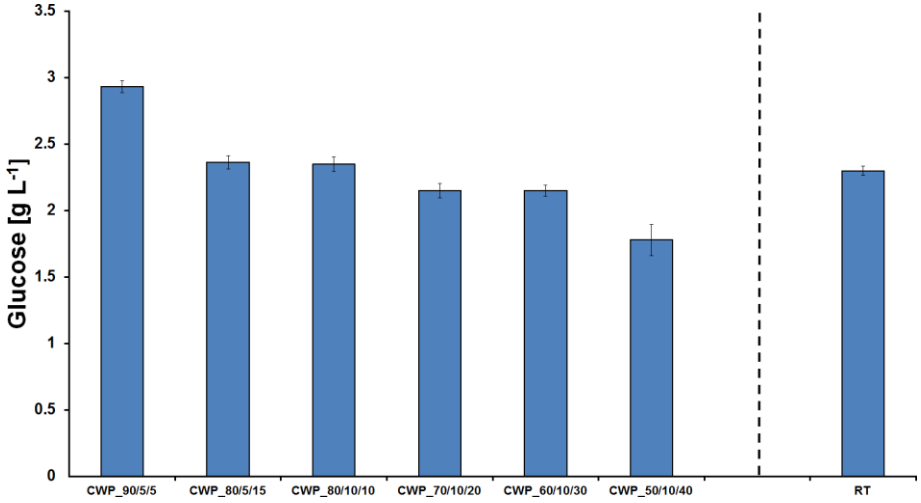

Figure 4 HPLC measurements of recovered glucose from enzymatic degradation of cellulose material depending on cellulose (C), wool (W) and polyester (P) content.

Generally, the data indicate the recycled glucose (1%) either from artificial blend (sample CWP_90/5/5 and CWP 50/10/40) and real textile waste was easily used as carbon source from the yeast. The amount of sugar drastically decreased after 6 hours and after 24 h there was no more sugar available. After 6 h of fermentation the maximum production of ethanol of around 0.3 g L^{-1} was observed. Afterwards the amount of ethanol decreased since the yeast started using it as carbon source.

Glucose recovered from real textile waste as carbon source showed an intermediary trend, the yeast growth was marginally affected than the growth with artificial blends. In comparison with the highest value of produced ethanol (0.3 g L^{-1}) after 6 h the incubation

with real textile waste produced 0.2 g L^{-1}. Certainly, the amount of ethanol produced was lower than at industrial scale[36]; but the fermentation with yeast was performed in small scale just as proof of concept that the use of recovered glucose from enzymatic recycling processes could indeed be suitable for ethanol production provided that the process is further optimized.

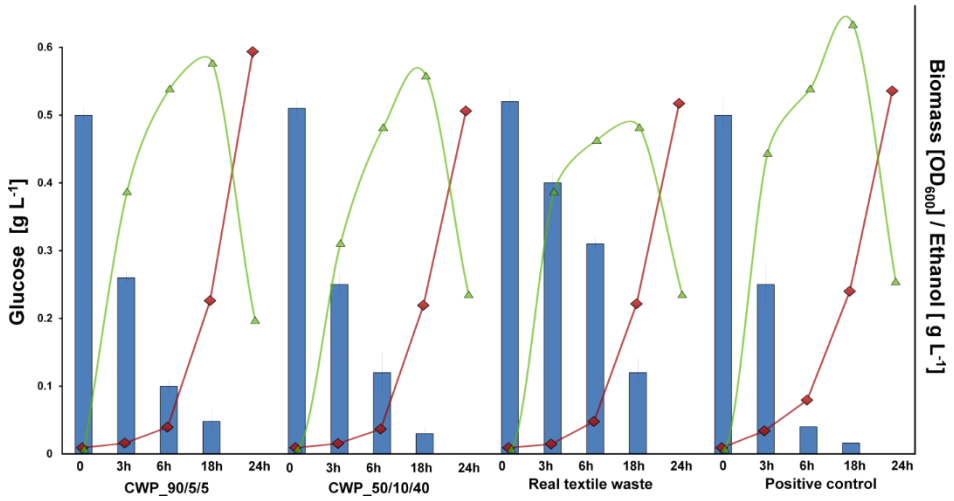

Figure 5 Fermentation of *S. cerevisiae* with glucose recovered. Time points collected after time 0, 3, 6 and 24 hours of incubation of yeast. The concentration of glucose (blue bars) and ethanol (green line) were quantified via HPLC analysis (experiments performed in triplicate). Biomass (red line) was quantified *via* spectrophotometric measurement of OD_{600}.

5.3.4 Poly(ethylene terephthalate) characterization

The high durability and crystallinity of PET is a major concern for the environment. On the other hand, its separation from other fibers can avoid the release in the environment[37] and allow recycling which is otherwise impossible with e.g cellulose impurities. As already defined, the two enzymatic steps have the aim to separate the polyester from the two initial natural fibers. FT-IR analysis demonstrated that in the samples CWP_90/5/5-CWP_80/10/10, the polymer obtained after the enzymatic treatments was 96% pure, due to absence of the cellulose peaks, as shown in the blank with pure cotton. On the other hand the presence of the in the area of 3300 and 870 cm^{-1} in samples CWP_60/10/30

and CWP_50/10/40 indicated the traces of cellulose (**Figure S6**). According to the yield, when a higher content of PET content (more than 30%) is present, lead to less cellulose removal by the enzyme cocktail the cellulose cocktail. Regarding the spectra of the real textile waste sample, after the enzymatic treatments small signals from cellulose material were also presents around 870 cm^{-1} with the purity of the recovered PET that was around 92%. However, in general most of the natural fibres in blended textiles were successfully removed.

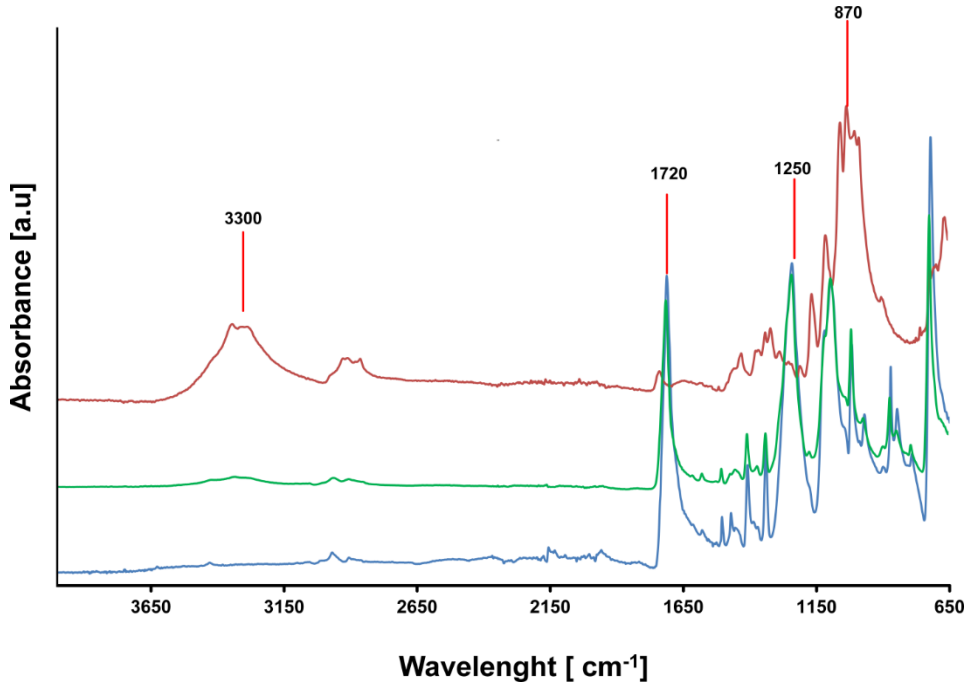

Figure 6 FT-IR real textile waste sample. Pure PET (blue line), pure cotton (red line), real textile waste sample (green line). All the spectra were normalized in the area 2500-2200 cm^{-1}.

Finally, as an alternative to recycling of PET as polymer, in another enzymatic step the building block could potentially be recovered. Incubation of the residual PET with the cutinase HiC demonstrated a partial degradation of PET, still not sufficient for complete recycling (**Figure S7**). As shown in our previous work, a complete degradation of PET would be possible using a synergistic combination of neutral chemical and enzymatic hydrolysis[38].

5.4 Conclusions

Enzymatic treatment has proven to be an environmentally friendly alternative tool towards the reduction of textile waste. The enzymatic hydrolysis of wool and cellulose based fibers led to yields of approximately 95 % and 85 %, respectively. The purity of the resulting poly(ethylene terephthalate) was comparable to the pure PET as demonstrated by FT-IR measurements, allowing recycling. Furthermore, in line with circular economy concepts, the recovered building blocks from wool and cellulose fibers components in blended textiles can likewise be reused. The amino acids and oligopeptides (with molecular weight lower than 10 KDa) obtained from wool degradation can be used as replacement of carbon and nitrogen sources for germination or phenolic related compounds for resins according to previous reports. On the other hand, in this paper recovered glucose (around 0.62 g L^{-1}) was successful used as carbon source for yeast fermentation to produce ethanol (0.3 g L^{-1}). In summary, such step-wise enzymatic process are especially attractive for the recycling of blended materials which are otherwise rather difficult to recycle with other technologies.

5.5 Author contributions

The manuscript was written through contributions of all authors. All authors have given approval to the final version of the manuscript.

Notes

The authors declare no competing financial interest.

Acknowledgments

This project received funding from the European Union's Horizon 2020 research and innovation program under the grant agreement 641942 (Resyntex project). A.P. thanks the FWF Erwin Schrödinger fellowship (grant agreement J 4014-N34) for financial

support. The authors want to thank Ms. Sumetzberger-Hasinger for the assistance with the TOC and TN analysis.

5.6 References

[1] Youjiang Wang, *No Title*. Woodhead Publishing, 2006.

[2] B. Zamani, G. Peters, and M. Svasntröm, “Towards Understanding Sustainable Textile Waste Management: Environmental impacts and social indicators,” *Chem. Biol. Eng.*, p. 52, 2014.

[3] A. Payne, *Open-and closed-loop recycling of textile and apparel products*. Elsevier Ltd, 2015.

[4] Oakdene Hollins, “Chemical recycling – A solution for Europe’s waste textile mountain ?,” no. December, pp. 10–12, 2016.

[5] E. Gentil, J. Clavreul, and T. H. Christensen, “Global warming factor of municipal solid waste management in Europe,” *Waste Manag. Res.*, vol. 27, no. 9, pp. 850–860, 2009.

[6] J. M. Hawley, “Textile Recycling,” *Handb. Recycl. State-of-the-art Pract. Anal. Sci.*, pp. 211–217, 2014.

[7] F. Cucchiella, I. D’Adamo, and M. Gastaldi, “Sustainable management of waste-to-energy facilities,” *Renew. Sustain. Energy Rev.*, vol. 33, pp. 719–728, 2014.

[8] C. Cole, M. Osmani, M. Quddus, A. Wheatley, and K. Kay, “Towards a zero waste strategy for an english local authority,” *Resour. Conserv. Recycl.*, vol. 89, pp. 64–75, 2014.

[9] L. Y. N. Richards and T. O. M. Richards, “Tools and methods :,” pp. 1–48, 2004.

[10] European technology Platform, “Towards a 4 th Industrial Revolution of Textiles and Clothing,” no. October, 2016.

[11] N. M. Van Der Velden, M. K. Patel, and J. G. Vogtländer, “LCA benchmarking study on textiles made of cotton, polyester, nylon, acryl, or elastane,” *Int. J. Life Cycle Assess.*, vol. 19, no. 2, pp. 331–356, 2014.

[12] R. Araújo, M. Casal, and A. Cavaco-Paulo, “Application of enzymes for textile fibres processing,” *Biocatal. Biotransformation*, vol. 26, no. 5, pp. 332–349, 2008.

[13] R. Chavan, “Environmental Sustainability through Textile Recycling,” *J. Text. Sci.*

Eng., vol. s2, no. 1, pp. 1–5, 2014.

[14] A. Pellis, S. Cantone, C. Ebert, and L. Gardossi, “Evolving biocatalysis to meet bioeconomy challenges and opportunities,” *N. Biotechnol.*, vol. 40, pp. 154–169, 2018.

[15] G. M. Guebitz and A. Cavaco-Paulo, “Enzymes go big: surface hydrolysis and functionalisation of synthetic polymers,” *Trends Biotechnol.*, vol. 26, no. 1, pp. 32–38, 2008.

[16] G. Buschle-Diller, S. H. Zeronian, N. Pan, and M. Y. Yoon, “Enzymatic Hydrolysis of Cotton, Linen, Ramie, and Viscose Rayon Fabrics,” *Text. Res. J.*, vol. 64, no. 5, pp. 270–279, 1994.

[17] N. Eslahi, F. Dadashian, and N. H. Nejad, “An investigation on keratin extraction from wool and feather waste by enzymatic hydrolysis,” *Prep. Biochem. Biotechnol.*, vol. 43, no. 7, pp. 624–648, 2013.

[18] C. Gamerith *et al.*, “Enzymatic recovery of polyester building blocks from polymer blends,” *Process Biochem.*, vol. 59, pp. 58–64, 2017.

[19] S. Vecchiato *et al.*, “Enzymatic Recycling of High-Value Phosphor Flame-Retardant Pigment and Glucose from Rayon Fibers,” *ACS Sustain. Chem. Eng.*, p. acssuschemeng.7b03840, 2017.

[20] S. Weinberger *et al.*, “Enzymatic surface hydrolysis of poly(ethylene furanoate) thin films of various crystallinities,” *Green Chem.*, vol. 19, no. 22, pp. 5381–5384, 2017.

[21] N. Eslahi, F. Dadashian, and N. H. Nejad, “Optimization of enzymatic hydrolysis of wool fibers for nanoparticles production using response surface methodology,” *Adv. Powder Technol.*, vol. 24, no. 1, pp. 416–426, 2013.

[22] Novozymes, “Novozymes Cellic® CTec3 - Secure your plant’s lowest total cost,” *Novozymes*, pp. 1–6, 2012.

[23] F. M. Brock, C. W. Forsberg, and J. G. Buchanan-smith, “Proteolytic activity of rumen microorganisms and effects of proteinase inhibitors . Proteolytic Activity of Rumen Microorganisms and Effects of Proteinase Inhibitors,” vol. 44, no. 3, pp. 561–569, 1982.

[24] P. Bhavsar *et al.*, *Superheated Water Hydrolysis of Waste Wool in a Semi-Industrial Reactor to Obtain Nitrogen Fertilizers*, vol. 4, no. 12. 2016.

[25] T. K. Ghose, “Measurement of cellulase activities,” *Pure Appl. Chem.*, vol. 59, no. 2, 1987.

[26] G. L. Miller, “Miller, G. L. 1959. Use of dinitrosalicylic acid reagent for determination of reducing sugar. Analytical Chemistry, 31: 426-428.,” *Anal. Chem*, vol. 31, pp. 426–428, 1959.

[27] J. E. Plowman, “Proteomic database of wool components,” *J. Chromatogr. B Anal. Technol. Biomed. Life Sci.*, vol. 787, no. 1, pp. 63–76, 2003.

[28] K. Röper, J. Föhles, and H. Klostermeyer, “[5] Complete Enzymatic Hydrolysis of Wool and Its Morphological Components,” *Methods Enzymol.*, vol. 106, no. C, pp. 58–69, 1984.

[29] C. Betzel, S. Klupsch, G. Papendorf, S. Hastrup, S. Branner, and K. S. Wilson, “Crystal structure of the alkaline proteinase Savinase™from Bacillus lentus at 1.4 Å resolution,” *J. Mol. Biol.*, vol. 223, no. 2, pp. 427–445, 1992.

[30] M. Nustorova, D. Braikova, A. Gousterova, E. Vasileva-Tonkova, and P. Nedkov, “Chemical, microbiological and plant analysis of soil fertilized with alkaline hydrolysate of sheep’s wool waste,” *World J. Microbiol. Biotechnol.*, vol. 22, no. 4, pp. 383–390, 2006.

[31] P. Bhavsar, M. Zoccola, A. Patrucco, A. Montarsolo, G. Rovero, and C. Tonin, “Comparative study on the effects of superheated water and high temperature alkaline hydrolysis on wool keratin,” *Text. Res. J.*, vol. 87, no. 14, pp. 1696–1705, 2017.

[32] I. C. Valverde, L. H. Castilla, D. F. Nuñez, E. Rodriguez-Senín, and R. De La Mano Ferreira, “Development of new insulation panels based on textile recycled fibers,” *Waste and Biomass Valorization*, vol. 4, no. 1, pp. 139–146, 2013.

[33] A. Moubarik, A. Pizzi, A. Allal, F. Charrier, A. Khoukh, and B. Charrier, “Cornstarch-mimosa tannin-urea formaldehyde resins as adhesives in the particleboard production,” *Starch/Staerke*, vol. 62, no. 3–4, pp. 131–138, 2010.

[34] H. Binici, M. Eken, M. Kara, and M. Dolaz, “An environment-friendly thermal insulation material from sunflower stalk, textile waste and stubble fibers,” *Proc. 2013 Int. Conf. Renew. Energy Res. Appl. ICRERA 2013*, vol. 51, pp. 833–846, 2013.

[35] M. Dimarogona, E. Topakas, and P. Christakopoulos, “Cellulose Degradation By Oxidative Enzymes,” *Comput. Struct. Biotechnol. J.*, vol. 2, no. 3, p. e201209015, 2012.

[36] J. C. López-Linares, I. Romero, C. Cara, E. Ruiz, M. Moya, and E. Castro, “Bioethanol production from rapeseed straw at high solids loading with different process configurations,” *Fuel*, vol. 122, pp. 112–118, 2014.

[37] A. Pellis, E. Herrero Acero, V. Ferrario, D. Ribitsch, G. M. Guebitz, and L. Gardossi,

"The Closure of the Cycle: Enzymatic Synthesis and Functionalization of Bio-Based Polyesters," *Trends Biotechnol.*, vol. 34, no. 4, pp. 316–328, 2016.

[38] F. Quartinello *et al.*, "Synergistic chemo-enzymatic hydrolysis of poly(ethylene terephthalate) from textile waste," *Microb. Biotechnol.*, vol. 10, no. 6, pp. 1376–1383, 2017.

5.7 Supporting information

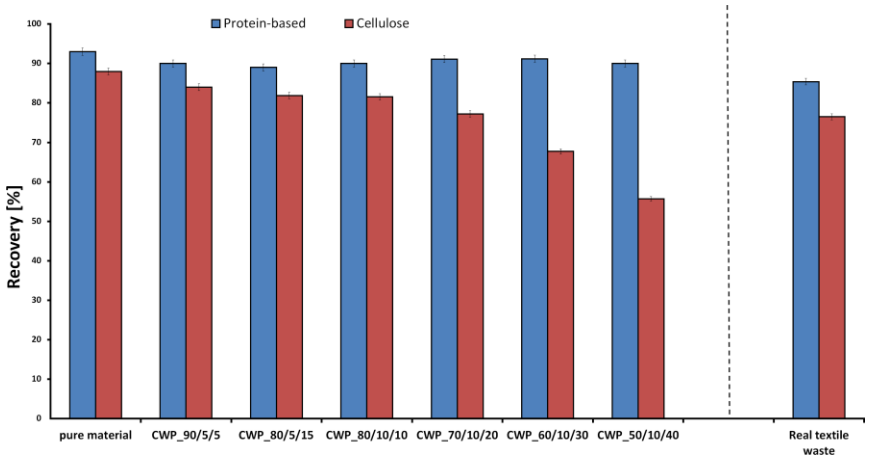

Figure S15 Recovery of protein and cellulose fibre building blocks after sequential treatment of textile waste and model mixtures with proteases and cellulases, respectively depending on cellulose (C), wool (W) and polyester (P) content. The data are given in (%) related to weight loss from the starting material (test performed in triplicates).

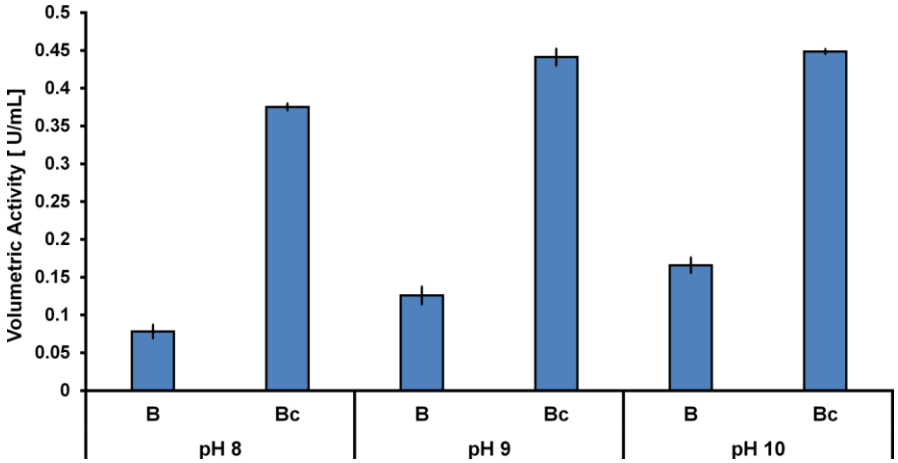

Figure S2 Volumetric activity of protease with (B) and without SDS and sodium bisulfite (B_c) at pH 8, 9 and 10 with azocasein assay. Experiments were performed in triplicate

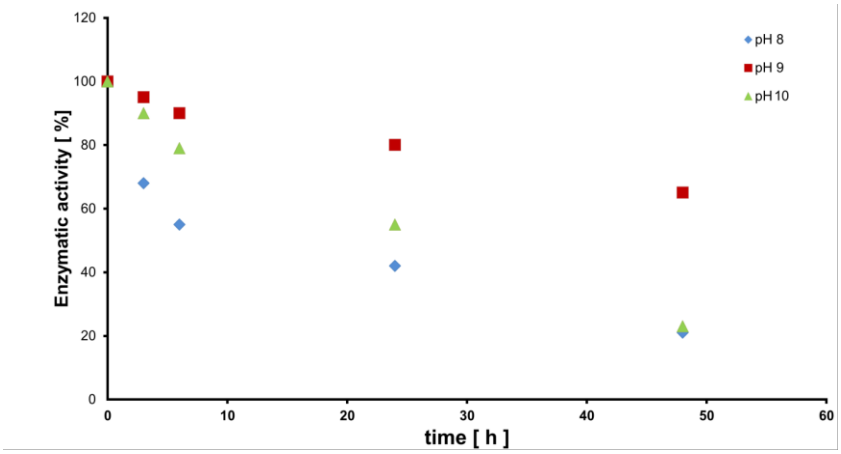

Figure S3 Volumetric activity of protease with SDS and sodium bisulfite at pH 8, 9 and 10, with azocasein assay. Experiments were performed in triplicate.

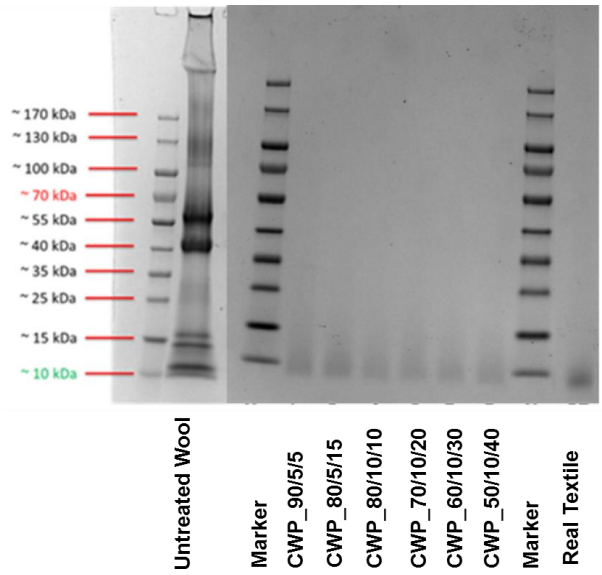

Figure S4 SDS-Page of protein bands after protease treatment.

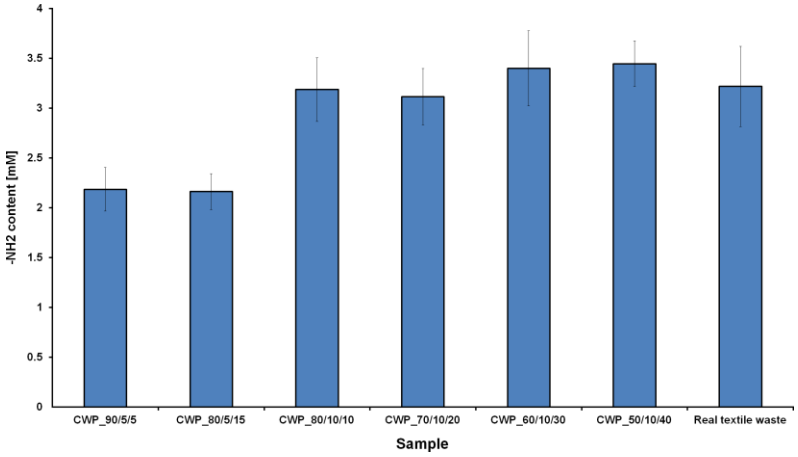

Figure S5 Amino groups content from wool hydrolysate supernatants.

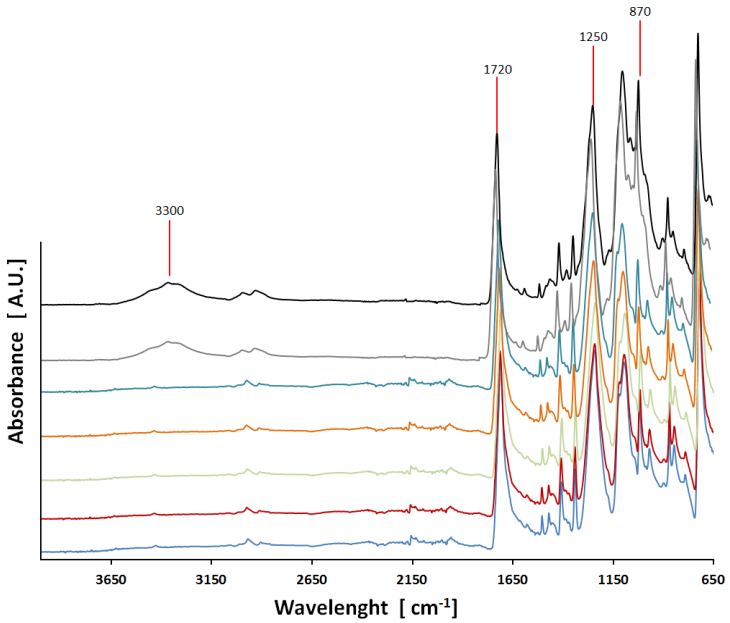

Figure S6 FT-IR spectra of: pure PET (blue line), CWP_90/5/5 (red line), CWP_80/5/15 (grey line), CWP_80/10/10 (orange line), CWP_70/10/20 (light blue line), CWP_60/10/30 (dark grey line), CWP_50/10/40 (black line). All the spectra were normalized in the area 2500-2200 cm^{-1}.

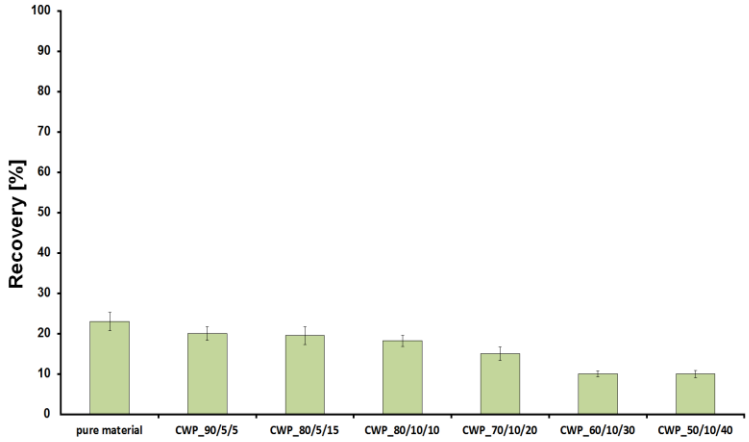

Figure S7 Recovery of PET building blocks with *Humicola insolens* cutinase

6

Synergistic chemo-enzymatic hydrolysis of poly(ethylene terephthalate) from textile waste.

Published in: Microbial Biotechnology (2017)

DOI: 10.1111/1751-7915.12734

F. Quartinello, S. Vajnhandl, J. Volmajer Valh, B. Vončina, A. Lobnik,

E. Herrero Acero, A. Pellis, G. M. Guebitz

Abstract

Due to the rising global environment protection awareness, recycling strategies that comply with the circular economy principles are needed. Polyesters are among the most used materials in the textile industry, therefore achieving a complete poly(ethylene terephthalate) (PET) hydrolysis in an environmentally-friendly way is a current challenge. In this work a chemo-enzymatic treatment was developed in order to recover the PET building blocks, namely terephthalic acid (TA) and ethylene glycol. To monitor the monomer and oligomer content in solid samples, a Fourier-Transformed Raman method was successfully developed. A shift of the free carboxylic groups (1,632 cm^{-1}) of TA into the deprotonated state (1,604 and 1,398 cm^{-1}) was observed and bands at 1,728 and

1,398 cm^{-1} were used to assess purity of TA after the chemo-enzymatic PET hydrolysis. The chemical treatment, performed under neutral conditions (T=250 °C, P=40 bar) led to conversion of PET into 85% TA and small oligomers. The latter were hydrolysed in a second step by using the *Humicola insolens* cutinase (HiC) yielding 97% pure TA, therefore comparable with the commercial synthesis grade TA (98%).

Graphical abstract

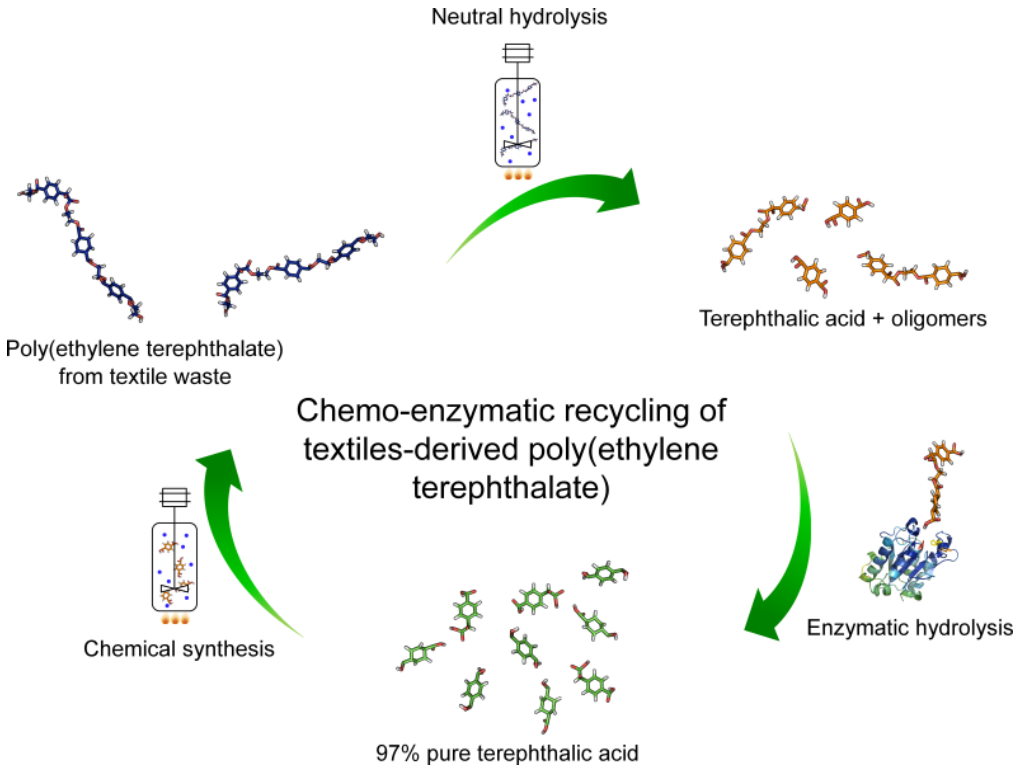

6.1. Introduction

Global population and rising living standards are directly correlated to the continuous increase of textile waste [1]. Over-production of fabrics since 2010 is driven by the increased rate of replacement of products. In 2008, around 14 M tons of textile waste were generated in Europe, but only 5 M tons were recovered [2]. About 75% of the recovered fabrics were reused or recycled mainly in industrial applications[3]. The remaining collected waste textiles is either landfilled or incinerated. However, the recycling of used textiles would lead to several environmental benefits such as energy saving, since this

process requires less energy than the production of the same products from virgin materials and reduction of the carbon footprint of the overall process [4].

The textile and clothing industry is a heterogeneous business which covers different types of fibers, with a consistent 54% that is represented by man-made synthetic materials. The consumption of these synthetic fibers increased by 77% between 2000 and 2012 [5]. On the other hand, the growth share of synthetic fibers in global consumption results in the rising demand for petroleum-based chemicals [6]. Among the synthetic textiles, poly(ethylene terephthalate) (PET) is one of the most widely used polymers in the global textile industry [7]. PET is a semi-crystalline thermoplastic polymer which shows excellent tensile strength, chemical resistance and high thermal stability. Two PET grades are dominating the global market: the fiber grade PET, with a M_w of 15-20 Kg mol^{-1} and intrinsic viscosity between 0.4 and 0.75 dL g^{-1} and the bottle grade PET, which refers to a higher M_w polymer (>20 Kg mol^{-1}) with an intrinsic viscosity above 0.95 dL g^{-1} [8], [9]

Due its wide production and utilization [10], PET represents a broad disposal inert textile. The non-toxic nature, durability and crystal-clear transparency of PET during use are the principal advantages of this polyester, while its rather slow biodegradability is the major cause of concern to the environmentalists. Recycling the textile waste-derived polyesters can significantly cut down the energy usage, resource depletion and greenhouse gas emissions. Unfortunately, different factors such as coloring dyes and other chemicals such as detergents, fuels and pesticides, reduce the quality of recycled PET reducing the number of the possible applications. When compared to mechanical recycling and incineration, chemical hydrolysis could lead to higher-value products. The most common chemical-based PET hydrolysis processes are alkaline hydrolysis using 4-20% NaOH/KOH solutions, phase transfer catalysts and acidic hydrolysis using concentrated sulfuric acid or other mineral acids. All these processes are very costly and toxic due the chemicals required and laborious purification steps needed. In recent years, more environmentally friendly PET recycling strategies based on neutral hydrolysis (carried out using water or steam at 1-4 MPa and temperatures of 200-300 °C) were reported. In last decade, the interest of biotechnologies towards polyesters biodegradation and recycling is gaining a key role. Yoshida *et al.* [11] showed a novel bacterium, *Ideonella sakaiensis*

201-F6, able to break down the plastic using two enzymes to hydrolyze PET and assimilate its building block for growth. Earlier, various studies demonstrated that a class of enzymes belonging to the α/β hydrolase family, namely cutinases, are able to hydrolize the ester bonds of PET and several other polyesters[12]–[14]. Among them, cutinase are currently under investigation for the bioprocessing of PET textiles on an industrial scale[15]. Earlier, it was reported that cutinases from *Thermobifida fusca* and *Humicola insolens* were able to hydrolyze low crystallinity PET while complete hydrolysis by enzymes only seems to be difficult if not impossible for PET with higher crystallinity[14]. In this work, we propose an innovative synergistic chemo-enzymatic hydrolysis of PET for the production of high purity TA (97%) avoiding harsh chemical treatments.

6.2 Materials and Methods

6.2.1 Chemicals, substrates and enzymes

Buffer components, bovine serum albumin (BSA), *para*-nitrophenyl-butyrate (*p*-NPB), methanol, zinc acetate, TA and formic acid were purchased from Sigma-Aldrich (USA). All other chemicals and reagents used in this work were of analytical grade and used without further purification if not otherwise specified. *Humicola insolens* cutinase (HiC) was a gift from Novozymes (Beijing, China). All hydrolysis were performed using Wellman PET fiber with a viscosity of 0.62 dL g^{-1}.

6.2.2 Water-based PET hydrolysis

Water based PET hydrolysis was performed in 1 L stainless steel steel high pressure and high temperature reactor at different temperatures (180 and 250 °C) and with and without the addition of zinc acetate as catalyst. All experiments were carried out with 25 g of virgin PET fiber in 250 mL deionized water. The reactions were stopped after 60 and 90 min respectively (30 min after reaching the steady state), and two different ratios PET/H_2O were assessed. A temperature and pressure profile of a typical reaction is shown in figure S1. At the end of the process, H_2O and EG were removed and a white powder was obtained (Figure S7b). The EG stream can be further processed anaerobically due to the current low cost of the compound.

6.2.3 ATR FT-IR analysis

ATR FT-IR spectra were recorded on a Perkin Elmer Spectrum GX spectrometer. The ATR accessory (supplied by Specac Ltd.,UK) contained a diamond crystal. A total of 16 scans for each sample were taken with a resolution of 4 cm^{-1}. All spectra were recorded at 21 °C over the wavelength interval between 4,000 and 650 cm^{-1}.

6.2.4 FT-Raman analysis

In order to remove the water, terephthalic acid (TA), bis(2-Hydroxyethyl) terephthalate (BHET), dimethyl terephthalate (DMT) and poly(ethylene terephthalate) PET as standards were lyophilized for 24 h. 50 mg of samples were incubated with different volumes of pure triethylamine in 10 mL of chloroform for 6 h. Afterwards, chloroform was removed by evaporation at 21 ºC for 24 h. The virgin material and the powders obtained from the chemical process and after the enzymatic treatment were also incubated as described above. The FT-Raman spectra were recorded using a Perkin Elmer Raman station 400, coupled with a 785 nm laser. Spectra were collected at a resolution of 2 cm^{-1} for 25 scans and normalized in the region 2,200-2,400 cm^{-1} before any data processing. The bands were assigned as follows: 3,000-2,700 cm^{-1} $\nu(Et\text{-}NH_4^+)$, 1,728 cm^{-1} $\nu(C=O$, bended), 1,632-1,604 cm^{-1} $\nu_{as}(C=O)$, single band 1,398 cm^{-1} $\delta(C\text{-}O)$, single band 1,286 cm^{-1} coupled mode $\nu(C=O)+\delta(COH)$.

6.2.5 Protein quantification and SDS-PAGE analysis

Protein concentration was measured using the Bio-Rad Protein Assay Kit (Bio-Rad, USA). BSA was used as protein standard. 10 µL of the sample was added into the wells of a 96 well-plate. Afterwards, 200 µL of the prepared Bio-Rad reagent solution were added (BioRad Reagent diluted 1:5 with MQ-water). The plate was incubated for 5 min at 21 °C and 400 rpm. Buffer (100 mM Tris-HCl pH 7) was used as blank. The absorption after 5 min was measured at λ = 595 nm in a plate reader (Tecan INFINITE M200) and the concentration calculated from the average of triplicates. Sodium dodecyl sulfate-polyacrylamide gel electrophoresis (SDS-PAGE) was performed according to Laemmli using 4% stacking gels and 15% separating gels and run at 150 V. Pre-stained protein marker IV (Peqlab, Germany) was used as a molecular mass marker. Proteins were stained with Coomassie method.

6.2.6 Esterase activity assay

Esterase activity was measured at 25 ˚C using *p*-nitrophenyl-butyrate (*p*-NPB) as a substrate according to Biundo et al[16]. The final assay was carried out by mixing 200 µL of the substrate stock solution, in 100 mM Tris-HCl buffer pH 7, with 20 µL of enzyme solution. The increase of the absorbance at 405 nm due to the release of *p*-nitrophenol (ε 405 nm= 10.27 mL (µmol cm)$^{-1}$) was measured for 5 min, every 18 sec with a plate reader. A blank was included using 20 µL of buffer instead of enzyme solution. The activity was calculated in units (U), where 1 unit is defined as the amount of enzyme required to hydrolyze 1 µmol of substrate per minute under the given assay conditions. The activity assay was also performed in presence of 1, 5, 10, 25 or 50 mM of the chemical catalyst (zinc acetate). All the experiments were performed in triplicates.

6.2.7 Enzymatic hydrolysis of PET oligomers

The enzymatic hydrolysis of the PET powder resulting from the chemical treatments were performed as previously described with some modifications[7], [12]. Briefly, 10 mg of pre-treated PET powder and 2.0 mL of enzyme solution (diluted in 100 mM Tris-HCl buffer pH 7) were added in a test tube. The mixture was incubated for 24 h at 50 °C and 14,000 rpm in an orbital shaker. Different concentrations 0.1, 0.5, 1 and 2 mg mL^{-1} of enzyme were used in order to understand the optimal concentration of HiC. All the experiments were performed in triplicates.

6.2.8 High Performance Liquid Chromatography

Proteins were removed using a 1:1 (v v^{-1}) ice-cold methanol precipitation. Therefore, samples were centrifuged at 14,000 rpm (Centrifuge Berkman JU-MI) at 0 °C for 15 min. The supernatant was acidified by adding 8 µL of 6 M HCl and then transferred into HPLC vials. The released products were analyzed by High Performance Liquid Chromatography (HPLC) (Agilent Technologies) coupled with a UV-detector, at 241 nm, using a water/methanol linear gradient (**Table S1**). In order to determine the TA percentage in the mixture, 10 mg of PET powder resulting from before and after the enzymatic hydrolysis were diluited in 100 mL of 100 mM Tris-HCl buffer pH 7 and analyzed as described before.

6.2.9 ^{1}H-NMR analysis

^{1}H nuclear magnetic resonance was performed on a Bruker Avance II 400 spectrometer (resonance frequency of 400.13 MHz for ^{1}H) equipped with a 5 mm observe broadband probe head (BBFO) with z-gradients. DMSO-d_6 was used as NMR solvent for all samples.

6.3. Results

6.3.1 FT-Raman analysis

In the past, several methods, mainly HPLC-related, have been established to follow enzymatic hydrolysis of PET in aqueous solutions[7], [13]. However, water insoluble oligomers would obviously escape quantification of TA in presence of unsoluble oligomers, hence, a novel method based on FT-Raman and triethylamine was adapted for this study. TA, *p*-$C_6H_4(COOH)_2$ has two carboxylic groups which are detectable using Fourier-transform Raman spectroscopy. The analysis of benzene dicarboxylic acids such as isophthalate and terephthalate using FT-Raman was previously described by Arenas and Tellez [17]. According to these reports the -COOH group of solid TA reveals a typic centered band at 1,631 cm^{-1}, mainly given by the asymmetric stretching (v_{as}) of C=O. As described by Tellez, a coupled vibrational mode is characteristic of the single band at 1,286 cm^{1}. The discrimination of monomeric TA from esterified species was performed converting these functional groups into the corresponding anions. The simplest reaction of carboxylic acid is salification by a base. This reaction causes the shift of (v_{as}) of the C=O group and appearance of new bands due to the in-phase and out of phase -$COO^{(-)}$ stretching vibration. The shift of the acid peak of the carboxylic group from 1,720 cm^{-1} to 1,580 cm^{-1} after alkaline treatment was previously reported for the grafting of cotton with cyclodextrins or for detection of end groups of fluoropolymers [18].

The conversion of the -COOH group into the carboxylate species was carried out using tryethilamine (TEA) in chloroform solution. The deprotonation ion obtained *via* incubation with tertiary aliphatic amine caused the shift of v_{as}C=O and the increase of the single band of the symmetric stretching (v_s) of C=O at 1,400 cm^{-1} and an ammonium-related band in the 2,700 cm^{-1} region.

Figure 1 shows the shift of the acid peak of solid TA from 1,631 cm^{-1} to 1,604 cm^{-1} after deprotonation with TEA. Furthermore, the clear appearance of a peak at 1,398 cm^{-1} was observed due the symmetric stretching mode of the carboxylate moiety. On the other hand, the peak at 1,286 cm^{-1} was strongly reduced. The 1:5 TA/TEA ratio showed the best signal for the monomers due to a complete conversion of the desired groups (Figure S2).

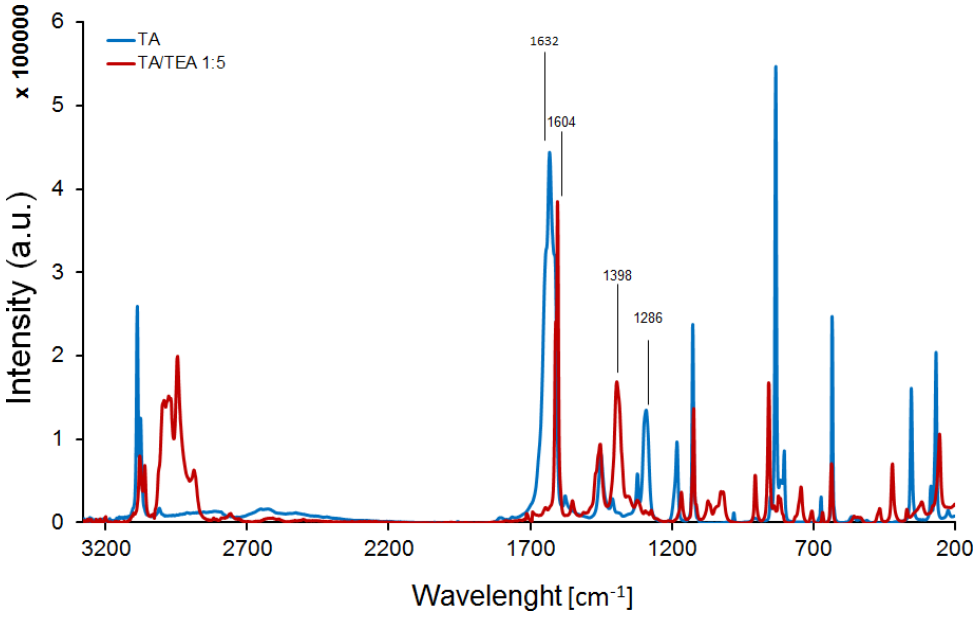

Figure 1. Monitoring of chemical and enzymatic hydrolysis of PET. FT-Raman analysis shows the deprotonation of the TA's carboxylic acid moieties *via* incubation with different TA/TEA ratios.Spectra were normalized between the region 2,000-2,200 cm^{-1}.

To assess the suitability of this method to quantify TA in the presence of oligomers, BHET, DMT and PET were incubated with the tertiary aliphatic amine (1:5 ratio). Expectedly the shift of 1,632 and 1,395 cm^{-1} typical for TA did not occur since all carboxylic groups of these oligomers are esterified (Figure S3-S5).

6.3.2 Water-based PET hydrolysis

Preliminary experiments showed that water-based PET depolimerization was not achieved with ratio 1:4 PET/H_2O and incubating 90 min. Therefore, a series of experiments were performed, in order to define the appropriate depolymerization conditions (**Table1**).

Table 1. Performed water-based PET hydrolysis experiments based on a design of experiments strategy.

Experiment	Initial MW (IV) range of PET	T [°C]	PET/H_2O ratio[a]	Steady state time [min][b]
1	0.62	180	1/4	0
2			1/10	30
3		250	1/4	
4			1/10	0
5		180	1/4	
6			1/10	30
7		250	1/4	
8			1/10	0

[*] Zinc acetate was added to the reaction mixture.

[a] 25 g of PET

[b] after the transient period (to reach the desired T)

The incubation of PET fiber at 180 °C and 12 bar did not lead to any depolymerization of the sample and hence there was no difference of spectra. In Figure S6 is possible to observe how the spectra of raw PET fiber and Sample 2 are very similar with no remarkable differences that could be spotted, showing that reaction temperature and pressure were not optimal for the hydrolysis of the polymer. Finally, when temperature and pressure were increased to 250 °C and 39 bar respectively the polymer was completely reduced in a whitish powder (Figure S7). In Figure S8, it is possible to see, that spectrum of PET depolymerization product for Sample 4 (blue) was similar to the spectrum of commercial TA. Using these conditions, a powder consisting of 85% TA was obtained from the water-based PET depolymerization according to HPLC analysis. Unfortunately, further variation of the reaction conditions including addition of zinc acetate did not lead to a higher yield of TA. Hence, enzymatic hydrolysis of the remaining oligomers was assessed in the next step.

6.3.3 Enzymatic PET hydrolysis

The kinetics of the formation of degradation products *via* enzymatic treatment depends on varius factors, including the chemical-physical structure of polyester substrate[19].Already various authors have previsouly demonstrated that cutinase preferentially hydrolase the amorphous region on PET[20], [21]. On the other hand, it was shown thatenzymatic hydrolysis of PET oligomers is way faster than of a long chain polymer [22].Therefore, due to the high cristallinity of the PET fibers used in the textile industry, a chemical pre-hydrolysis was established in this work.

The sample from chemical pretreatment with the highest degree of hydrolysis (Sample 4, 85% TA) was further incubated with different concentrations of *Humicola insolens* cutinase (HiC) to hydrolyze remaining oligomers (**Figure 2**). The highest amount of soluble TA (6.5 mM) was obtained after 6 h of incubation both when 1 or 2 mg mL^{-1} of HiC were applied without any further increase until 24 h of incubation. The lower concentrations of enzyme of 0.1 and 0.5 mg mL^{-1} led to the release of 0.53 and 1.9 mM of TA, respectively.

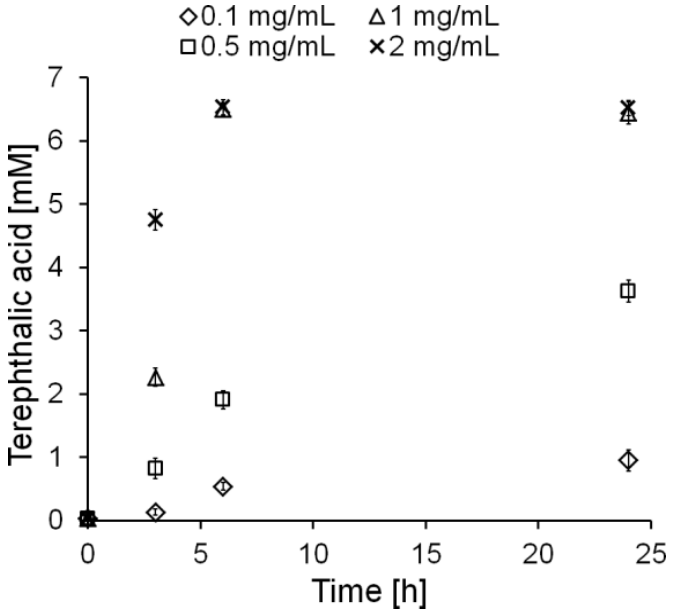

Figure 2. Enzymatic hydrolysis of chemically pretreated PET with different concentrations of *Humicola insolens* cutinase (HiC).

TA with 97% purity was obtained after enzymatic treatment of the chemical-treated PET which is comparable to synthesis-grade TA (98% pure). When chemical pre-hydrolysis of PET was performed in the presence of zinc acetate as a catalyst, a negative influence on enzymatic hydrolysis was observed (**Figure 3**). In fact, there was no further increase of the amount of TA seen (**Figure 3**). Zinc and other metal ions are well known to be potential inhibitors of many enzymes, including cutinases as recently reported by Chen et *al.* that biochemically characterited *Thermobifida fusca* cutinases [23]

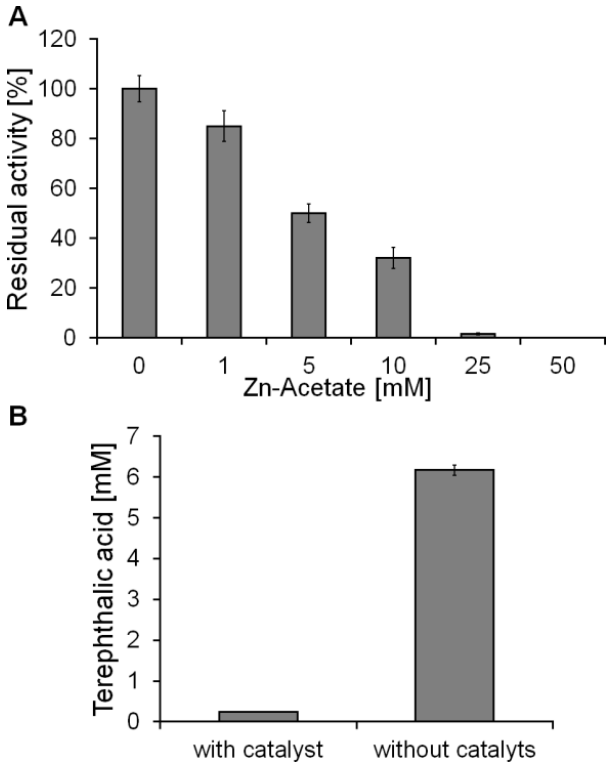

Figure 3. Residual activity of HiC in the presence of Zn-acetate (A) and enzymatic hydrolysis of PET chemically pre-treted in the presence of Zn acetate (B).

6.3.3.1 FT-Raman detection of depolymerized PET

While in the chemically pre-treated sample oligomers were present, the peak at 1,728 cm^{-1} indicative of ester bond was considerably reduced after enzymatic hydrolysis (**Figure 4**). In parallel, the increase of the band at 1,398 cm^{-1} indicated formation of TA. Finally, the signal at 1,286 cm^{-1}, as expected, had the opposite trend of the asymmetric stretching of CO, further confirming the reduction of the oligomers to TA (**Figure 5**).

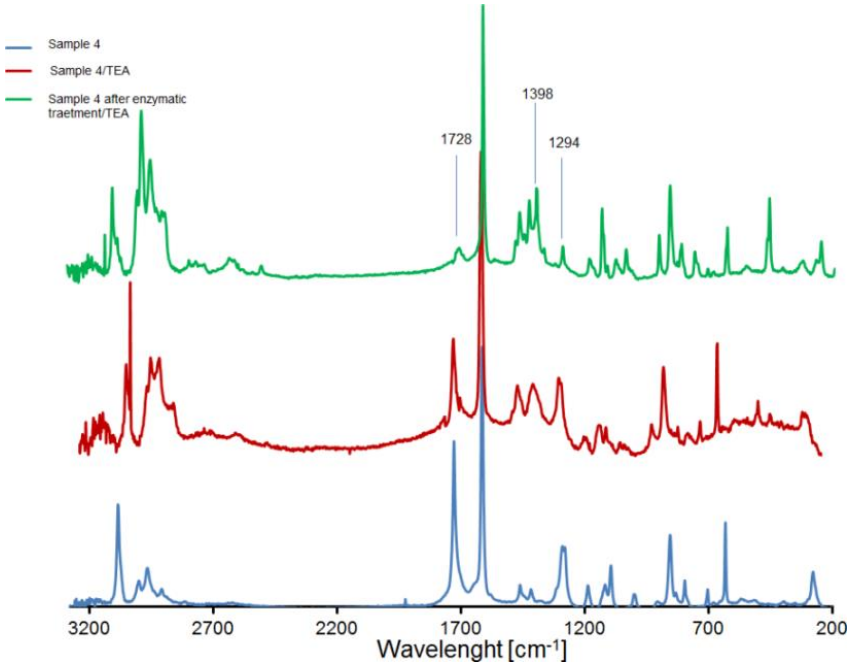

Figure 4. Incubation of Sample 4 with TEA 1:5 before and after enzymatic hydrolysis Spectra were normalized between the region 2,000-2,200 cm^{-1}

In addition to FT-Raman, ^{1}H-NMR analysis was performed. Likewise, ^{1}H spectra (recorded in DMSO-d_6) indicate the presence of some longer oligomers in the chemically pretreated sample while the spectra of the reaction product after subsequent enzymatic hydrolysis suggest their conversion into TA. Based on the ^{1}H-NMR performed calculations (see ESI for details), the oligomers are mostly comprised of less than four (but nearer two) constitutional repeat units, and TA end groups dominate over EG suggesting the oligomerization is more effective at releasing free EG than free TA, or that the purification steps involved preferentially remove EG.

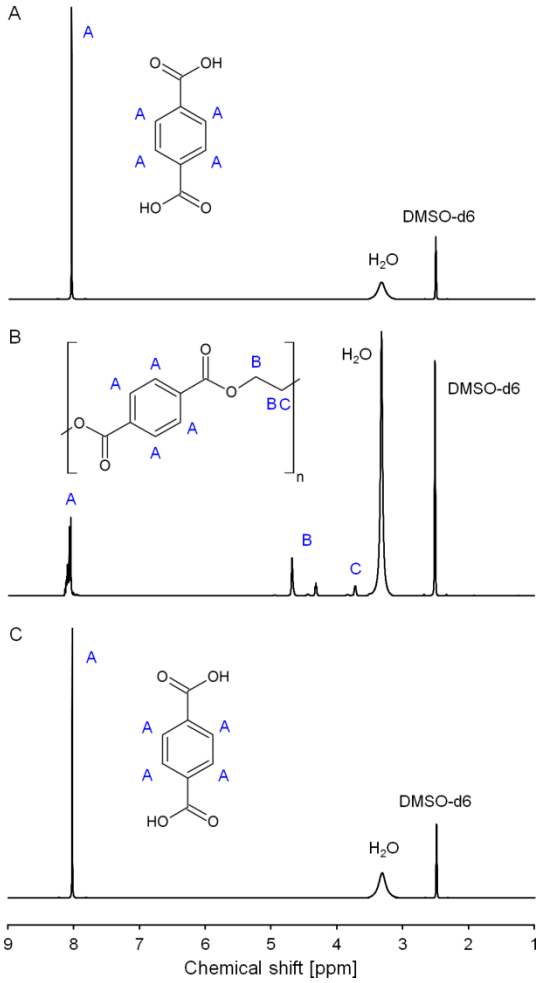

Figure 5. ^{1}H-NMR of pure TA (A), PET degradation after chemical treatment (Sample 4, B) and PET degradation after enzymatic finishing (C). All spectra were recored in DMSO-d_6. All samples were fully soluble in the selected solvent.

6.4. Conclusions

In this study, the synergism of chemical and enzymatic hydrolysis of PET was demonstrated on a multi-gram scale. To monitor the PET hydrolysis and formation of TA a FT-Raman method based on the deprotonation of the –COOH group was established. The chemical pre-treatment performed in an environmentally-friendly way under neutral conditions, therefore avoiding harsh chemicals, lead to depolymerization of the polyester-composed waste textiles yielding about 85% TA. The enzymatic hydrolysis performed in a second reaction step lead to further hydrolysis of the remaining oligomers yielding TA

with a purity of 97%. Future studies should consider the chemo-enzymatic treatment of different PET containing textiles wastes as well as studies on synthesis of PET based on the recovered TA.

6.5 Author contributions

The manuscript was written through contributions of all authors. All authors have given approval to the final version of the manuscript.

Notes

The authors declare no competing financial interest.

Acknowledgments

This project received funding from the European Union's Horizon 2020 research and innovation program under the grant agreement 641942 (Resyntex project).

6.6 References

[1] J. Allwood, S. Laursen, C. de Rodriguez, and N. Bocken, "Well dressed?: The present and future sustainability of clothing and textiles in the United Kingdom," *J. Home Econ. Inst. Aust.*, 2015.

[2] B. Zamani, G. Peters, and M. Svasntröm, "Towards Understanding Sustainable Textile Waste Management: Environmental impacts and social indicators," *Chem. Biol. Eng.*, p. 52, 2014.

[3] A. Jørgensen, A. Le Bocq, L. Nazarkina, and M. Hauschild, "Methodologies for social life cycle assessment," *Int. J. Life Cycle Assess.*, vol. 13, no. 2, pp. 96–103, 2008.

[4] J. H. Clark, T. J. Farmer, L. Herrero-Davila, and J. Sherwood, "Circular economy design considerations for research and process development in the chemical sciences," *Green Chem.*, vol. 18, no. 14, pp. 3914–3934, 2016.

[5] R. Harder, Y. Kalmykova, G. M. Morrison, F. Feng, M. Mangold, and L. Dahlén, "Quantification of goods purchases and waste generation at the level of individual households," *J. Ind. Ecol.*, vol. 18, no. 2, pp. 227–241, 2014.

[6] A. Pellis, E. Herrero Acero, V. Ferrario, D. Ribitsch, G. M. Guebitz, and L. Gardossi, "The Closure of the Cycle: Enzymatic Synthesis and Functionalization of Bio-Based Polyesters," *Trends Biotechnol.*, vol. 34, no. 4, pp. 316–328, 2016.

[7] E. Herrero Acero *et al.*, "Enzymatic surface hydrolysis of PET: Effect of structural diversity on kinetic properties of cutinases from Thermobifida," *Macromolecules*, vol. 44, no. 12, pp. 4632–4640, 2011.

[8] F. Tasca *et al.*, "Increasing the coulombic efficiency of glucose biofuel cell anodes by combination of redox enzymes," *Biosens. Bioelectron.*, vol. 25, no. 7, pp. 1710–1716, 2010.

[9] A. M. Al-Sabagh, F. Z. Yehia, G. Eshaq, A. M. Rabie, and A. E. ElMetwally, "Greener

routes for recycling of polyethylene terephthalate," *Egypt. J. Pet.*, vol. 25, no. 1, pp. 53–64, 2016.

[10] G. M. Guebitz and A. Cavaco-Paulo, "Enzymes go big: surface hydrolysis and functionalisation of synthetic polymers," *Trends Biotechnol.*, vol. 26, no. 1, pp. 32–38, 2008.

[11] S. Yoshida *et al.*, "A bacterium that degrades and assimilates poly(ethyleneterephthalate)," *Science (80-.).*, vol. 351, no. 6278, pp. 1196–1199, 2016.

[12] A. Pellis *et al.*, "Biocatalyzed approach for the surface functionalization of poly(L-lactic acid) films using hydrolytic enzymes," *Biotechnol. J.*, vol. 10, no. 11, pp. 1739–1749, 2015.

[13] A. Pellis, C. Gamerith, G. Ghazaryan, A. Ortner, E. Herrero Acero, and G. M. Guebitz, "Ultrasound-enhanced enzymatic hydrolysis of poly(ethylene terephthalate)," *Bioresour. Technol.*, vol. 218, pp. 1298–1302, 2016.

[14] Å. M. Ronkvist, W. Xie, W. Lu, and R. A. Gross, "Cutinase-Catalyzed hydrolysis of poly(ethylene terephthalate)," *Macromolecules*, vol. 42, no. 14, pp. 5128–5138, 2009.

[15] C. Silva, R. Ara, M. Casal, M. G. Georg, and A. Cavaco-paulo, "Influence of mechanical agitation on cutinases and protease activity towards polyamide substrates," vol. 40, pp. 1678–1685, 2007.

[16] A. Biundo *et al.*, "Characterization of a poly(butylene adipate-co-terephthalate)-hydrolyzing lipase from Pelosinus fermentans," *Appl. Microbiol. Biotechnol.*, vol. 100, no. 4, pp. 1753–1764, 2016.

[17] J. F. Arenas and J. I. Marcos, "Infrared and Raman spectra of phtalate, isophtalate and terephtalate ions," *Spectrochim. Acta Part A Mol. Spectrosc.*, vol. 35, no. 4, pp. 355–363, 1979.

[18] M. Pianca, E. Barchiesi, G. Esposto, and S. Radice, "End groups in fluoropolymers," *J. Fluor. Chem.*, vol. 95, no. 1–2, pp. 71–84, 1999.

[19] A. Eberl *et al.*, "Enzymatic surface hydrolysis of poly(ethylene terephthalate) and bis(benzoyloxyethyl) terephthalate by lipase and cutinase in the presence of surface active molecules," *J. Biotechnol.*, vol. 143, no. 3, pp. 207–212, 2009.

[20] I. Donelli, P. Taddei, P. F. Smet, D. Poelman, V. A. Nierstrasz, and G. Freddi, "Enzymatic surface modification and functionalization of PET: A water contact angle, FTIR, and fluorescence spectroscopy study," *Biotechnol. Bioeng.*, vol. 103, no. 5, pp. 845–856, 2009.

[21] C. Gamerith, M. Gajda, A. Ortner, E. H. Acero, G. M. Guebitz, and M. Ulbricht, "Enzymatic hydrolysis of poly(ethyleneterephthalate) used for and analysed by pore modification of track-etched membranes," *N. Biotechnol.*, vol. 39, pp. 42–50, 2017.

[22] D. Ribitsch *et al.*, "Hydrolysis of polyethyleneterephthalate by p-nitrobenzylesterase from Bacillus subtilis," *Biotechnol. Prog.*, vol. 27, no. 4, pp. 951–960, 2011.

[23] S. Chen, L. Su, S. Billig, W. Zimmermann, J. Chen, and J. Wu, "Biochemical characterization of the cutinases from Thermobifida fusca," *J. Mol. Catal. B Enzym.*, vol. 63, no. 3–4, pp. 121–127, 2010.

6.7 Supporting information

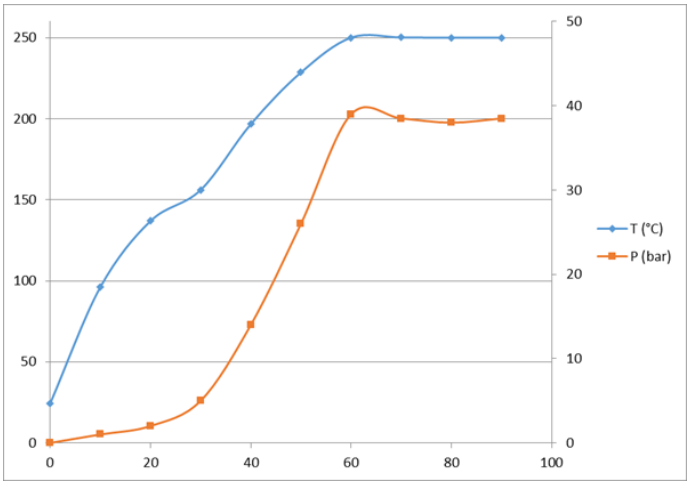

Figure S1. Temperature (blue, Y-axis left) and pressure (red, Y-axis right) increase according to the reaction time (X-axis).

Table S3. Mobile phase gradient used for the HPLC-DAD analysis of the PET degradation release products.

Time (min)	H_2O	Methanol	Formic acid	Flow (mL/min)	Pressure (bar)
1	80	10	10	0.75	600
8	40	50	10	0.75	600
10	0	90	10	0.75	600

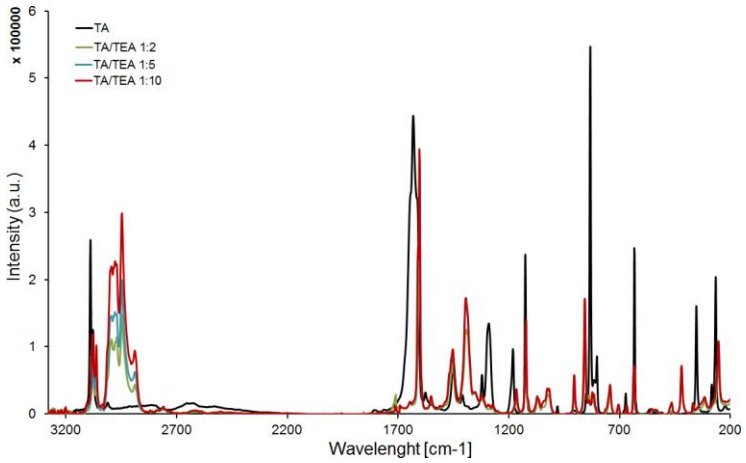

Figure S2. FT-Raman analysis showing the deprotonation of the TA's carboxylic acid moieties *via* incubation with different TA/TEA ratio

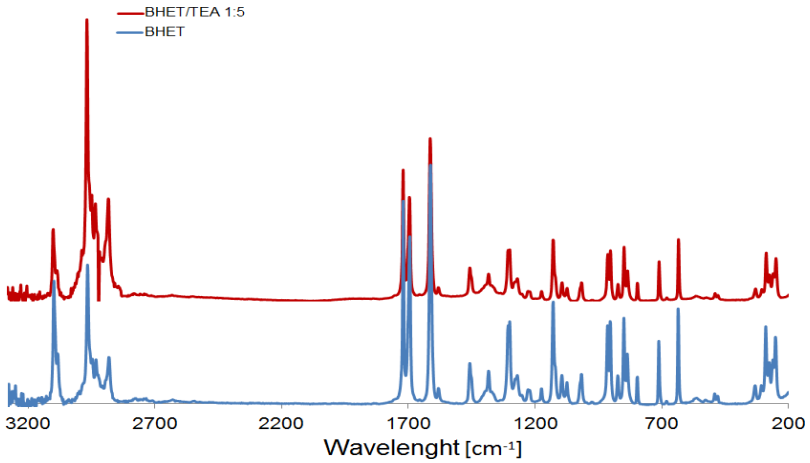

Figure S3. FT-Raman analysis showing the deprotonation of the BHET *via* incubation with TEA 1:5

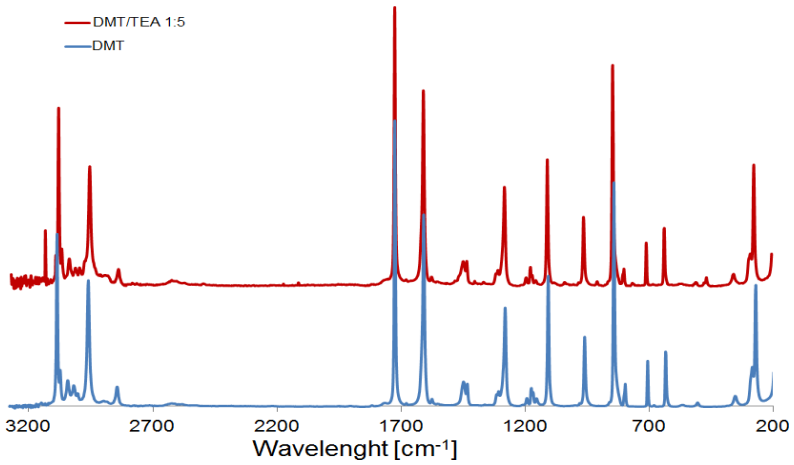

Figure S4. FT-Raman analysis showing the deprotonation of the DMT *via* incubation with TEA 1:5

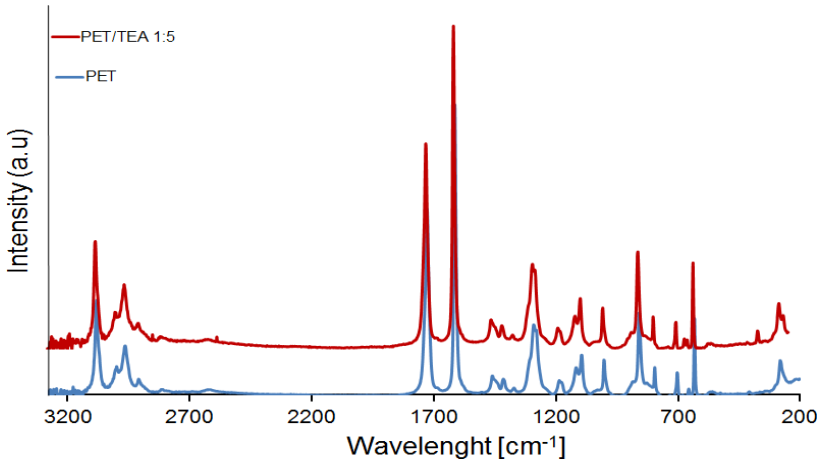

Figure S5. FT-Raman analysis showing the deprotonation of the PET *via* incubation with TEA 1:5

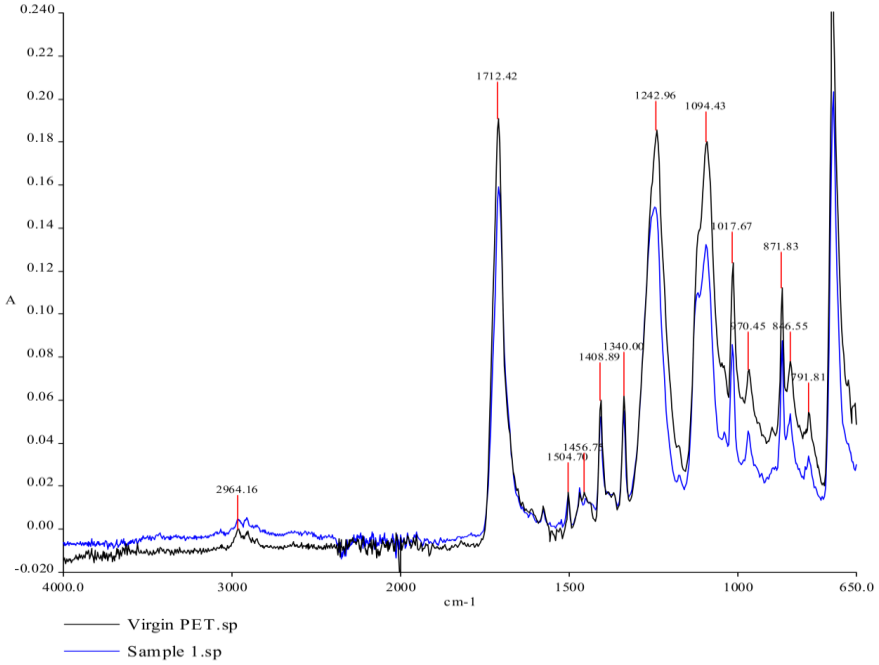

Figure S6. FT-IR spectrum of Sample 1 (black) and spectrum of untreated virgin PET (blue)

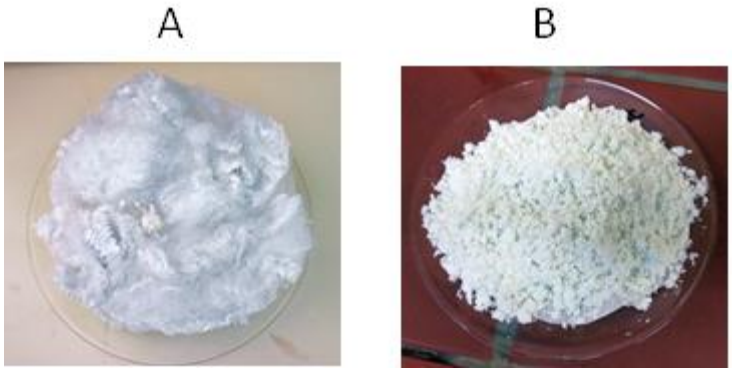

Figure S7. Samples obtained by 3 different depolymerisation operational conditions

A - Sample obtained by experiment: T=180°C, P=12 bars, t=0 min after reaching steady state conditions.

B - Sample obtained by experiment: T=250°C, P=39 bars, t=0 min after reaching steady state conditions

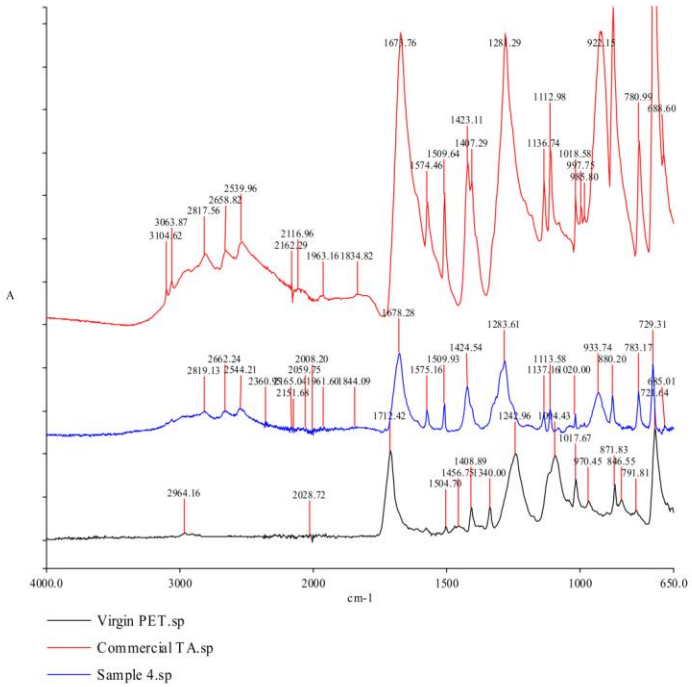

Figure S8. FT-IR spectra of Sample 4 (blue), untreated virgin PET (black) and pure TA (red).

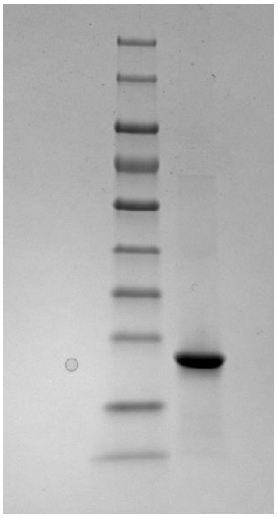

Figure S9. SDS-PAGE of HiC. Lane 1 Protein Marker IV (bands 10-170 KDa). Lane 2 HiC (dilution 1:10), MW~ 24 KDa.

^{1}H-NMR calculations on the released products

Chemical shift (ppm)	Assignment	Integral	No. of protons	Notes
8.05	A = Ar-H (bulk+end-group)	4.0	4	Set as reference
4.67	B+C = EG bulk (ArOC**H2**C**H2**OAr)	1.69	4	
4.31	B* = EG end-group (ArOC**H2**CH2OH)	0.59	2	
3.72	C* = EG end-group (ArOCH2C**H2**OH)	0.59	2	

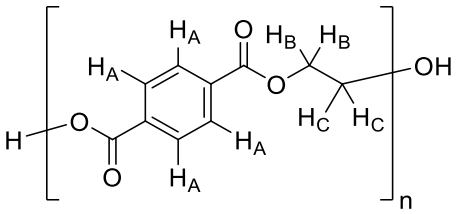

Constitutional repeat unit (CRU)

Note: B = B* and C = C* when EG is an end-group

Ratio of TA to EG:

[A/4] : [(B+C+B+C*)/4] = [4.0/4] : [(1.69+0.59+0.59)/4] = 1 : 0.72 TA:EG*

Therefore there is an excess of TA, this being either as oligomers or free TA

End-group Analysis: We are unable to distinguish between the bulk (i.e. within the chain), end-group or free TA units via ^{1}H-NMR spectroscopy but based on the above ratio there is a 1 : 0.72 excess of TA relative to EG. This excess must be either as end-groups or free TA therefore ~28% (i.e. 100% - 72%) of the TA units are assumed to be end-groups but virtue of there excess relative to EG.

We can distinguish whether the EG units are bulk or end-group, and would also see free EG but this is not evident in the sample. Therefore a ratio of bulk : end-group EG can be determined:

EG_{bulk} : $EG_{end\text{-}group}$ = [B+C/4] : [(B+C*)/4] = [1.69/4] : [(0.59+0.59)/4] = 0.42 : 0.30 = 1 : 0.70*

Based on this ratio of 1 : 0.70 EG_{bulk} : $EG_{end\text{-}group}$ we can determine that 41% of the EG units are end-groups.

As some of the EG are end-groups despite the excess of TA calculated above there must therefore be additional units of TA that are also end-groups (i.e. those as a result of EG becoming end-groups thus freeing more carboxylic acid end-groups). This can be estimated based on the amounts of $EG_{end\text{-}group}$. We had already determined that ~28% of all TA was end-groups due to it being in excess, but a further 41% of the remaining (72%) TA is also end-groups. As 41% of the remaining 72% = 30% then a total of 58% (i.e. 30% + 28%) of all TA must be end-groups or free TA.

7

General Conclusion

Textile and Clothing industry products are almost omnipresent in our daily life, including high -performance fabrics and medical applications. On the other hand, textile technology is the one of the oldest sectors, thus the aim of this thesis was to assess the potential of new technology in this field, including more innovative and environmentally friendly systems. In the last two decades, different enzymatic approaches have been proved to be a potential substitute of classic chemistry methods used in such field.

Focusing on surface technology, in this thesis a cutinase from *Humicola insulens* was exploited for limited surface functionalization on synthetic polymers, such as poly(ethylene terephthalate) and polyamide-6. The released products from the partial cleavage of fabrics were determined *via* HPLC (1 mM BHET for PET and 0.07 mM caprolactam for nylon at 50 °C after 72 h). Due to their chemical structure different flame retardant compounds (FRC) have been defined highly hazard for human health. Thereafter, the development of less toxic FRC is unequivocally required. As results of its chemical structure, DNA can achieve the same intuminescent properties as the halogenated flame retardant compounds, for example. Immobilization of DNA on activated synthetic polymer surfaces was studied *via* different coupling system (EDC/NHS, dopamine and tyrosine). Hereby, DNA immobilization was at first instance confirmed by FT-IR, using its typical bands at

1220, 970 and 840 cm^{-1}. Among the mentioned coupling systems, tyrosine (as cross-linker) resulted the most effective. Specifically, the tyrosine/DNA coupling on nylon-6 surface shown the lowest burning rate and total burning time (35 sec,150 mm and 4.3 $mm*sec^{-1}$ for the blank and 3.5 sec, 17.5 mm and 5 $mm*sec^{-1}$ for nylon/tyrosine/DNA), which was also confirmed by FT-IR, ESEM and EDS (*via* determination of phosphorous group present in DNA). Moreover, thermogravimetric analysis confirmed that tyrosine coupling system allows a lower thermal degradation measured between 450 and 625 °C compared to the blanks.

Nosocomial infections and extensive abuse of antibiotics lead a strong necessity of new alternative medical strategies. For this reason, it is also presented the covalent coupling of natural antimicrobial compounds (eugenol) loaded on pH-responsive human serum albumin/silk fibroin nanocapsules onto cotton/PET blends. HSA and SF, mixed with eugenol were used to produced using ultrasound, with a final particles size (hydrodynamic radii) between 319.73±17.5 and 574± 92.76 nm and zeta-potential ranging from -10.39±1.99 mV to -12.11±0.59 mV. Different release studies of eugenol were conducted and evaluated in different artificial sweats varying in pH (5.5, 6.5 and 8.00) as simulation of sweat gland contribution in wound reepithelialisation. Particles formulation with 10 % of silk fibroin with the lower degradation degree demonstrated the highest release around 41 % at pH 6.5. After coupling onto surface activated cotton/PET (using HiC) *via* EDC/NHS system, the blends shown antimicrobial activity against *Staphylococcus aureus* (Gram positive) and *Escherichia coli* (Gram negative), with inhibition of 81 and 33 % respectively.

The end-life of textile material is mostly landfilling and only a small percentage of this kind of waste is used for energy recovery. Taking into account textile composition, these discarded materials still present valuable products that could be reused. Hereby, un-wearable fabric can reduce the environmental impact of textile and clothing industry and moreover save landfill space and GHG emissions. It is well known the higher specificity and selectivity of enzymes. Following a circular economy view, artificial and real textile blends were used to extract to recover value-added products from wool (with 95 % of efficiency) and cellulose-based materials (85 % of yield).The amino-acids and oligomers

(with molecular weight lower than 5 KDa) could replace carbon and nitrogen sources for germination or for replacement of phenolic compounds for resin preparation. Glucose, obtained from cellulose degradation, (around 0.62 $g*L^{-1}$) was used for bio-ethanol (0.3 $g*L^{-1}$) via yeast fermentation. The purity of polyester, as residual polymer from the blends, was determined with FT-IR, which it was equivalent to pure PET.

The high crystallinity degree of PET used in textile application makes difficult its complete depolymerization with esterases. Therefore, a synergistic combination of chemical and enzymatic depolymerization was performed. In a fist step, PET was degraded using water at 250 °C, 40 bar (ratio PET/water 1:10) with yield of 85 % into TPA and small oligomers. The oligomers were further converted into monomer after 6 h incubations with *Humicola insulens* cutinase, which yielded a final 97 % pure TPA. The ability of deprotonation of free carboxylic group of TPA was used to monitor the degree of the depolymerization process, in presence of tryethylamine (ratio 1:5) using FT-Raman.

this thesis demonstrates the high versatility and specificity of the enzymes. It possible to conclude that enzymatic approaches are capable of surface modification of polymers and as well be involved in recycling process. Despite enzymes are well described, optimization of the processes are needed in order to achieve a more economical and feasible industrial process. The improvement in terms of production, purification and finally recycling of enzymes will lead the boosting of their applications in several industrial fields, including textile and clothing industry

8

Appendix

8.1 List of figures

Chapter 2

Appendix

Chapter 3

Pag

Appendix

Figure 3 FT-IR analayis of hydrolyzed PET after coating with tyrosine (blue line)and after tyrosine/DNA coupling (red line)

Figure 4 FT-IR analayis of hydrolyzed nylon-6 after coating with tyrosone (blue line) and after tyrosine/DNA coupling (red line

Figure 5 Scanning electron microscopy images of the samples (A) untreated PET1000x (B)PET_tyrosine_DNA 1000x magnification (C) PET_tyrosine_DNA 5000x magnification (D) untreated nylon-6 1000x magnification (E) nylon_tyrosine_DNA 1000x magnification (F) nylon_tyrosine_DNA 5000x magnification

Figure 6 DNA washing stability. Washing of PET (A) and nylon (B) samples treated with DNA absorbed on untreated polymer (white dots),DNA absorbed on enzymatic treated polymer (red dots), and three coupling conditions: EDC coupling (orange dots), dopamine coupling (green dots) and tyrosine coupling (blue dots)

Figure 7 Results of flammability tests of enzymatically activated and tyrosine and tyrosine/DNA treated PET

Figure 8 Results of flammability tests of enzymatically activated and tyrosine and tyrosine/DNA treated nylon

Figure 9 ESEM image of nylon/blank burne (100x)(A) and nylon/tyrosine/DNA burned (100x) (B) in the upper part and PET/blank burned (100x) (C),PET/tyrosone/DNA burned (100x), (D) and PET/tyrosine/DNA burned (1000x) (E)

Chapter 4

Pag

(A) Dynamic light scattering based hydrodynamic radii in nm. (B) Zeta potential in mV compared to unloaded HSA/SF nanocapsules with ident protein concentrations. (C) Secondary structure ratios (β/α ratios) calculated from ATR-FTIR spectra of unloaded and eugenol loaded HSA/SF nanocapsules for the amid I bands (β: 1626 cm^{-1}; α: 1648 cm^{-1}), whereby the increase in β-sheets structures is separately indicated for nanocapsules containing 30 or 60 mb SF by dashed lines

Figure 4 Average cumulative release of eugenol from HSA/SF nanocapsules with lower degradation degree (30 mb) and 10 or 25% SF over a time period of 168 h in artificial sweats prepared as previously described by Callewaert *et al.* [36]. (A) ISO pH 5.5, (B) ISO pH 8.0 and (C) EN pH 6.0. All time points were measured in triplicates.

Figure 5 Effect of SF content, concentration of HSA and HSA/SF nanocapsules on cell viability of human THP-1 monocyte cells. (A) unloaded and (B) eugenol loaded particles of indicated formulations and at final concentrations of 1 mg mL^{-1}, 250 µg mL^{-1} or 62.5 µg mL^{-1} were incubated with THP-1 monocytes for 24 hours. Cell viability was determined via MTT assay and normalized to untreated control cells (CTRL; 100% viability). DMSO was used at 30% final concentration to obtain a cytotoxicity control (DMSO). (n=4; mean ± SD; Kruskal-Wallis test with Dunn's multiple comparison test; all samples were compared to corresponding untreated control (CTRL); difference of p-

Chapter 5

Pag

Appendix

Chapter 6

Pag

8.2 List of tables

Chapter 3

Pag

Chapter 4

Pag

Chapter 5

Chapter 6

8.3 Scientific publications

Papers:

1 **Quartinello Felice**, Simona Vajnhandl, Julija Volmajer Valh, Thomas J. Farmer, Bojana Vončina, Alexandra Lobnik, Enrique Herrero Acero, Alessandro Pellis, and Georg M. Guebitz. "Synergistic chemo-enzymatic hydrolysis of poly (ethylene terephthalate) from textile waste." *Microbial biotechnology* 10, no. 6 (2017): 1376-1383.

2 **Quartinello, Felice**, Sara Vecchiato, Simone Weinberger, Klemens Kremser, Lukas Skopek, Alessandro Pellis, and Georg M. Guebitz.

"Highly selective enzymatic recovery of building blocks from wool-cotton-polyester textile waste blends." *Polymers* 10, no. 10 (2018): 1107.

3 **Quartinello, Felice**, Klemens Kremser, Sara Vecchiato, Herta Schoen, Robert Vielnascher, Leon Ploszanski, Alessandro Pellis, and Georg M. Guebitz. "Increased flame retardancy of enzymatic functionalized PET and Nylon fabrics via DNA immobilization." *Frontiers in chemistry* 7 (2019): 685.

4 **Quartinello Felice**, Claudia Tallian, Julia Auer, Herta Schön, Robert Vielnascher, Simone Weinberger, Karin Wieland et al. "Smart textiles in wound care: functionalization of cotton/PET blends with antimicrobial nanocapsules." *Journal of materials chemistry B* 7, no. 42 (2019): 6592-6603.

5 Gigli, Matteo, **Felice Quartinello**, Michelina Soccio, Alessandro Pellis, Nadia Lotti, Georg M. Guebitz, Silvia Licoccia, and Andrea Munari. "Enzymatic hydrolysis of poly (1, 4-butylene 2, 5-thiophenedicarboxylate)(PBTF) and poly (1, 4-butylene 2, 5-furandicarboxylate)(PBF) films: A comparison of mechanisms." *Environment international* 130 (2019)

6 **Quartinello Felice**, and Georg M. Gübitz. "Bioprocessing of polyesters." In *Advances in Textile Biotechnology*, pp. 37-48. Woodhead Publishing, 2019.)

7 **Quartinello Felice**, Georg M. Guebitz, and Doris Ribitsch. "Surface functionalization of polyester." In *Methods in enzymology*, vol. 627, pp. 339-360. Academic Press, 2019.

8 Weinberger, Simone, Judit Canadell, **Felice Quartinello**, Bahar Yeniad, Andrea Arias, Alessandro Pellis, and Georg M. Guebitz. "Enzymatic degradation of poly (ethylene 2, 5-furanoate) powders and amorphous films." *Catalysts* 7, no. 11 (2017): 318.

9 Pellis, Alessandro, Marco Vastano, **Felice Quartinello**, Enrique Herrero Acero, and Georg M. Guebitz. "His-tag immobilization of cutinase 1 from Thermobifida cellulosilytica for solvent-free synthesis of polyesters." *Biotechnology journal* 12, no. 10 (2017): 1700322.

10 Haske-Cornelius, Oskar, Simone Weinberger, **Felice Quartinello**, Claudia Tallian, Florian Brunner, Alessandro Pellis, and Georg M. Guebitz. "Environmentally friendly covalent coupling of proteins onto oxidized cellulosic materials." *New Journal of Chemistry* 43, no. 36 (2019): 14536-14545.

11 Perz, Veronika, **Felice Quartinello**, Christoph Provasnek, Georg M. Guebitz, Gabriele Berg, and Christina Andrea Müller. "Polyesterases from moss-associated microorganisms." (2016).

8.4 Oral presentations as presenting author:

1- Autex Conference (Corfu´, Greece-2017)

Enzymatic separation of poly(ethylene terephthalate) from cotton blends

Felice Quartinello, Alessandro Pellis, Georg M. Guebitz

2- ICET Conference (Wuxi, China-2018)

Enzymatic separation of polymers from textile waste

Felice Quartinello, Alessandro Pellis, Georg M. Guebitz

8.5 Poster presentations (most relevant):

1- Autex Conference (Ljubliana, Slovenia- 2016)

Cutinase-catalyzed and chemical hydrolysis of recycled poly(ethylene terephthalate)-

Felice Quartinello, Barbara Zartl, Simona Vajnhandl, Julia Volmajer, Enrique Herrero Acero, Georg M. Guebitz

2- ECAB Conference (Florence, Italy- 2019)
Enzymatic recovery of building blocks from texitile blends

Felice Quartinello, Alessandro Pellis, Georg M. Guebitz

8.6 Acknowledgments

It´s time say some

thank you!

I would like to thank my supervisor **Prof. Georg Guebitz**, for giving me the opportunity to do my PhD in his working group and for his scientific input during all the PhD.

I would like also to thank my consortium partners from the EU Project **Resyntex** and for introducing me in the textile world and giving me the possibility to do and finish my PhD.

Honourable thank goes to **Dr Alessandro Pellis**, for the daily supervision, the scientific discussions; I learned a lot from him and during my time here he became a real friend to me.

Thank you **Dr Doris Ribitsch** for being patient every time I knock on your door and you reply to my many questions.

All the **IFA-people** but a HUGE thanks goes to **Elke, Petra**, **Marion, Marcus Pruckner** and our **Robsi**: no PhD student would survive without your support.

Now it´s time to mention a thanks to the all the members of the **BET-group** and it´s well spent time during these years. I´ve been really lucky to meet and work with **Herta**, thanks for your support especially when I come to you with my crazy ideas and we make our great “homemade solutions”.

Some days have been really heavy and stressful but I´m glad to share my **Hogwarts Office** with **Klemens** (my former master student and now Gryffindor friend), **Oskar** (the crazy and nice German Slytherin), **Miguel** (our new entry Hufflepuff “cook”) and even if for a short time, it was enjoyable to meet and know **Magda** (the Muggle).

Sometimes colleagues become your close friends and your share a big part of your life also outside of work. So now I have to say thanks to:

Sara: for being always present in my “roller coaster “life

Claudia: partner in crime in”IFA- happiness and craziness “times

Simone: Oh my Dear there are no words how I can say Thank You for all these years and pleasant time with you.

Now it is time to say thank you someone outside of work!

I think it is essential in the life of a person to have some people on which you can always count on, so thanks to my **parents** and **my brother**.

Vienna and Tulln gave me the opportunity to know and get close to many different friends. I can easily say that via a twisted connection a deep friendship was born, then i´m glad to have in my life “**Le Arancine” (Valentina** and **Alessandra)** and **Matteo**.

It's always nice to meet people with so many different coloured personalities, so I am happy to be part of the group of “**Italienischer Regenbogen**”, proudly organized by **Alessandra D**.(thank you lil girl). Among this group I met **Valeria, Federica, Davide** e **Federico** who fully took part in my life in Vienna.

There is no distance that can destroy a bond like ours, even when we are forced to talk only via messages or calls, we are able to laugh and to support each other.

Thank you Big Sis **Elisabeth!**

8.7 Statutory declaration

I declare that I have authored this thesis independently, that I have not used other than the declared sources/resources, and that I have explicitly marked all material which has been quoted either literally or by content from the used source.

_____ _____

Date Signature